GEOMETRIZED VACUUM PHYSICS. PART 7:
"ELECTRON" AND "POSITRON"

Mikhail Batanov-Gaukhman[1]

(1) Moscow Aviation Institute (National Research University),
Institute No. 2 "Aircraft and rocket engines and power plants",
st. Volokolamsk highway, 4, Moscow – Russia, 125993
(e-mail: alsignat@yandex.ru)

12.09.2024

ABSTRACT

This article is the seventh part of the scientific project under the general title "Geometrized Vacuum Physics Based on the Algebra of Signature " [1,2,3,4,5,6]. In this article, the metric-dynamic model of two simplest mutually opposite stable spherical vacuum formations is considered - "electron" and "positron". These stable vacuum formations are an integral part of the hierarchical cosmological model proposed in the previous article [6]. The methods of geometrized vacuum physics and the mathematical apparatus of the Algebra of Signature used in this article to study the metric-dynamic model of "electron" and "positron" are suitable for studying all other more complex stable vacuum formations of the same scale: "quarks", "nucleons", "mesons", "atoms" and "molecules", etc., as well as all stable vacuum formations of any scale, for example, "planets", "stars" and "galaxies". This article examines issues related to deformations and accelerated flows of various vacuum layers inside the "electron" and "positron". Paths for the development of geometrized vacuum electrostatics are outlined. Some aspects of the "electron"-"photon", "electron"-"positron" and "electron"-"electron" interactions are considered. The "eelectron" and "positron" are infinitely complex vacuum formations, but the algorithms and mathematical techniques of the Algebra of signature proposed in the article can allow permanently pushing back darkness into the abyss of the unknown, gradually transforming transcendence into immanence.

Keywords: electron, positron, geometrized physics, vacuum, Algebra of signature, vacuum equations, elementary particle models, mass gap.

BACKGROUND AND INTRODUCTION

This paper is the seventh in a series of articles under the general title "Geometrized Vacuum Physics Based on the Algebra of Signature". The previous six articles are listed in the bibliography [1,2,3,4,5,6].

The paper [6] presented a hierarchical cosmological model, within the framework of which the Universe is filled with an uncountable number of spherical vacuum formations (corpuscles) of various scales, which are nested inside each other like Russian dolls (see Figure 10 in [6]).

Within the framework of the hierarchical cosmological model [6], all spherical vacuum formations (corpuscles) of the universal, galactic, stellar-planetary, microscopic (i.e. cellular-bacterial), picoscopic (i.e. atomic-molecular), etc. scales are arranged practically identically. Therefore, in the article [6], only the level of elementary particles is considered in detail. In particular, metric-dynamic models of sixteen types of colored "quarks" (see Table 1 and the set of metrics (71) in [6]) and colored photons were obtained, on the basis of which completely geometrized representations of practically all elements of the Standard Model of elementary particles were constructed: "leptons", "mesons", "baryons", "bosons" (see §4 in [6]), as well as "atoms" and "molecules".

Let's recall that we have agreed to put the names of metric-dynamic models of "particles" of all scales in quotation marks, because, firstly, these are not exactly particles, and, secondly, these geometrized models only partially correspond to modern ideas about these elements of matter.

In the article [6], only sets of metrics-solutions of Einstein's vacuum equations are given, which make up the metric-dynamic models of spherical vacuum formations ("corpuscles"), however, how to extract information about the structure of these "corpuscles" from these sets of metrics based on the methods of geometrized vacuum physics and the Algebra of Signature was not presented.

In this article, as an example, we will study in detail the structure and interaction of only the "electron" and "positron". The structure and interaction of all other spherical vacuum formations ("corpuscles") of any scale ("quarks", "planets", "stars", "galaxies", etc.) are described similarly, and are partly planned to be considered in subsequent articles of this project.

Let's recall that the metric-dynamic models of a free "electron" and a free "positron" are determined respectively by sets of metrics (50) and (60) taking into account §4.12 in [6]

<div align="center">

"ELECTRON" (1)

free, valence

On average, spherical stable "convex" multilayer spherical

curvature of $\lambda_{-12,-15}$-vacuum with signature $(+ - - -)$, consisting of:

I   The outer shell of free valence "electron"

in the interval $[r_2, r_6]$ (see Figure 1)

</div>

$$I \qquad ds_1^{(+---)2} = \left(1 - \frac{r_6}{r} + \frac{r^2}{r_2^2}\right)c^2 dt^2 - \frac{dr^2}{\left(1 - \frac{r_6}{r} + \frac{r^2}{r_2^2}\right)} - r^2(d\theta^2 + \sin^2\theta\, d\phi^2), \qquad (2)$$

$$H \qquad ds_2^{(+---)2} = \left(1 + \frac{r_6}{r} - \frac{r^2}{r_2^2}\right)c^2 dt^2 - \frac{dr^2}{\left(1 + \frac{r_6}{r} - \frac{r^2}{r_2^2}\right)} - r^2(d\theta^2 + \sin^2\theta\, d\phi^2), \qquad (3)$$

$$V \qquad ds_3^{(+---)2} = \left(1 - \frac{r_6}{r} - \frac{r^2}{r_2^2}\right)c^2 dt^2 - \frac{dr^2}{\left(1 - \frac{r_6}{r} - \frac{r^2}{r_2^2}\right)} - r^2(d\theta^2 + \sin^2\theta\, d\phi^2), \qquad (4)$$

$$H' \qquad ds_4^{(+---)2} = \left(1 + \frac{r_6}{r} + \frac{r^2}{r_2^2}\right)c^2 dt^2 - \frac{dr^2}{\left(1 + \frac{r_6}{r} + \frac{r^2}{r_2^2}\right)} - r^2(d\theta^2 + \sin^2\theta\, d\phi^2); \qquad (5)$$

<div align="center">

H   The core of free valence "electron"

in the interval $[r_6, r_7]$ (Figure 1)

</div>

$$I \qquad ds_1^{(+---)2} = -\left(1 - \frac{r_7}{r} + \frac{r^2}{r_6^2}\right)c^2 dt^2 - \frac{dr^2}{-\left(1 - \frac{r_7}{r} + \frac{r^2}{r_6^2}\right)} - r^2(d\theta^2 + \sin^2\theta\, d\phi^2), \qquad (6)$$
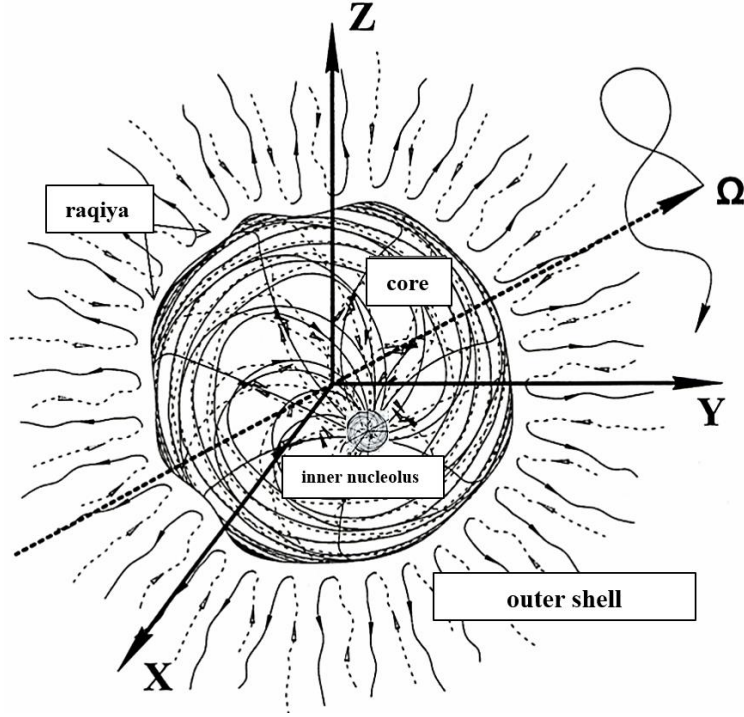
$$H \qquad ds_2^{(+---)2} = -\left(1 + \frac{r_7}{r} - \frac{r^2}{r_6^2}\right)c^2 dt^2 - \frac{dr^2}{-\left(1 + \frac{r_7}{r} - \frac{r^2}{r_6^2}\right)} - r^2(d\theta^2 + \sin^2\theta\, d\phi^2), \qquad (7)$$

$$V \qquad ds_3^{(+---)2} = -\left(1 - \frac{r_7}{r} - \frac{r^2}{r_6^2}\right)c^2 dt^2 - \frac{dr^2}{-\left(1 - \frac{r_7}{r} - \frac{r^2}{r_6^2}\right)} - r^2(d\theta^2 + \sin^2\theta\, d\phi^2), \qquad (8)$$

$$H' \qquad ds_4^{(+---)2} = -\left(1 + \frac{r_7}{r} + \frac{r^2}{r_6^2}\right)c^2 dt^2 - \frac{dr^2}{-\left(1 + \frac{r_7}{r} + \frac{r^2}{r_6^2}\right)} - r^2(d\theta^2 + \sin^2\theta\, d\phi^2); \qquad (9)$$

<div align="center">

i   **The substrate of the "electron"**

in the interval $[0, \infty]$

</div>

$$i \qquad ds_5^{(+---)2} = c^2 dt^2 - dr^2 - r^2(d\theta^2 + \sin^2\theta\, d\phi^2). \qquad (10)$$

Fig. 1. Illustration of a fully geometrized model of a stable spherical vacuum formation
(in particular, a free "electron") with four clearly defined regions:
The **core** of the "electron" is the central closed spherical region of λ-12,-15-vacuum;
The **outer shell** of the "electron" is the region of λ-12,-15-vacuum surrounding the core of the "electron";
The **raqiya** of the "electron" is a multilayer spherical abyss-crack separating the core of the "electron" from its outer shell;
The **inner nucleolus** is a small closed spherical region of λ-12,-15-vacuum inside the core of the "electron";
The **substrate** of the "electron" is the original undeformed region of vacuum in which the "electron" is located. This is a kind of memory of what this vacuum region was like before it was deformed and took on the stable form of an "electron"

<div align="center">

"POSITRON" (11)

free, valence

On average, spherical stable " concave " multilayer spherical
curvature of λ-12,-15-vacuum with signature $(+ - - -)$, consisting of:

V   The outer shell of free valence "positron"

in the interval $[r_2, r_6]$ (see Figure 1)

</div>

$$I \qquad ds_1^{(-+++)2} = -\left(1 + \frac{r_6}{r} - \frac{r^2}{r_2^2}\right)c^2 dt^2 + \frac{dr^2}{-\left(1 - \frac{r_6}{r} + \frac{r^2}{r_2^2}\right)} + r^2(d\theta^2 + \sin^2\theta \, d\phi^2), \qquad (12)$$

$$H \qquad ds_2^{(-+++)2} = -\left(1 - \frac{r_6}{r} + \frac{r^2}{r_2^2}\right)c^2 dt^2 + \frac{dr^2}{-\left(1 + \frac{r_6}{r} - \frac{r^2}{r_2^2}\right)} + r^2(d\theta^2 + \sin^2\theta \, d\phi^2), \qquad (13)$$

$$V \qquad ds_3^{(-+++)2} = -\left(1 + \frac{r_6}{r} + \frac{r^2}{r_2^2}\right)c^2 dt^2 + \frac{dr^2}{-\left(1 - \frac{r_6}{r} - \frac{r^2}{r_2^2}\right)} + r^2(d\theta^2 + \sin^2\theta \, d\phi^2), \qquad (14)$$

$$H' \qquad ds_4^{(-+++)2} = -\left(1 - \frac{r_6}{r} - \frac{r^2}{r_2^2}\right)c^2 dt^2 + \frac{dr^2}{-\left(1 + \frac{r_6}{r} + \frac{r^2}{r_2^2}\right)} + r^2(d\theta^2 + \sin^2\theta \, d\phi^2); \qquad (15)$$

3

<div align="center">

H′   The core of free valence " positron "

in the interval $[r_6, r_7]$ (Figure 1)

</div>

I
$$ds_1^{(-+++)2} = -\left(1 - \frac{r_7}{r} + \frac{r^2}{r_6^2}\right)c^2 dt^2 + \frac{dr^2}{\left(1 - \frac{r_7}{r} + \frac{r^2}{r_6^2}\right)} + r^2(d\theta^2 + \sin^2\theta\, d\phi^2), \tag{16}$$

H
$$ds_2^{(-+++)2} = -\left(1 + \frac{r_7}{r} - \frac{r^2}{r_6^2}\right)c^2 dt^2 + \frac{dr^2}{\left(1 + \frac{r_7}{r} - \frac{r^2}{r_6^2}\right)} + r^2(d\theta^2 + \sin^2\theta\, d\phi^2), \tag{17}$$

V
$$ds_3^{(-+++)2} = -\left(1 - \frac{r_7}{r} - \frac{r^2}{r_6^2}\right)c^2 dt^2 + \frac{dr^2}{\left(1 - \frac{r_7}{r} - \frac{r^2}{r_6^2}\right)} + r^2(d\theta^2 + \sin^2\theta\, d\phi^2), \tag{18}$$

H′
$$ds_4^{(-+++)2} = -\left(1 + \frac{r_7}{r} + \frac{r^2}{r_6^2}\right)c^2 dt^2 + \frac{dr^2}{\left(1 + \frac{r_7}{r} + \frac{r^2}{r_6^2}\right)} + r^2(d\theta^2 + \sin^2\theta\, d\phi^2); \tag{19}$$

<div align="center">

i   The substrate of the "positron"

in the interval $[0, \infty]$

</div>

i
$$ds_5^{(-+++)2} = -c^2 dt^2 + dr^2 + r^2(d\theta^2 + \sin^2\theta\, d\phi^2). \tag{20}$$

where in metrics (2) – (9) and (12) – (19), according to hierarchy (44a) in [6], presumably:

$r_2 \sim 10^{29}$ cm is the approximate radius of the observable Universe;

$r_6 \sim 10^{-13}$ cm is the approximate radius of the radius of the core of the "electron";

$r_7 \sim 10^{-24}$ cm is the approximate radius of the core of the "proto-quark".

The radii r_2, r_6, r_7, taken from the hierarchy (44a) in [6] are approximate and can be refined as further research progresses. These radii do not have a significant effect on the structure of the valence "electron" and valence "positron" if $r_2 \gg r_6 \gg r_7$.

As already noted in [6], the sets of metrics (1) and (11) differ only in signature. That is, the "electron" and "positron" are completely identical, but antipodal (mutually opposite) copies of each other. If the "electron" is conventionally called a "convex" stable spherical $\lambda_{-12,-15}$-vacuum formation (Figure 1), then the "positron" is exactly the same conventionally "concave" stable spherical $\lambda_{-12,-15}$-vacuum formation (negative of Figure 1). Recall that the concept of $\lambda_{m,n}$-vacuum was introduced in §2.1 in [1]. Such a mutually opposite pair of $\lambda_{-12,-15}$-vacuum formations fully corresponds to the condition of vacuum balance (see the Introduction in [1], since they compensate each other's manifestations (i.e. if we add or average all the metrics (2) – (10) and (12) – (20), the result will be zero).

MATERIALS AND METHOD

1 Infinite "electron" and "positron"

The sets of metric solutions (1) and (11) are the most simplified metric-dynamic models of the "electron" and "positron". They are called valence (from the Latin valentis - strong, durable; influential, by analogy with valence quarks in nuclear physics), since the sets of metric solutions (1) and (11) determine the average stable structure of the "electron" and "positron".

Firstly, the vacuum constantly and everywhere chaotically oscillates and curves, so its structure is revealed only by averaging these fluctuations. Second, according to the fundamentals of the Algebra of signature (see §2.9 in [2] and §2.7 in [5]), any pair of metrics with mutually opposite signatures can be represented as a sum (or average) of $7 + 7 = 14$ metrics with other signatures.

For example, a mutually opposite pair of metrics $ds^{(-++-)2}$ and $ds^{(+--+)2}$ with opposite signatures $(-+++)$ and $(+---)$ can be expressed by summing (or averaging) $7 + 7 = 14$ metrics with signatures

(21)

$$
\begin{array}{rclcrcl}
(+\ +\ +\ +) & + & (-\ -\ -\ -) & =0 \\
(-\ -\ -\ +) & + & (+\ +\ +\ -) & =0 \\
(+\ -\ -\ +) & + & (-\ +\ +\ -) & =0 \\
(-\ -\ +\ -) & + & (+\ +\ -\ +) & =0 \\
(+\ +\ -\ -) & + & (-\ -\ +\ +) & =0 \\
(-\ +\ -\ -) & + & (+\ -\ +\ +) & =0 \\
\underline{(+\ -\ +\ -)} & + & \underline{(-\ +\ -\ +)} & =0 \\
(+-\ -\ -)_+ & + & (-\ +\ +\ +)_+ & =0.
\end{array}
$$

Recall that each signature corresponds to a topology of metric extension (see §4 in [2]).

For example, the mutually opposite (conjugate) pair of metrics (2) and (12)

$$
ds_1^{(+---)2} = \left(1 - \frac{r_6}{r} + \frac{r^2}{r_2^2}\right)c^2 dt^2 - \frac{dr^2}{\left(1 - \frac{r_6}{r} + \frac{r^2}{r_2^2}\right)} - r^2(d\theta^2 + \sin^2\theta\, d\phi^2) \quad \text{with signature } (+---), \tag{2'}
$$

$$
ds_1^{(-+++)2} = -\left(1 + \frac{r_6}{r} - \frac{r^2}{r_2^2}\right)c^2 dt^2 + \frac{dr^2}{-\left(1 - \frac{r_6}{r} + \frac{r^2}{r_2^2}\right)} + r^2(d\theta^2 + \sin^2\theta\, d\phi^2) \quad \text{with signature } (-+++) \tag{12'}
$$

can be represented as a sum (or average) of $7 + 7 = 14$ sub-metrics with the same components

$$
g_{00} = \left(1 - \frac{r_6}{r} + \frac{r^2}{r_2^2}\right), \quad g_{11} = \left(1 - \frac{r_6}{r} + \frac{r^2}{r_2^2}\right)^{-1}, \quad g_{22} = r^2, \quad g_{33} = r^2\sin^2\theta, \tag{22}
$$

and signatures from rankings (21):

(23)

$$
\begin{array}{lcll}
ds^{(++++)2} = & g_{00}dx_0^2 + g_{11}dx_1^2 + g_{22}dx_2^2 + g_{33}dx_3^2 & + \quad ds^{(----)2} = -g_{00}dx_0^2 - g_{11}dx_1^2 - g_{22}dx_2^2 - g_{33}dx_3^2 & = 0 \\
ds^{(---+)2} = & -g_{00}dx_0^2 - g_{11}dx_1^2 - g_{22}dx_2^2 + g_{33}dx_3^2 & + \quad ds^{(+++-)2} = g_{00}dx_0^2 + g_{11}dx_1^2 + g_{22}dx_2^2 - g_{33}dx_3^2 & = 0 \\
ds^{(+--+)2} = & g_{00}dx_0^2 - g_{11}dx_1^2 - g_{22}dx_2^2 + g_{33}dx_3^2 & + \quad ds^{(-++-)2} = -g_{00}dx_0^2 + g_{11}dx_1^2 + g_{22}dx_2^2 - g_{33}dx_3^2 & = 0 \\
ds^{(--+-)2} = & -g_{00}dx_0^2 - g_{11}dx_1^2 + g_{22}dx_2^2 - g_{33}dx_3^2 & + \quad ds^{(++-+)2} = g_{00}dx_0^2 + g_{11}dx_1^2 - g_{22}dx_2^2 + g_{33}dx_3^2 & = 0 \\
ds^{(-+--)2} = & -g_{00}dx_0^2 + g_{11}dx_1^2 - g_{22}dx_2^2 - g_{33}dx_3^2 & + \quad ds^{(+-++)2} = -g_{00}dx_1^2 + g_{11}dx_2^2 + g_{22}dx_2^2 + g_{33}dx_3^2 & = 0 \\
ds^{(+--+)2} = & g_{00}dx_0^2 - g_{11}dx_1^2 + g_{22}dx_2^2 - g_{33}dx_3^2 & + \quad ds^{(-+-+)2} = -g_{00}dx_0^2 + g_{00}dx_1^2 - g_{22}dx_2^2 + g_{33}dx_3^2 & = 0 \\
ds^{(++--)2} = & g_{00}dx_0^2 + g_{11}dx_1^2 - g_{22}dx_2^2 - g_{33}dx_3^2 & + \quad ds^{(--++)2} = -g_{00}dx_0^2 - g_{11}dx_1^2 + g_{22}dx_2^2 + g_{33}dx_3^2 & = 0 \\
\hline
ds^{(+---)2} = & g_{00}dx_0^2 - g_{11}dx_1^2 - g_{00}dx_2^2 - g_{00}dx_3^2 & + \quad ds^{(-+++)2} = -g_{00}dx_0^2 + g_{11}dx_1^2 + g_{22}dx_2^2 + g_{33}dx_3^2 & = 0
\end{array}
$$

Summation (or averaging) in rankings (23) is performed by columns and by rows (§2.9 in [2] and §2.7 in [5]).

Similarly, all other conjugate pairs of metrics (3) – (10) and (12) – (20) can be decomposed into $7 + 7 = 14$ sub-metrics.

In turn, mutually opposite pairs of sub-metrics from rankings (23) can be decomposed in exactly the same way into sums of $7 + 7 = 14$ sub-sub-metrics. This can continue ad infinitum, provided that the condition of complete "vacuum balance" is met (i.e., if the

summation of the entire infinite set of mutually exclusive metrics with different signatures is equal to zero) (see the Introduction in [1]).

Based on such decompositions of sets of metrics (1) and (11) into additive components with different signatures, one can form an idea of a seething sea of so-called colored "quarks" and "antiquarks" (see Table 1 in [5]), similar to the quark-gluon sea in nuclear physics.

Thus, the "electron" and "positron" are infinitely complex, but on average they are stable spherical vacuum formations.

That is, the "electron" is an extremely complex iridescent, but on average stable "convexity" of the outer side of the $\lambda_{-12,-15}$-vacuum (see Figure 2), and its antipode, the "positron", is an extremely complex iridescent, but on average stable "concavity" of the inner side of the $\lambda_{-12,-15}$-vacuum.

As a result of averaging the most complex fluctuations of the $\lambda_{-12,-15}$-vacuum (see the illustration in Figure 1), a stable metric-dynamic structure of the valence "electron" (1) and valence "positron" (11) emerges from chaos, which are studied below.
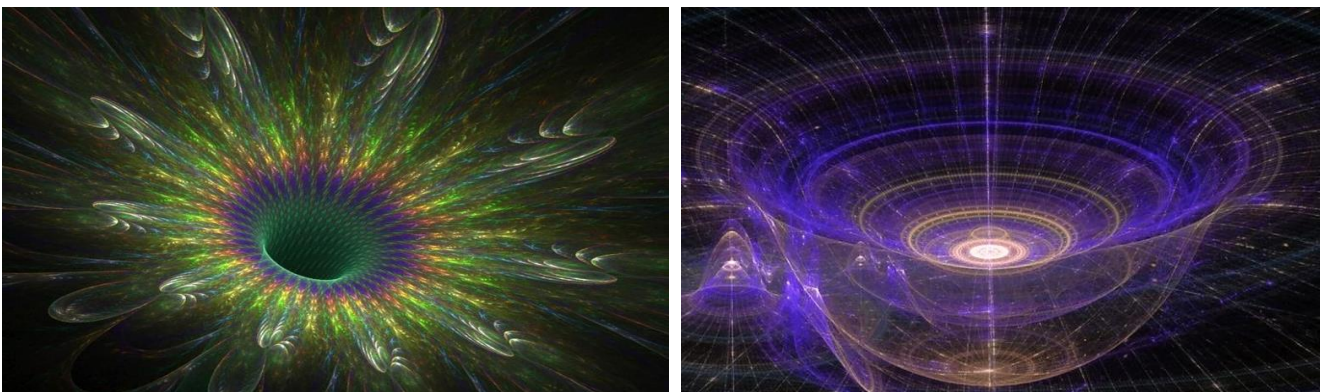
Fig. 2. Illustrations of complex iridescent but on average
stable spherical deformation of $\lambda_{-12,-15}$-vacuum

2 Free valence "electron" and "positron"

Let's consider the average structure of a free valence "electron" based on a set of metrics-solutions (1) and the methods of Geometricized Vacuum Physics and the Algebra of signature" [1,2,3,4,5,6].

The structure of a free valence "positron", and all other valence colored "quarks" from Table 1 in [6], is studied similarly.

2.1 Deformation of the outer shell and core of a free valence "electron" and "positron"

We recall that in §2.7 in [2] it was conventionally accepted that metrics with the signature $(+ - - -)$ describe the metric-dynamic state of the external side of the $\lambda_{-12,-15}$-vacuum (i.e., the subcont), and metrics with the signature $(- + + +)$ describe the metric-dynamic state of the internal side of the $\lambda_{-12,-15}$-vacuum (i.e., the antisubcont). The concepts of "subcont" (short for substantial continuum) and "antisubcont" were introduced, on the one hand, to shorten the long terms "external side of the $\lambda_{-12,-15}$-vacuum" and "internal side of the $\lambda_{-12,-15}$-vacuum", and on the other hand, to create the illusion of two conjugate continuous elastic-plastic media, for the convenience of describing and perceiving intra-vacuum processes. But let us note once again that "subcont" and "antisubcont" are not real continuous media, but auxiliary mental constructs, the same as "space" and "time" in Kant's philosophy. Let's also recall that according to §2.1 in [1], the $\lambda_{-12,-15}$-vacuum is a 3-dimensional landscape (i.e., a 3D-network) illuminated from emptiness (i.e., the Einstein vacuum) by probing it with mutually perpendicular light beams with a wavelength of $\lambda_{-12,-15}$ from the range $\Delta\lambda = 10^{-12} \div 10^{-15}$ cm.

2.1.1 Averaged deformation of the outer shell of the "electron"

Within the framework of the theory developed here, the averaged metric-dynamic model of the outer shell of a free valence "electron" is determined by the metrics-solutions (2) – (5), (10) of the second Einstein vacuum equation $R_{ik} + \Lambda g_{ik} = 0$: :

$$ds_1^{(+---)2} = \left(1 - \frac{r_6}{r} + \frac{r^2}{r_2^2}\right)c^2 dt^2 - \frac{dr^2}{\left(1 - \frac{r_6}{r} + \frac{r^2}{r_2^2}\right)} - r^2(d\theta^2 + sin^2\theta \, d\phi^2), \tag{2'}$$

$$ds_2^{(+---)2} = \left(1 + \frac{r_6}{r} - \frac{r^2}{r_2^2}\right)c^2 dt^2 - \frac{dr^2}{\left(1 + \frac{r_6}{r} - \frac{r^2}{r_2^2}\right)} - r^2(d\theta^2 + sin^2\theta \, d\phi^2), \tag{3'}$$

$$ds_3^{(+---)2} = \left(1 - \frac{r_6}{r} - \frac{r^2}{r_2^2}\right)c^2 dt^2 - \frac{dr^2}{\left(1 - \frac{r_6}{r} - \frac{r^2}{r_2^2}\right)} - r^2(d\theta^2 + sin^2\theta \, d\phi^2), \tag{4'}$$

$$ds_4^{(+---)2} = \left(1 + \frac{r_6}{r} + \frac{r^2}{r_2^2}\right)c^2 dt^2 - \frac{dr^2}{\left(1 + \frac{r_6}{r} + \frac{r^2}{r_2^2}\right)} - r^2(d\theta^2 + sin^2\theta \, d\phi^2), \tag{5'}$$

$$ds_5^{(+---)2} = c^2 dt^2 - dr^2 - r^2(d\theta^2 + sin^2\theta \, d\phi^2). \tag{10'}$$

In this section, we are interested in the neighborhood of the "electron" core in the range from $r_6 \sim 10^{-13}$ cm to $r \sim 10^{12}$ cm. In this region of the $\lambda_{-12,-15}$-vacuum, the third terms $r^2/r_2^2 \sim 10^{12}/10^{58}$ in the brackets of metrics (2) – (5) can be neglected. Therefore, as a result of averaging metrics (2´) and (4´), as well as metrics (3´) and (5´), we obtain

$$ds_1^{(+)2} = \left(1 - \frac{r_6}{r}\right)c^2 dt^2 - \frac{dr^2}{\left(1 - \frac{r_6}{r}\right)} - r^2(d\theta^2 + sin^2\theta \, d\phi^2), \tag{24}$$

$$ds_2^{(+)2} = \left(1 + \frac{r_6}{r}\right)c^2 dt^2 - \frac{dr^2}{\left(1 + \frac{r_6}{r}\right)} - r^2(d\theta^2 + sin^2\theta \, d\phi^2), \tag{25}$$

$$ds_5^{(+)2} = c^2 dt^2 - dr^2 - r^2(d\theta^2 + sin^2\theta \, d\phi^2). \tag{26}$$

Let's use a similar situation considered in §2.8 in [5].

Both metrics (24) and (25) are solutions of the same first Einstein vacuum equation $R_{ik} = 0$ under the same conditions. Therefore, we consider the result of their averaging (see §2.8 in [5])

$$ds_{12}^{(+)2} = \frac{1}{2}\left(ds_1^{(+)2} + ds_2^{(+)2}\right) = c^2dt^2 - \frac{r^2}{r^2-r_6^2}dr^2 - r^2d\theta^2 - r^2\sin^2\theta\,d\phi^2. \tag{27}$$

The relative elongation of the outer side of the $\lambda_{-12,-15}$-vacuum (i.e., the subcont) is determined by expression (47) in [3]

$$l_i^{(+)} = \sqrt{1 + \frac{g_{ii}^{(+)} - g_{ii0}^{(+)}}{g_{ii0}^{(+)}}} - 1, \tag{28}$$

where
$g_{ii}^{(+)}$ are the components of the metric tensor of the curved area of the $\lambda_{-12,-15}$-vacuum;

$g_{ii0}^{(+)}$ are the components of the metric tensor of the same area of the $\lambda_{-12,-15}$-vacuum before the curvature (i.e. in the absence of its curvature).

Let's substitute into Ex. (28) the components $g_{ii}^{(+)}$ from the averaged metric (27), and the components $g_{ii0}^{(+)}$ from the original metric (26), as a result we obtain

Fig. 3. Graph of the relative elongation function (29) $l_r^{(+)} = \frac{\Delta r}{r}$

$$l_r^{(+)} = \frac{\Delta r}{r} = \sqrt{\frac{r^2}{r^2-r_6^2}} - 1, \quad l_\theta^{(+)} = 0, \quad l_\phi^{(+)} = 0. \tag{29}$$

The graph of the radial component of the relative elongation of the subcont (29) $l_r^{(+)} = \Delta r/r$ in the outer shell of the "electron" is shown in Figure 2. At $r = r_6 \sim 10^{-13}$ cm, this function tends to infinity ($\Delta r/r = \infty$).

2.1.2 Average deformation of the "electron" core

The metric-dynamic model of the core of a free valence "electron" is determined by metrics (6) – (9) and (10)

$$ds_1^{(+)2} = -\left(1 - \frac{r_7}{r} + \frac{r^2}{r_6^2}\right)c^2dt^2 - \frac{dr^2}{-\left(1 - \frac{r_7}{r} + \frac{r^2}{r_6^2}\right)} - r^2(d\theta^2 + \sin^2\theta\,d\phi^2), \tag{30}$$

$$ds_2^{(+)2} = -\left(1 + \frac{r_7}{r} - \frac{r^2}{r_6^2}\right)c^2dt^2 - \frac{dr^2}{-\left(1 + \frac{r_7}{r} - \frac{r^2}{r_6^2}\right)} - r^2(d\theta^2 + \sin^2\theta\,d\phi^2), \tag{31}$$

$$ds_3^{(+)2} = -\left(1 - \frac{r_7}{r} - \frac{r^2}{r_6^2}\right)c^2dt^2 - \frac{dr^2}{-\left(1 - \frac{r_7}{r} - \frac{r^2}{r_6^2}\right)} - r^2(d\theta^2 + \sin^2\theta\,d\phi^2), \tag{32}$$

$$ds_4^{(+)2} = -\left(1 + \frac{r_7}{r} + \frac{r^2}{r_6^2}\right)c^2dt^2 - \frac{dr^2}{-\left(1 + \frac{r_7}{r} + \frac{r^2}{r_6^2}\right)} - r^2(d\theta^2 + \sin^2\theta\,d\phi^2), \tag{33}$$

$$ds_5^{(+)2} = c^2dt^2 - dr^2 - r^2(d\theta^2 + \sin^2\theta\,d\phi^2). \tag{34}$$

We use a similar situation considered in §4 in [5].

Let's average the metrics (30) – (33)

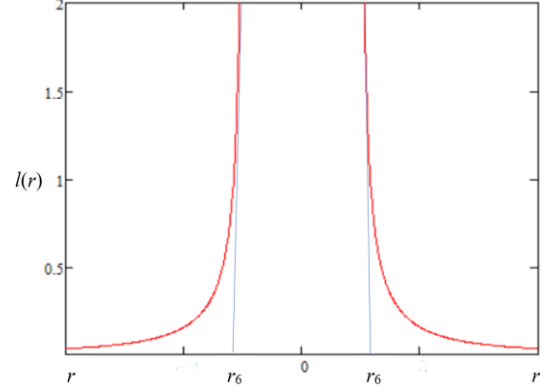$$ds_{1-4}^{(+)2} = \frac{1}{4}(ds_1^{(+)2} + ds_2^{(+)2} + ds_3^{(+)2} + ds_4^{(+)2}). \tag{35}$$

As a result, we obtain an average metric

$$ds_{1-4}^{(+)2} = c^2 dt^2 + g_{11}^{(+)}(r)dr^2 - r^2(d\theta^2 + \sin^2\theta\, d\phi^2), \tag{36}$$

where

$$g_{11}^{(+)}(r) = \frac{1}{4}\left[\frac{1}{\left(1 - \frac{r_{10}}{r} + \frac{r^2}{r_6^2}\right)} + \frac{1}{\left(1 + \frac{r_{10}}{r} - \frac{r^2}{r_6^2}\right)} + \frac{1}{\left(1 - \frac{r_{10}}{r} - \frac{r^2}{r_6^2}\right)} + \frac{1}{\left(1 + \frac{r_{10}}{r} + \frac{r^2}{r_6^2}\right)}\right]. \tag{37}$$

We substitute the components $g_{ii}^{(+)}$ (37) of the averaged metric (36) into the expressions for the relative elongation (28), where the components $g_{ii0}^{(+)}$ are taken from the uncurved metric (34).

As a result, we obtain the relative elongation of the outer side of the $\lambda_{-12,-15}$-vacuum (i.e., the subcont) inside the core of the "electron" (i.e. in the range from $r_7 \sim 10^{-24}$ cm to $r_6 \sim 10^{-13}$ cm)

$$l_r^{(+)} = \frac{\Delta r}{r} = \sqrt{g_{11}^{(+)}(r)} - 1 = \sqrt{\frac{1}{4}\left[\frac{1}{\left(1 - \frac{r_{10}}{r} + \frac{r^2}{r_6^2}\right)} + \frac{1}{\left(1 + \frac{r_{10}}{r} - \frac{r^2}{r_6^2}\right)} + \frac{1}{\left(1 - \frac{r_{10}}{r} - \frac{r^2}{r_6^2}\right)} + \frac{1}{\left(1 + \frac{r_{10}}{r} + \frac{r^2}{r_6^2}\right)}\right]} - 1, \tag{38}$$

$$l_t^{(+)} = 0, \qquad l_\theta^{(+)} = 0, \qquad l_\phi^{(+)} = 0.$$

The graph of the radial component of the relative elongation of the subcont (38) $l_r^{(+)} = \Delta r/r$ in the "electron" core is shown in Figure 4. At $r = r_6 \sim 10^{-13}$ cm, this function also tends to infinity ($\Delta r/r = \infty$).
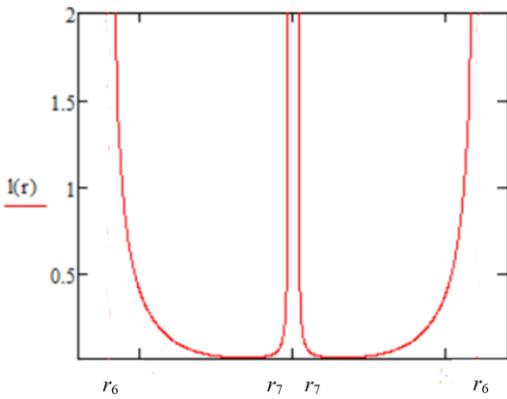
Fig. 4. Graph of the function (38) of the relative elongation $l_r^{(+)}$ of the outer side of the $\lambda_{-12,-15}$-vacuum (i.e., the subcont) inside the core of the "electron"
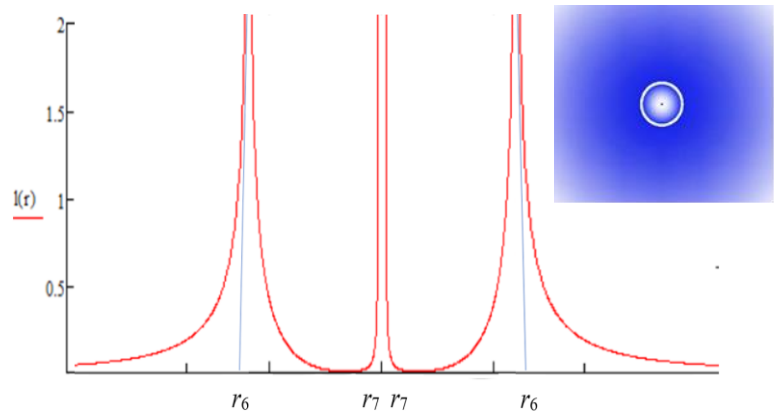
Fig. 5. Combined graphs of functions (29) and (38) of the relative elongation $l_r^{(+)}$ of the outer side of the $\lambda_{-12,-15}$-vacuum (i.e., the subcont) outside and inside the core of the "electron"

The combination of the graphs of functions (29) and (38) is shown in Figure 5. These graphs show that the outer side of the $\lambda_{-12,-15}$-vacuum (i.e., the subcont) is strongly deformed (more precisely, stretched in the radial direction to infinity) on both sides of the edge of the "electron" core with a radius of $r_6 \sim 10^{-13}$ cm. With distance from the edge of the core, the deformation of the subcont decreases. However, as we approach the center of the "electron" core, the radial stretching of the subcont increases again as we approach the inner nucleolus (i.e., the "proto-quark" core) with a radius of $r_7 \sim 10^{-24}$ cm.

9

Radial extension of the subcont to infinity seems unrealistic. However, as noted in §5.2 in [5], if in the area of raqiya (see Figure 1 and §4.11 in [6]) the subcont seems to boil (i.e. becomes more and more broken and twisted, see the illustrations in Figure 18 in [5]), then its geodesic lines can extend almost to infinity, just as the Koch curve extends to infinity as the iterations of this fractal increase (see Figure 16 in [5]). It is interesting that the Koch curve was described by the Swedish mathematician Helge von Koch, but A. Einstein's mother was also called Pauline Koch. There is another coincidence: A. Einstein's teacher of Judaism was called Heinrich Friedman, and the author of the theory of a non-stationary Universe was Alexander Friedman.

2.1.3 Average deformation of the outer shell and core of the "positron"

The deformation of the outer shell and core of the free valence "positron", the metric-dynamic model of which is determined by the set of metrics (11), completely coincide with the deformations of the "electron" with the only difference that in this case the inner side of the $\lambda_{-12,-15}$-vacuum (i.e. the antisubcont) is radially extended.

2.2 Subcont flows in the outer shell and in the core of a free valence "electron" and "positron"

As has been noted more than once in [1,2,3,4,5,6], the theory developed here has a significant conceptual difference from Einstein's general theory of relativity (GTR) in the matter of the physical interpretation of the zero components of the metric tensor $g_{00}^{(+)}$ and $g_{0i}^{(+)} = g_{i0}^{(+)}$. In GTR, the zero components affect the rate of time, while in the geometrized vacuum physics developed here, the zero components are associated with the rectilinear and rotational motion of the layers of the $\lambda_{m,n}$-vacuum (see §6 in [3] and §2.8.4 in [5]).

Apparently, both interpretations of the zero components of the metric tensor do not exclude, but complement each other. In a number of tasks it is convenient to assume that the curvature of space-time affects natural phenomena. In other tasks it is more convenient to assume that vacuum layers have elastic-plastic properties (similar to material continuous media), and the same zero components of the metric tensor are associated with the velocities and accelerations of these media.

Let's return to the study of metrics (24) and (25), which describe the metric-dynamic (MD) state of the subcont in the outer shell of the "electron" (see §§2.8.3 and 2.8.4 in [5])

$$ds_1^{(+)2} = \left(1 - \frac{r_6}{r}\right)c^2 dt^2 - \frac{dr^2}{\left(1 - \frac{r_6}{r}\right)} - r^2(d\theta^2 + \sin^2\theta\, d\phi^2) \; - \text{ MD state of the } a\text{-subcont,} \tag{24'}$$

$$ds_2^{(+)2} = \left(1 + \frac{r_6}{r}\right)c^2 dt^2 - \frac{dr^2}{\left(1 + \frac{r_6}{r}\right)} - r^2(d\theta^2 + \sin^2\theta\, d\phi^2) \; - \text{MD state of the } b\text{-subcont,} \tag{25'}$$

$$ds_5^{(+)2} = c^2 dt^2 - dr^2 - r^2(d\theta^2 + \sin^2\theta\, d\phi^2) \; - \text{MD state of the subcont before deformation.} \tag{26'}$$

In §6.2 in [3] several kinematic cases of motion of layers of two-sided $\lambda_{m,n}$-vacuum were considered. We apply this kinematic approach to the use of metrics (24) and (25).

2.2.1 Velocities of subcont currents and countercurrents in the outer shell of the "electron"

For metrics (24´) and (25´) is suitable the metric (91) in [3] with the signature $(+ - - -)$

$$ds^{(+)2} = \left(1 + \frac{v_{ra}^2}{c^2}\right)c^2 dt^2 - dr^2 - r^2 d\theta^2 - r^2 \sin^2\theta\, d\phi^2, \tag{39}$$

since in this metric, as well as in metrics (24′) and (25′), the components of the metric tensor $g_{i0}^{(+)} = g_{i0}^{(+)} = 0$.

Let's compare $g_{00}^{(+)}$ in metrics (24′) and (39), and as a result we get

$$1 - \frac{r_6}{r} = 1 + \frac{v_{ra}^2}{c^2},$$

from where we determine the components of the velocity vector of the a-subcont in the outer shell of the "electron"

$$- v_{ra}^2 = \frac{c^2 r_6}{r} \quad \text{or} \quad v_{ra} = \sqrt{-\frac{c^2 r_6}{r}} = i\sqrt{\frac{c^2 r_6}{r}} \qquad (40)$$

$$\text{or} \quad -i v_{ra} = \sqrt{\frac{c^2 r_6}{r}}, \quad v_{\theta a} = 0, \quad v_{\phi a} = 0.$$

Now let us compare $g_{00}^{(+)}$ in metrics (25′) and (39), as a result we get

$$1 + \frac{r_6}{r} = 1 + \frac{v_{rb}^2}{c^2},$$

from where we determine the components of the velocity vector of the b-subcont in the outer shell of the "electron"

$$v_{rb}^2 = \frac{c^2 r_6}{r} \quad \text{или} \quad v_{rb} = \sqrt{\frac{c^2 r_6}{r}}, \quad v_{\theta b} = 0, \quad v_{\phi b} = 0. \qquad (41)$$

Also compare $g_{00}^{(+)}$ in the original metric (26′), and in the averaged metric (36) with $g_{00}^{(+)}$ in the metric (39), and we obtain

$$1 = 1 + \frac{v_r^{(+)2}}{c^2}.$$

As a result, we obtain for the subcont velocity in the case of no deformations and in the case of averaging

$$v_r^{(+)2} = 0, \quad v_\theta^{(+)} = 0, \quad v_\phi^{(+)} = 0. \qquad (42)$$

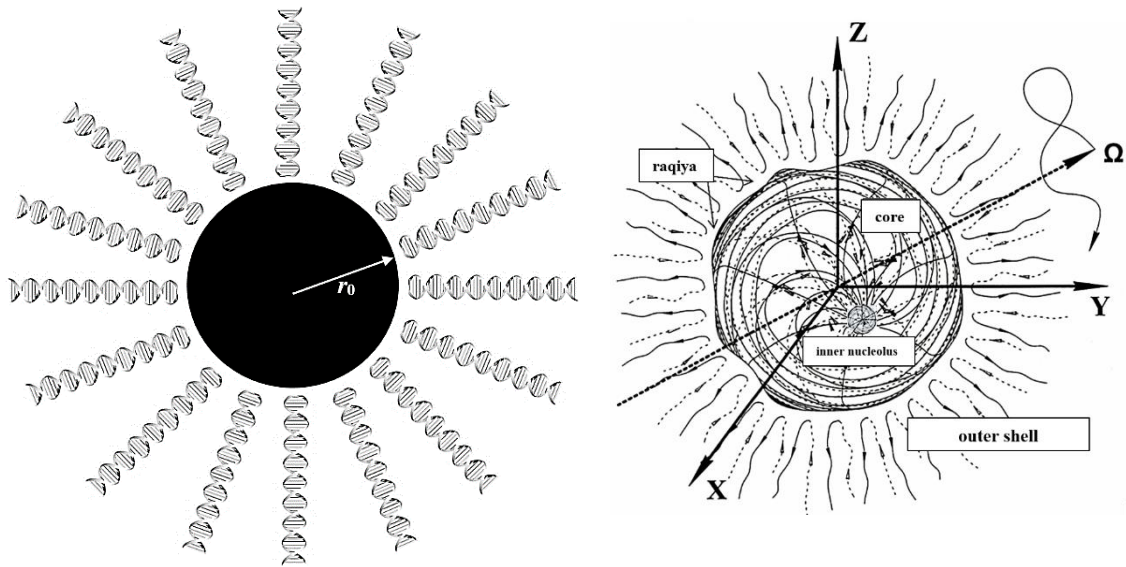According to Exs. (40), (41) and (42), in all radial directions from the core of the "electron", the average velocity of the subcont (or ab-subcont) in the outer shell of the "electron" is equal to zero everywhere

Fig. 6. An attempt to recreate a schematic picture of the inflow of a-subcont and the outflow of b-subcont to/from the "electron" *raqiya*

$$v_{rab}^{(+)2} = \frac{1}{2}(v_{rb}^2 - v_{ra}^2) = 0 \quad \text{or} \quad |v_{rab}^{(+)}| = \frac{1}{\sqrt{2}}\left|\sqrt{\frac{c^2 r_6}{r}} - i\sqrt{\frac{c^2 r_6}{r}}\right| = 0. \qquad (43)$$

This means that the a-subcont flows in the form of thin streams (currents) from all sides to the "electron" *raqiya* along a multitude of spirals, i.e., wrapping around all radial directions (see Figures 6 and 7). In this case, the a-subcont velocity gradually increases practically from zero to reaching the speed of light c at $r \approx r_6 \sim 10^{-13}$ cm. That is, in the area of the *raqiya*, the a-subcont falls with a speed close to the speed of light into the spherical abyss-crack between the outer shell and the "electron" core (see Figures 6 and 7). At the same time, the b-subcont flows away from the spherical abyss-crack in the form of thin streams (currents) in all directions along a multitude of counter-spirals (wrapping around radial directions), starting from the speed of light c at $r \approx r_6$, and gradually decreasing to zero.
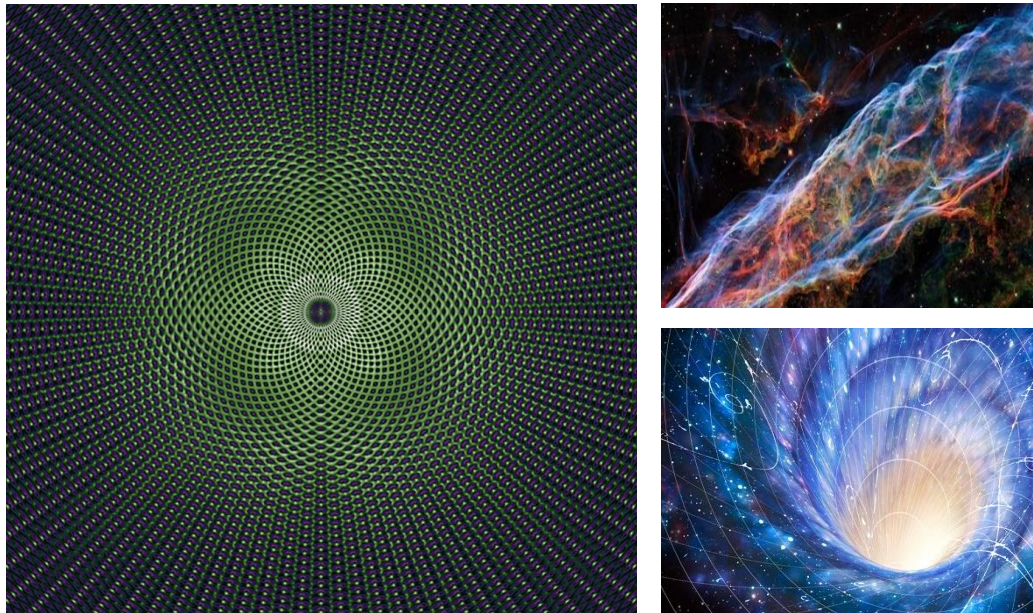
Fig. 7. Illustration of subcont currents in the outer shell of the "electron": the *a*-subcont flows in the form of thin streams (currents) along spirals twisted around all radial directions to the "electron" *raqiya* with a radius $r_0 = r_6$, gradually increasing the speed from zero to the speed of light *c*. At the same time, the *b*-subcont flows out in the form of thin streams (currents) along counter-spirals around all radial directions from the "electron" *raqiya*, starting from the speed of light and gradually decreasing to zero.

In total, the *a*-subcont and *b*-subcont currents are twisted into counter double spirals (see Figure 7), which, on average, in each local region of the outer shell of the "electron" completely compensate for each other's manifestations. That is, in each local region, a balance of subcont currents and countercurrents is maintained along the threads (lines) twisted into double spirals (see Figures 7 and 8).

Fig. 8. Illustration of the interweaving of subcont currents and countercurrents
in the vicinity of the core of a free valence "electron"

The relative radial elongation of these double helices was considered in the previous paragraph (see Figure 3). In this case, the greater the radial deformation of the subcont as it approaches the "electron" *raqiya*, the greater the speed of the subcont currents and countercurrents. It should be expected that when the speed of the radial subcont currents and countercurrents reaches a certain critical value $v_{r\ \text{кр}}^{(+)}$

$$v_{r\ cr}^{(+)} = \sqrt{\frac{c^2 r_6}{r_{cr}}},$$
(44)

their laminar flow becomes turbulent, which corresponds to an increase in the brokenness and twisting of the subcon radial lines as they approach the "electron" *raqiya*. It is possible that for the subcont currents and countercurrents it will subsequently be possible to obtain a number corresponding to the Reynolds number in hydrodynamics.

Thus, from the metric solutions (24') and (25') of the Einstein vacuum equations, the soliton character of a stable spherical vacuum formation (in particular, an "electron") was revealed. Since local radial deformations of the subcont are supported by the corresponding velocities (more precisely, accelerations, see the next paragraph) of the subcont currents and countercurrents. With an increase in the radial deformation of the subcont, the velocities and accelerations of the radial subcont currents and countercurrents also increase proportionally. When the radial lines of the subcont are in a broken and twisted state in the region of the "electron" *raqiya*, the subcont currents and countercurrents change from laminar to turbulent flow.

Comparison of the kinematic metric (39) with the metrics-solutions of the vacuum equation (24) and (25) is quite logically justified, but is of a heuristic nature. However, we will show that the relativistic method of determining the velocity leads to absurd results. In GTR, the velocity is determined by the formula [7]

$$v^{(+)} = \frac{dl}{d\tau} = \frac{\sqrt{\left(-g_{\alpha\beta}^{(+)} + \frac{g_{0\alpha}^{(+)} g_{0\beta}^{(+)}}{dg_{00}^{(+)}}\right) dx^\alpha dx^\beta}}{\sqrt{g_{00}^{(+)}}\, dt}.$$

Substituting the components $g_{\alpha\beta}^{(+)}$, $g_{0\alpha}^{(+)}$ and $g_{00}^{(+)}$ from the metric (24´) into this expression, we obtain the components of the velocity vector of the *a*-subcont

$$v_{ra}^{(+)} = \sqrt{\frac{-g_{11}^{(+a)}}{g_{00}^{(+a)}}}\frac{dr}{dt} = \frac{1}{\left(1-\frac{r_6}{r}\right)}\frac{dr}{dt} = \frac{c}{\left(1-\frac{r_6}{r}\right)}, \quad v_{\theta a}^{(+)} = 0, \quad v_{\phi a}^{(+)} = 0.$$

From these expressions it is clear that the radial component of the velocity at $r = r_6$ tends to infinity, and at large r this velocity tends to the speed of light c. Obviously, this result is absurd.

2.2.2 Acceleration of subcont currents and countercurrents in the outer shell of a free valence "electron"

In §5 in [4], Ex. (108) was written for the acceleration of the $\lambda_{m,n}$-vacuum layer in the stationary case

$$\mathbf{a} = \vec{a} = \frac{1}{\sqrt{1-\frac{v^2}{c^2}}}c^2\left\{-grad(ln\sqrt{g_{00}}) + \sqrt{g_{00}}\left[\frac{\vec{v}}{c} \times rot\vec{g}\right]\right\} = \mathbf{E}v + [\mathbf{v} \times \mathbf{B}v],$$
(45)

where $\vec{g}(g_1, g_2, g_3)$ is a 3-dimensional vector with components

$$g_1 = -\frac{g_{01}}{g_{00}}, \quad g_2 = -\frac{g_{02}}{g_{00}}, \quad g_3 = -\frac{g_{03}}{g_{00}};$$
(46)

$$\mathbf{E}_v = \vec{E}_v = -\gamma_c \; grad \; \varphi; \tag{47}$$

$$\mathbf{B}_v = \vec{B}_v = \gamma_c \sqrt{g_{00}} \; rot \frac{\vec{A}}{c}; \tag{48}$$

$\varphi = ln\sqrt{g_{00}}$ is geometrized scalar potential; $\qquad$ (49)

$\vec{A} = \vec{g}$ $\qquad$ is geometrized vector potential; $\qquad$ (50)

$\gamma_c = \dfrac{c^2}{\sqrt{1-\frac{v^2}{c^2}}},$ $\quad$ is Lorentz factor multiplied by c^2. $\qquad$ (51)

$\mathbf{E}_v$ is geometrized vector of eclectic intensity with components:

$$E_{v1} = \gamma_c \frac{\partial \, ln\sqrt{g_{00}}}{\partial x^1}, \qquad E_{v2} = \gamma_c \frac{\partial \, ln\sqrt{g_{00}}}{\partial x^2}, \qquad E_{v3} = \gamma_c \frac{\partial \, ln\sqrt{g_{00}}}{\partial x^3}. \tag{52}$$

$\mathbf{B}_v$ is geometrized magnetic induction vector with components:

$$B_{v1} = \gamma_c \sqrt{g_{00}} \left(\frac{\partial g_3}{\partial x^2} - \frac{\partial g_2}{\partial x^3} \right), \quad B_{v2} = \gamma_c \sqrt{g_{00}} \left(\frac{\partial g_1}{\partial x^3} - \frac{\partial g_3}{\partial x^1} \right), \quad B_{v3} = \gamma_c \sqrt{g_{00}} \left(\frac{\partial g_2}{\partial x^1} - \frac{\partial g_1}{\partial x^2} \right). \tag{53}$$

In metrics (24´) and (25´), describing the metric-dynamic state of the subcont in the outer shell of the "electron", all mixed zero components of the metric tensor are equal to zero ($g_{0\alpha}{}^{(+)} = g_{0\alpha}{}^{(+)} = 0$). Therefore, Eq. (45) for the acceleration of the subcont in the stationary case is simplified to a vector equation of the geometrized electric field

$$E_{v\mu}^{(+)} = a_\mu^{(+)} = -\frac{c^2}{\sqrt{1-\frac{v^{(+)2}}{c^2}}} \frac{\partial \, ln\sqrt{g_{00}^{(+)}}}{\partial x^\mu}, \quad \text{where} \; \mu = 1,2,3. \tag{54}$$

Let's substitute into Ex. (54) the zero component of the metric tensor $g_{00}^{(+)}$ from the metric (24´) and the corresponding velocity (40) $v^{(+)2} = v_{ra}^2 = -\dfrac{c^2 r_6}{r}$, as a result we obtain

$$E_{vr}^{(+a)} = a_r^{(+a)} = -\frac{c^2}{\sqrt{1+\frac{r_6}{r}}} \frac{\partial \, ln\sqrt{\left(1-\frac{r_6}{r}\right)}}{\partial r^{*a}} = -\frac{c^2 r_6}{2r^2 \sqrt{\left(1+\frac{r_6}{r}\right)}}, \qquad E_\theta^{(+a)} = 0, \qquad E_\phi^{(+a)} = 0, \tag{55}$$

where $\quad \dfrac{\partial}{\partial r^{*a}} = g^{11(+a)} \dfrac{\partial}{\partial r} = \left(1-\dfrac{r_6}{r}\right) \dfrac{\partial}{\partial r}.$

Let's substitute into Ex. (54) the zero component of the metric tensor $g_{00}^{(+)}$ from the metric (25′) and the corresponding velocity (41) $v^{(+)2} = v_{rb}^2 = \dfrac{c^2 r_6}{r}$, as a result we obtain

$$E_{vr}^{(+b)} = a_r^{(+b)} = -\frac{c^2}{\sqrt{1-\frac{r_6}{r}}} \frac{\partial \, ln\sqrt{\left(1+\frac{r_6}{r}\right)}}{\partial r^{*b}} = \frac{c^2 r_6}{2r^2 \sqrt{\left(1-\frac{r_6}{r}\right)}}, \qquad E_\theta^{(+b)} = 0, \qquad E_\phi^{(+b)} = 0, \tag{56}$$

where $\dfrac{\partial}{\partial r^{*b}} = g^{11(+b)} \dfrac{\partial}{\partial r} = \left(1+\dfrac{r_6}{r}\right) \dfrac{\partial}{\partial r}.$

As shown in the previous paragraph, the inflowing currents of the a-subcont and the outflowing currents of the b-subcont are twisted into double spirals (see Figures 7 and 9). Therefore, according to §4.4 in [4], the total radial acceleration of the subcont $a_r^{(+ab)}$ is determined by the complex Ex. (104) in [4]

$$a_r^{(+ab)} = \frac{1}{\sqrt{2}} \left(a_r^{(+b)} + i a_r^{(+a)} \right) = \frac{1}{\sqrt{2}} \left(E_{vr}^{(+b)} + i E_{vr}^{(+a)} \right), \tag{57}$$

14

more precisely, the modulus of this expression

$$(58)$$

$$a_r^{(+ab)} = E_{vr}^{(+ab)} = \frac{1}{\sqrt{2}}\sqrt{E_r^{(+a)2} + E_r^{(+b)2}} = \frac{1}{\sqrt{2}}\sqrt{\left(-\frac{c^2 r_6}{2r^2\sqrt{\left(1+\frac{r_6}{r}\right)}}\right)^2 + \left(\frac{c^2 r_6}{2r^2\sqrt{\left(1-\frac{r_6}{r}\right)}}\right)^2} = \frac{1}{\sqrt{2}}\frac{c^2 r_6}{2r^2}\sqrt{\frac{1}{\left(1+\frac{r_6}{r}\right)}+\frac{1}{\left(1-\frac{r_6}{r}\right)}} = \frac{c^2 r_6}{2r^2\sqrt{1-\frac{r_6^2}{r^2}}}.$$

b)   a)   b)
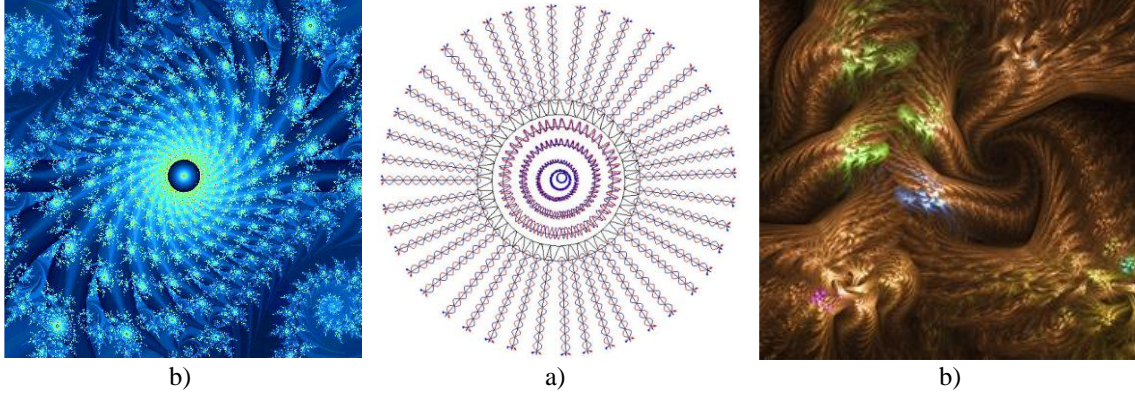
Fig. 9. a) Spirals consisting of inflowing a-subcont and outflowing b-subcont currents in the outer shell of the "electron"; b) fractal illustrations of intertwined intra-vacuum currents around a spherical object (in particular, around the core of the "electron" or the core of the "positron")

As a result, it turned out that the acceleration vector of the subcont (or the geometrized vector of the eclectic intensity of the subcont) in the outer shell of the "electron" is given by the components

$$a_r^{(+ab)} = E_{vr}^{(+ab)} = \frac{c^2 r_6}{2r^2\sqrt{1-\frac{r_6^2}{r^2}}}, \quad a_{\alpha\theta}^{(+)} = E_{v\theta}^{(+ab)} = 0, \quad a_{\alpha\phi}^{(\pm)} = E_{v\phi}^{(+ab)} = 0. \quad (59)$$

The graph of the radial component of acceleration $a_r^{(+ab)}$ is shown in Figure 10.

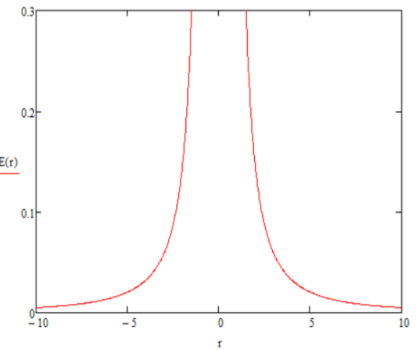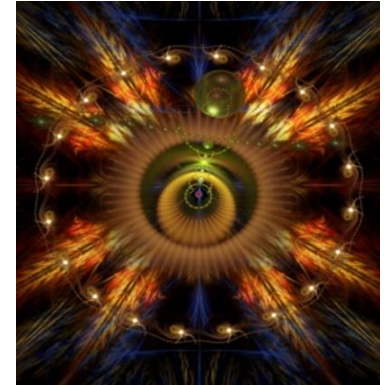From Exs. (59) it follows that at $r \gg r_6$

$$a_r^{(+ab)} = E_{vr}^{(+ab)} \approx \frac{c^2 r_6}{2r^2}, \qquad (60)$$

$$a_{\alpha\theta}^{(+)} = E_{v\theta}^{(+ab)} = 0, \quad a_{\alpha\phi}^{(+)} = E_{v\phi}^{(+ab)} = 0.$$

In classical electrostatics, the vector of the electric field strength of a point charge (in particular, an electron) in a vacuum is determined by the components:

$$E_r = \frac{e}{4\pi\varepsilon_0 r^2}, \quad E_\theta = 0, \quad E_\phi = 0, \qquad (61)$$

where $e = -1{,}60219\cdot10^{-19}$ C is the electron charge; $\varepsilon_0 = 8{,}85419\cdot10^{-12}$ F/m is the electric constant.


**Fig. 10.** Graph of function (59) $E_{vr}^{(+ab)}$

Comparing Exs. (60) and (61), we find the following correspondence between the parameters of classical electrostatics and the parameters of geometrized subcont statics (i.e., stable accelerated motion of the subcont in the outer shell of the "electron")

$$\frac{e}{4\pi\varepsilon_0} \leftrightarrow \frac{c^2 r_6}{2}. \tag{62}$$

In classical electrostatics, the heuristic concept of the "electric charge of an electron" e characterizes the intensity of its electromagnetic interaction with other particles. In the geometrized vacuum electrostatics developed here, the unclear ratio e/ε_0 is replaced by the product of clear concepts $c^2 r_6$. The speed of light c is a fundamental constant characterizing the elastic properties of a vacuum, r_6 is the radius of a *raqiya*, i.e. a spherical abyss-crack surrounding the core of a stable vacuum formation (in particular, an "electron"), see Figures 11 and 12.
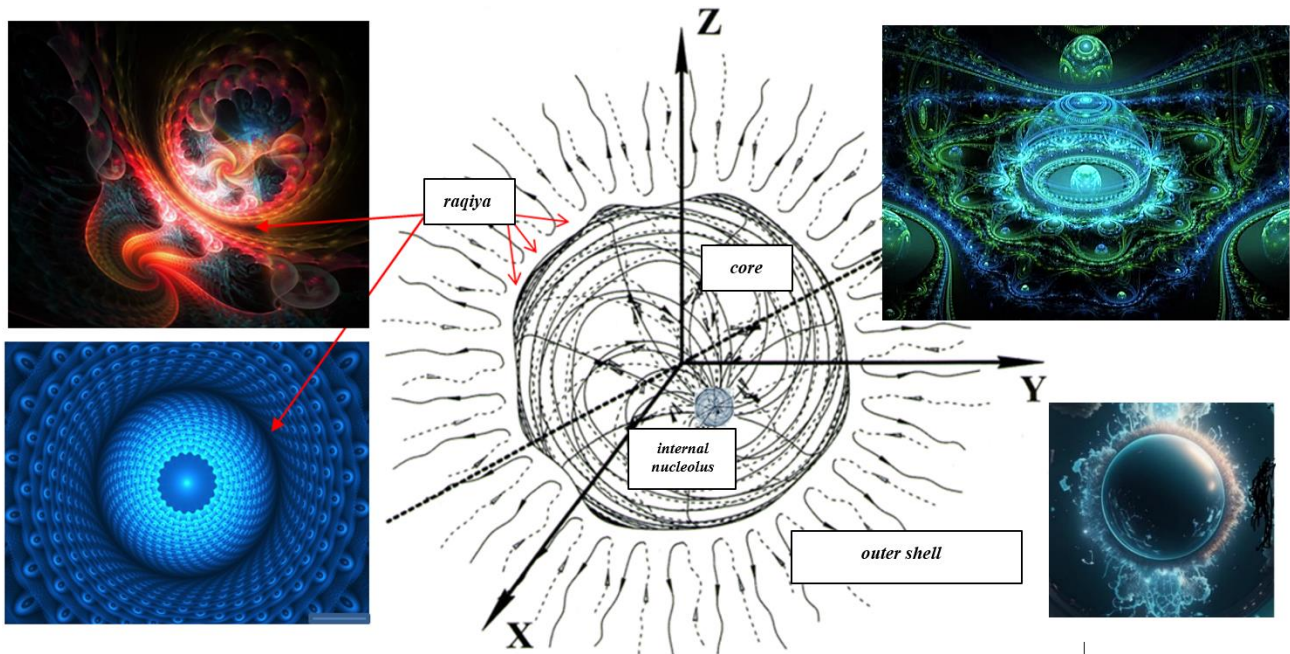
Fig. 11. The outer shell, multilayer raqiya (neck), core and inner nucleolus of a spherical vacuum formation (in particular, an "electron" or "positron") and its fractal illustrations
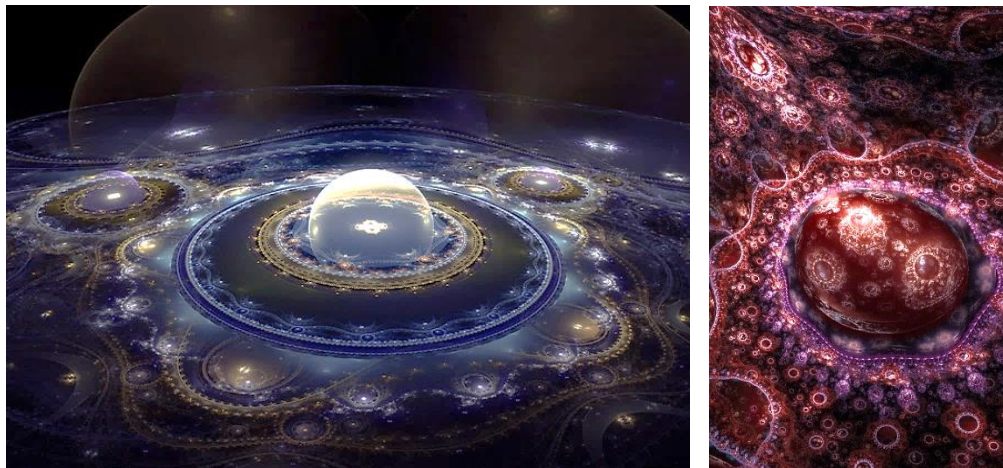
Fig. 12. Fractal illustrations of boiling subcont in the vicinity of the "electron" *raqiya* (i.e. spherical abyss-cracke)

16

In quantum electrostatics, the effect of polarization of the physical vacuum around a point charge is taken into account. The vacuum seems to boil in the environment of the electron core (see Figures 11 and 12). This allowed quantum theorists to introduce the concept of an effective electric charge

$$e_{eff} \approx \frac{e}{\sqrt{\left(1-\frac{e^2}{6\pi^2}ln\frac{\hbar}{4rm_e}\right)}}, \qquad \text{where } \hbar \text{ is the reduced Planck constant.}$$

The electric field strength around the effective charge takes the form

$$E_r \approx \frac{e}{4\pi\varepsilon_0 r^2\left(1-\frac{e^2}{6\pi^2}ln\frac{\hbar}{4rm_e}\right)^{\frac{1}{2}}}. \tag{63}$$

When comparing the radial components of the field strength vector (59) and (63), we again discover an obvious analogy

$$\frac{1}{\sqrt{\left(1-\frac{e^2}{6\pi^2}ln\frac{\hbar}{4rm_e}\right)}} \leftrightarrow \frac{1}{\sqrt{1-\frac{r_6^2}{r^2}}}. \tag{64}$$

In classical electrostatics, the potential of the electric field around a point charge e with strength (61) is determined by the expression

$$\phi_e = -\int E_r dr = -\int \frac{e}{4\pi\varepsilon_0 r^2}dr = -\frac{e}{4\pi\varepsilon_0}\int\frac{dr}{r^2} = \frac{e}{4\pi\varepsilon_0 r}, \tag{65}$$

while the potential energy contained between two spheres with radii r_1 and r_2

$$U_e = \int_0^{2\pi}\int_0^{2\pi}\int_{r_1}^{r_2}\phi_e\, drd\theta d\phi = 4\pi^2\int_{r_1}^{r_2}\frac{e}{4\pi\varepsilon_0 r}dr = \frac{\pi q_e}{\varepsilon_0}\int_{r_1}^{r_2}\frac{1}{r}dr = \frac{\pi e}{\varepsilon_0}(ln\, r_2 - ln\, r_1) = \frac{\pi e}{\varepsilon_0}ln\frac{r_2}{r_1}. \tag{66}$$

In the fully geometrized vacuum electrostatics developed here, a similar potential of the subcont field strength in the outer shell of the "electron", taking into account (59), is equal to

$$\phi_{ab}^{(+)}(r) = -\int a_{ar}^{(\pm)}dr = -\int E_{vr}^{(+ab)}dr = -\int\frac{c^2 r_6}{2r^2\sqrt{1-\frac{r_6^2}{r^2}}}dr = -\frac{c^2 r_6}{2}\int\frac{1}{r\sqrt{r^2-r_6^2}}dr = -\frac{c^2 r_6}{2}arc\, sec\frac{r}{r_6} + C, \tag{67}$$

where the table integral $\int\frac{dx}{x\sqrt{x^2-a^2}} = \frac{1}{a}arc\, sec\frac{x}{a} + C = \frac{1}{a}arccos\frac{a}{x} + C$ is used.

Thus, the fully geometrized subcont electrostatics corresponds to the experimental data and reveals the geometric nature of the electric charge of the electron.

Note that the relative elongation of the subcont (29), as well as the velocity (43) and acceleration (59) of the subcont current in the outer shell of the "electron" are determined relative to the initial substrate of the "electron" (34). A change in the substrate of the "electron" (for example, by transition to another coordinate system) can lead to instability of the vacuum formation.

2.2.3 Velocities of subcont currents and countercurrents in the core of a free valence "electron"

We compare the zero components $g_{00}^{(+)}$ in metrics (30) – (33), which define the metric-dynamic model of the "electron" core, with the zero component in the kinematic metric (39).

As a result, we obtain the velocities of four intertwined subcont currents inside the "electron" core

$$\left(1 + \frac{v_{ra}^2}{c^2}\right) = \left(1 - \frac{r_7}{r} + \frac{r^2}{r_6^2}\right) \rightarrow v_{ra}^2 = \left(\frac{r^2}{r_6^2} - \frac{r_7}{r}\right)c^2 \rightarrow v_{ra} = \sqrt{\frac{r^2 c^2}{r_6^2} - \frac{r_7 c^2}{r}} = c\sqrt{\frac{r^2}{r_6^2} - \frac{r_7}{r}} \quad \text{for } a\text{-subcont,} \tag{68}$$

$$\left(1 + \frac{v_{rb}^2}{c^2}\right) = \left(1 + \frac{r_7}{r} - \frac{r^2}{r_6^2}\right) \rightarrow v_{rb}^2 = \left(-\frac{r^2}{r_6^2} + \frac{r_7}{r}\right)c^2 \rightarrow v_{rb} = \sqrt{-\frac{r^2 c^2}{r_6^2} + \frac{r_7 c^2}{r}} = c\sqrt{\frac{r_7}{r} - \frac{r^2}{r_6^2}} \quad \text{for } b\text{-subcont,} \tag{69}$$

$$\left(1 + \frac{v_{rc}^2}{c^2}\right) = \left(1 - \frac{r_7}{r} - \frac{r^2}{r_6^2}\right) \rightarrow v_{rc}^2 = \left(-\frac{r^2}{r_6^2} - \frac{r_7}{r}\right)c^2 \rightarrow v_{rc} = \sqrt{-\frac{r^2 c^2}{r_6^2} - \frac{r_7 c^2}{r}} = ic\sqrt{\frac{r^2}{r_6^2} + \frac{r_7}{r}} \quad \text{for } c\text{-subcont,} \tag{70}$$

$$\left(1 + \frac{v_{rd}^2}{c^2}\right) = \left(1 + \frac{r_7}{r} + \frac{r^2}{r_6^2}\right) \rightarrow v_{rd}^2 = \left(\frac{r^2}{r_6^2} + \frac{r_7}{r}\right)c^2 \rightarrow v_{rd} = \sqrt{\frac{r^2 c^2}{r_6^2} + \frac{r_7 c^2}{r}} = c\sqrt{\frac{r^2}{r_6^2} + \frac{r_7}{r}}. \quad \text{for } d\text{-subcont.} \tag{71}$$

Since v_{ri} cannot exceed the speed of light, the conditions must be satisfied

$$0 \leq \frac{r^2}{r_6^2} + \frac{r_7}{r} \leq 1, \quad 0 \leq \frac{r^2}{r_6^2} - \frac{r_7}{r} \leq 1, \quad 0 \leq \frac{r_7}{r} - \frac{r^2}{r_6^2} \leq 1. \tag{72}$$

At $r \approx r_6$ (i.e. in the region of the periphery of the "electron" core) all velocities (68) – (61) tend to the speed of light c. Also at $r \approx r_7$ (i.e. in the region of the inner nucleolus, i.e. near the proto-quark core) all velocities (68) – (61) tend to the speed of light c.

Thus, at the level of consideration of the nucleus of the valence "electron" on each radial direction four intra-vacuum flows (currents) are wound.

Two of these helical flows (*b*-subcont current and *c*-subcont currents) flow away from the periphery of the core of the "electron", first at a speed close to the speed of light, then slowing down and then at the site of the inner nucleolus (i.e. near the proto-quark core) again accelerating to the speed of light.

Two other counter-rotating helical currents (the *a*-subcont current and the *d*-subcont currents) flow away from the inner nucleolus, first at a speed close to the speed of light, then slowing down, and then at the periphery of the "electron" core again accelerating to a speed close to the speed of light.

For clarity, it is convenient to assume that the *a*-subcont and *b*-subcont, as well as the counter-rotating *c*-subcont and *d*-subcont currents, flow along four sides of one twisted tetrahedron (see Figure 13).

At the same time, for an outside observer, the periphery of the "electron" core and the periphery of its inner nucleolus rotate intricately at a speed close to the speed of light.

Fig. 13. A twisted tetrahedron, along one side of which the *a*-subcont moves with acceleration, along the other side the *b*-subcont flows with acceleration, along the third and fourth sides the *c*-subcont and *d*-subcont flow towards them with acceleration.

The total velocity of each radial subcont current (i.e. a bundle twisted from 4 threads) inside the core of the "electron" is determined by the quaternion [4]

$$v_{r(abcd)} = \frac{1}{\sqrt{4}}(v_{ra} + iv_{rb} + jv_{rc} + kv_{rd}),$$

(73)

more precisely, its modulus

$$|v_{r(abcd)}| = \frac{1}{\sqrt{4}}\sqrt{v_{ra}^2 + v_{rb}^2 + v_{rc}^2 + v_{rd}^2} = \frac{c}{2}\sqrt{\left(\frac{r^2}{r_6^2} - \frac{r_7}{r}\right) + \left(-\frac{r^2}{r_6^2} + \frac{r_7}{r}\right) + \left(-\frac{r^2}{r_a^2} - \frac{r_7}{r}\right) + \left(\frac{r^2}{r_a^2} + \frac{r_7}{r}\right)} = 0.$$

(74)

That is, the intranuclear subcont currents and counter-currents on average completely compensate each other's manifestations.

To obtain the radial components of the acceleration vectors of the four sub-contact intra-nuclear currents, we sequentially substitute into expression (54).

2.2.4 Acceleration of subcontact currents and countercurrents in the nucleus of a free valence "electron"

To obtain the radial components of the acceleration vectors of the four subcont intracore currents, we sequentially substitute into expression (54)

$$E_{vr}^{(+)} = a_r^{(+)} = -\frac{c^2}{\sqrt{1 - \frac{v^{(+)2}}{c^2}}}\frac{\partial \ln\sqrt{g_{00}^{(+)}}}{\partial x^\mu} = -\frac{c^2}{\sqrt{1 - \frac{v^{(+)2}}{c^2}}}g^{11(+)}\frac{\partial \ln\sqrt{g_{00}^{(+)}}}{\partial r},$$

(54′)

the covariant and contravariant components of the metric tensor $g_{00}^{(+)}$ and $g^{11(+)}$ from metrics (30) – (33) and the corresponding velocities (68) – (71)

$$a_r^{(+a)} = c^2\sqrt{1 - \frac{r_7}{r} + \frac{r^2}{r_6^2}}\frac{\partial \ln\sqrt{1 - \frac{r_7}{r} + \frac{r^2}{r_6^2}}}{\partial r} = \frac{c^2\left(\frac{r_7}{r^2} + \frac{2r}{r_6^2}\right)}{2\sqrt{1 - \frac{r_7}{r} + \frac{r^2}{r_6^2}}} \qquad - a\text{-subcont acceleration,}$$

(75)

$$a_r^{(+b)} = c^2\sqrt{1 + \frac{r_7}{r} - \frac{r^2}{r_6^2}}\frac{\partial \ln\sqrt{1 + \frac{r_7}{r} - \frac{r^2}{r_6^2}}}{\partial r} = -\frac{c^2\left(\frac{r_7}{r^2} + \frac{2r}{r_6^2}\right)}{2\sqrt{1 + \frac{r_7}{r} - \frac{r^2}{r_6^2}}} \qquad - b\text{-subcont acceleration,}$$

(76)

$$a_r^{(+c)} = c^2\sqrt{1 - \frac{r_7}{r} - \frac{r^2}{r_6^2}}\frac{\partial \ln\sqrt{1 - \frac{r_7}{r} - \frac{r^2}{r_6^2}}}{\partial r} = \frac{c^2\left(\frac{r_7}{r^2} - \frac{2r}{r_6^2}\right)}{2\sqrt{1 - \frac{r_7}{r} - \frac{r^2}{r_6^2}}} \qquad - c\text{-subcont acceleration,}$$

(77)

$$a_r^{(+d)} = -c^2\sqrt{1 + \frac{r_7}{r} + \frac{r^2}{r_6^2}}\frac{\partial \ln\sqrt{1 + \frac{r_7}{r} + \frac{r^2}{r_6^2}}}{\partial r} = -\frac{c^2\left(\frac{r_7}{r^2} - \frac{2r}{r_6^2}\right)}{2\sqrt{1 + \frac{r_7}{r} + \frac{r^2}{r_6^2}}} \qquad - d\text{-subcont acceleration.}$$

(78)

The remaining components of the acceleration vectors of the four subcont currents are zero.

The total radial acceleration of the subcont inside the core of the "electron" is given by the averaged quaternion (§4 in [4])

$$a_{r(abcd)}^{(+)} = \frac{1}{\sqrt{4}}(a_r^{(+a)} + ia_r^{(+b)} + ja_r^{(+c)} + ka_r^{(+d)}),$$

(79)

which describes the interweaving of 4 subcont currents and countercurrents around each radial direction inside the core of the "electron" (see Figure 13).

The modulus of the averaged quaternion (79), taking into account expressions (75) – (78), is equal to

$$\left| a_{r(abcd)}^{(+)} \right| = \frac{1}{\sqrt{4}} \sqrt{ a_r^{(+a)2} + a_r^{(+b)2} + a_r^{(+c)2} + a_r^{(+d)2} } = \frac{c^2}{4} \sqrt{ \frac{\left(\frac{r_7}{r^2} + \frac{2r}{r_6^2} \right)^2}{\left(1 - \frac{r_7}{r} + \frac{r^2}{r_6^2} \right)^2} + \frac{\left(\frac{r_7}{r^2} + \frac{2r}{r_6^2} \right)^2}{\left(1 + \frac{r_7}{r} - \frac{r^2}{r_6^2} \right)^2} + \frac{\left(\frac{r_7}{r^2} - \frac{2r}{r_6^2} \right)^2}{\left(1 - \frac{r_7}{r} - \frac{r^2}{r_6^2} \right)^2} + \frac{\left(\frac{r_7}{r^2} - \frac{2r}{r_6^2} \right)^2}{\left(1 + \frac{r_7}{r} + \frac{r^2}{r_6^2} \right)^2} } . \qquad (80)$$

The graph of Function (80) is shown in Figure 14.
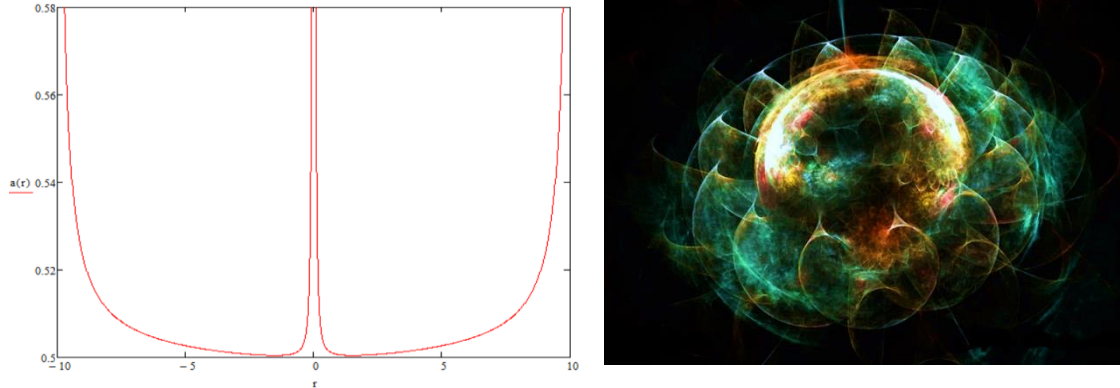
Fig. 14. Graph of Function (80) for the conventionally accepted $r_7 = 0{,}001$, $r_6 = 10$, $c = 1$.
This function determines the distribution of the spiral-radial component of the acceleration
vector of the subcont inside the core of the "electron"

From the graph in Figure 14 it is evident that the subcont has large accelerations near the periphery of the "electron" core and near the inner nucleolus (i.e. the core of the "proto-quark"). However, this is not the laminar acceleration of the subcont in the radial direction, but the averaged helical-radial acceleration of rotation of the four subcont currents along the intertwined 4-helix wound on each radial direction (see [4], Figures 13 and 15). Such an accelerated helical-rotational motion of the subcont currents and countercurrents around all radial directions creates an force that stretches the subcont, as shown in Figure 4. Moreover, the greater this helical-rotational acceleration, the greater the stretching of the subcont in the radial direction.
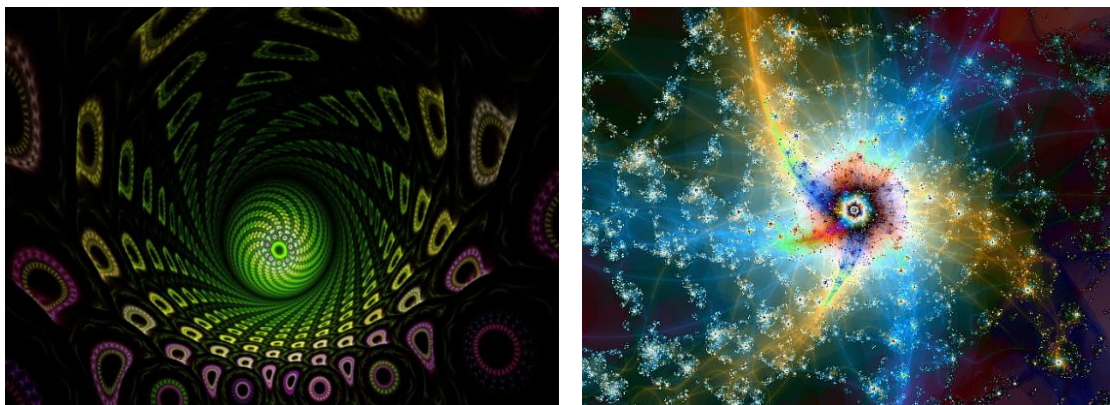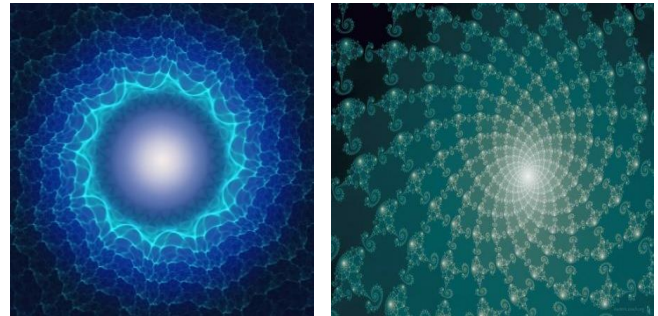
Fig. 15. Fractal illustrations of spiral-rotational and spiral-radial movements of subcont currents and countercurrents
around all radial directions both inside and outside the core of the "electron"

If we neglect the small terms r_7/r and r_7/r^2 (or when $r_7 = 0$) in Ex. (75) – (78), we obtain:

$$a_r^{(+a)} = \frac{c^2 r}{r_6^2 \sqrt{1 + \frac{r^2}{r_6^2}}} \quad – \text{ } a\text{-subcont acceleration,} \qquad a_r^{(+c)} = -\frac{c^2 r}{r_6^2 \sqrt{1 - \frac{r^2}{r_6^2}}} \quad – \text{ } c\text{-subcont acceleration,}$$

$$a_r^{(+b)} = -\frac{c^2 r}{r_6^2 \sqrt{1 - \frac{r^2}{r_6^2}}} \quad – \text{ } b\text{-subcont acceleration,} \qquad a_r^{(+d)} = \frac{c^2 r}{r_6^2 \sqrt{1 + \frac{r^2}{r_6^2}}} \quad – \text{ } d\text{-subcont acceleration.}$$

In this case, the total acceleration of the subcont in the core of the "electron" in this case is equal to

$$a_r^{(+)} = \frac{1}{\sqrt{4}} \sqrt{a_r^{(+a)2} + a_r^{(+b)2} + a_r^{(+c)2} + a_r^{(+d)2}} = \frac{c^2}{2 r_6^2} \sqrt{\frac{r^2}{1 + \frac{r^2}{r_6^2}} + \frac{r^2}{1 - \frac{r^2}{r_6^2}} + \frac{r^2}{1 - \frac{r^2}{r_6^2}} + \frac{r^2}{1 + \frac{r^2}{r_6^2}}} = \frac{c^2 \sqrt{r^2}}{r_6^2 \sqrt{1 - \frac{r^4}{r_6^4}}}. \tag{80a}$$

The graph of function (80a) is shown in Figure 16.
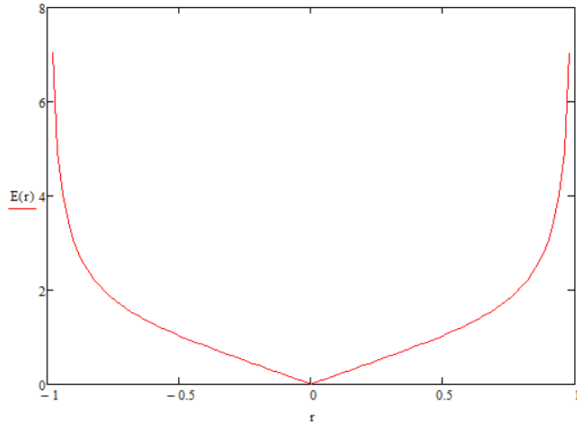
Fig. 16. Graph of the function (80a) of acceleration of the subcont (with conventionally accepted $r_6 = 1$, $c = 1$), in the case where there is no internal nucleolus inside the core of the "electron"

3 Low-intensity "electron" - "photon" interaction

Let's consider the interaction of a free valence "electron" with a "photon". A separate study is necessary for a full-fledged study of such interaction, but here we will present only the most basic aspects that concern the interaction of a stationary free valence "electron" with a "photon" whose wavelength λ is comparable to or slightly smaller than the size of the "electron" core ($r_6 \sim 10^{-13}$ cm).

The "photon" and "antiphoton" are defined in §4.8 in [6] as two mutually opposite wave disturbances of the $\lambda_{-12,-15}$-vacuum, which are described by solutions (130) and (131) in [6] of the lianized Einstein vacuum equation (127) in [6].

$$a_+ \exp\{i(\omega t - \mathbf{k} \cdot \mathbf{r})\} \quad \text{and} \quad a_- \exp -\{i(\omega t - \mathbf{k} \cdot \mathbf{r})\}, \quad \text{where } a_+ \text{ and } a_- – \text{ amplitudes of oscillations.} \tag{81}$$

We will study how these "photons" interact with the outer shell of the "electron", the metric-dynamic state of which is described by the metrics-solutions (24) and (25) with the signature $(+ - - -)$:

$$ds_1^{(+)2} = \left(1 - \frac{r_6}{r}\right) c^2 dt^2 - \frac{dr^2}{\left(1 - \frac{r_6}{r}\right)} - r^2 d\theta^2 - r^2 \sin^2 \theta \, d\phi^2 \quad – \text{ state } a\text{-subcont,} \tag{24'}$$

$$ds_2^{(+)2} = \left(1 + \frac{r_6}{r}\right) c^2 dt^2 - \frac{dr^2}{\left(1 + \frac{r_6}{r}\right)} - r^2 d\theta^2 - r^2 \sin^2 \theta \, d\phi^2 \quad – \text{ state } b\text{-subcont,} \tag{25'}$$

21

or the averaged metric (27)

$$ds_{12}^{(+)2} = \tfrac{1}{2}\left(ds_1^{(+)2} + ds_2^{(+)2}\right) = c^2dt^2 - \frac{1}{1-\frac{r_6^2}{r^2}}dr^2 - r^2d\theta^2 - r^2\sin^2\theta\,d\phi^2. \tag{27'}$$

We represent the wave solutions (81) as a two-component column matrix and its Hermitian conjugate row matrix (§11 in [2])

$$\left(\bar{a}_+^* e^{i\frac{2\pi}{\lambda}(ct-r)} \quad \bar{a}_-^* e^{-i\frac{2\pi}{\lambda}(ct-r)}\right), \quad \begin{pmatrix} \bar{a}_+ e^{-i\frac{2\pi}{\lambda}(ct-r)} \\ \bar{a}_- e^{i\frac{2\pi}{\lambda}(ct-r)} \end{pmatrix}. \tag{82}$$

In this case, the metric (27′) must be represented as a spintensor (see §10 and §11 in [2]).

Recall that the quadratic form $s^{(+\,-\,-\,-)2} = x_0^2 - x_1^2 - x_2^2 - x_3^2$ is the determinant of all the following 2×2-matrices (i.e. Hermitian spintensors) (see matrices (64) in [2]):

$$\begin{pmatrix} x_0+x_3 & x_1+ix_2 \\ x_1-ix_2 & x_0-x_3 \end{pmatrix} \begin{pmatrix} x_0-x_3 & x_1-ix_2 \\ x_1+ix_2 & x_0+x_3 \end{pmatrix} \begin{pmatrix} x_0+x_3 & x_1-ix_2 \\ x_1+ix_2 & x_0-x_3 \end{pmatrix} \begin{pmatrix} x_0-x_3 & x_1+ix_2 \\ x_1-ix_2 & x_0+x_3 \end{pmatrix} \begin{pmatrix} ix_1-x_2 & -x_0+x_3 \\ x_0+x_3 & ix_1+x_2 \end{pmatrix}$$

$$\begin{pmatrix} x_0+x_1 & x_3+ix_2 \\ x_3-ix_2 & x_0-x_1 \end{pmatrix} \begin{pmatrix} x_0-x_1 & x_3-ix_2 \\ x_3+ix_2 & x_0+x_1 \end{pmatrix} \begin{pmatrix} x_0+x_1 & x_3-ix_2 \\ x_3+ix_2 & x_0-x_1 \end{pmatrix} \begin{pmatrix} x_0-x_1 & x_3+ix_2 \\ x_3-ix_2 & x_0+x_1 \end{pmatrix} \begin{pmatrix} ix_2-x_1 & -x_0+x_3 \\ x_0+x_3 & ix_2+x_1 \end{pmatrix}$$

$$\begin{pmatrix} x_0+x_2 & x_1+ix_3 \\ x_1-ix_3 & x_0-x_2 \end{pmatrix} \begin{pmatrix} x_0-x_2 & x_1-ix_3 \\ x_1+ix_3 & x_0+x_2 \end{pmatrix} \begin{pmatrix} x_0+x_2 & x_1-ix_3 \\ x_1+ix_3 & x_0-x_2 \end{pmatrix} \begin{pmatrix} x_0-x_2 & x_1+ix_3 \\ x_1-ix_3 & x_0+x_2 \end{pmatrix} \begin{pmatrix} ix_1-x_3 & -x_0+x_2 \\ x_0+x_2 & ix_1+x_3 \end{pmatrix}$$

$$\begin{pmatrix} x_0+x_3 & x_2+ix_1 \\ x_2-ix_1 & x_0-x_3 \end{pmatrix} \begin{pmatrix} x_0-x_3 & x_2-ix_1 \\ x_2+ix_1 & x_0+x_3 \end{pmatrix} \begin{pmatrix} x_0+x_3 & x_2-ix_1 \\ x_2+ix_1 & x_0-x_3 \end{pmatrix} \begin{pmatrix} x_0-x_3 & x_2+ix_1 \\ x_2-ix_1 & x_0+x_3 \end{pmatrix} \begin{pmatrix} ix_3-x_2 & -x_0+x_1 \\ x_0+x_1 & ix_3+x_2 \end{pmatrix}$$

$$\begin{pmatrix} x_0+x_1 & x_2+ix_3 \\ x_2-ix_3 & x_0-x_1 \end{pmatrix} \begin{pmatrix} x_0-x_1 & x_2-ix_3 \\ x_2+ix_3 & x_0+x_1 \end{pmatrix} \begin{pmatrix} x_0+x_1 & x_2-ix_3 \\ x_2+ix_3 & x_0-x_1 \end{pmatrix} \begin{pmatrix} x_0-x_1 & x_2+ix_3 \\ x_2-ix_3 & x_0+x_1 \end{pmatrix} \begin{pmatrix} ix_2-x_3 & -x_0+x_1 \\ x_0+x_1 & ix_2+x_3 \end{pmatrix}$$

$$\begin{pmatrix} x_0+x_2 & x_3+ix_1 \\ x_3-ix_1 & x_0-x_2 \end{pmatrix} \begin{pmatrix} x_0-x_2 & x_3-ix_1 \\ x_3+ix_1 & x_0+x_2 \end{pmatrix} \begin{pmatrix} x_0+x_2 & x_3-ix_1 \\ x_3+ix_1 & x_0-x_2 \end{pmatrix} \begin{pmatrix} x_0-x_2 & x_3+ix_1 \\ x_3-ix_1 & x_0+x_2 \end{pmatrix} \begin{pmatrix} ix_3-x_1 & -x_0+x_2 \\ x_0+x_2 & ix_3+x_1 \end{pmatrix}$$

$$\begin{pmatrix} ix_2-x_1 & -x_0+x_3 \\ x_0+x_3 & ix_2+x_1 \end{pmatrix} \begin{pmatrix} ix_2-x_1 & x_0+x_3 \\ -x_0+x_3 & ix_2+x_1 \end{pmatrix} \begin{pmatrix} ix_1-x_3 & x_0+x_2 \\ -x_0+x_2 & ix_1+x_3 \end{pmatrix} \begin{pmatrix} ix_2-x_3 & x_0+x_1 \\ -x_0+x_1 & ix_2+x_3 \end{pmatrix} \begin{pmatrix} ix_3-x_1 & x_0+x_2 \\ -x_0+x_2 & ix_3+x_1 \end{pmatrix}$$

For example, we write one of the variants of the spintensor representation of the metric (27′)

$$\begin{pmatrix} cdt + \dfrac{1}{\sqrt{1-\frac{r_6^2}{r^2}}}dr & r\sin\theta d\phi + ird\theta \\[3em] r\sin\theta d\phi - ird\theta & cdt - \dfrac{1}{\sqrt{1-\frac{r_6^2}{r^2}}}dr \end{pmatrix}. \tag{84}$$

To shorten the notation, we get rid of the differentials and represent the matrix (84) as a sum of matrices

$$\begin{pmatrix} 1+\dfrac{1}{\sqrt{1-\frac{r_6^2}{r^2}}} & r\sin\theta+ir \\ \\ r\sin\theta-ir & 1-\dfrac{1}{\sqrt{1-\frac{r_6^2}{r^2}}} \end{pmatrix} = \begin{pmatrix} 1 & 0 \\ 0 & 1 \end{pmatrix} + \begin{pmatrix} \dfrac{1}{\sqrt{1-\frac{r_6^2}{r^2}}} & 0 \\ \\ 0 & -\dfrac{1}{\sqrt{1-\frac{r_6^2}{r^2}}} \end{pmatrix} + \begin{pmatrix} 0 & r\sin\theta \\ r\sin\theta & 0 \end{pmatrix} + \begin{pmatrix} 0 & ir \\ -ir & 0 \end{pmatrix},$$

By analogy with example 2 in §11 in [2], we leave in this matrix only the spatial components

$$\begin{pmatrix} \dfrac{1}{\sqrt{1-\frac{r_6^2}{r^2}}} & r\sin\theta+ir \\ \\ r\sin\theta-ir & -\dfrac{1}{\sqrt{1-\frac{r_6^2}{r^2}}} \end{pmatrix} = \begin{pmatrix} \dfrac{1}{\sqrt{1-\frac{r_6^2}{r^2}}} & 0 \\ \\ 0 & -\dfrac{1}{\sqrt{1-\frac{r_6^2}{r^2}}} \end{pmatrix} + \begin{pmatrix} 0 & r\sin\theta \\ r\sin\theta & 0 \end{pmatrix} + \begin{pmatrix} 0 & ir \\ -ir & 0 \end{pmatrix}, \tag{85}$$

As shown in §2.11 in [2], the projections of the spin of the wave perturbation $\lambda_{12,-15}$-vacuum on the coordinate axis for the case when the metric 3-space has the signature $(+---)$ can be defined using the spintensor (77) in [2]

$$\tag{86}$$

$$(s_1^*, s_2^*)\begin{pmatrix} x_1 & x_3+ix_2 \\ x_3-ix_2 & -x_2 \end{pmatrix}\begin{pmatrix} s_1 \\ s_2 \end{pmatrix} =$$

$$= -x_1(s_1^*, s_2^*)\begin{pmatrix} 0 & -1 \\ -1 & 0 \end{pmatrix}\begin{pmatrix} s_1 \\ s_2 \end{pmatrix} - x_2(s_1^*, s_2^*)\begin{pmatrix} 0 & -i \\ i & 0 \end{pmatrix}\begin{pmatrix} s_1 \\ s_2 \end{pmatrix} - x_3(s_1^*, s_2^*)\begin{pmatrix} -1 & 0 \\ 0 & 1 \end{pmatrix}\begin{pmatrix} s_1 \\ s_2 \end{pmatrix} =$$

$$= -(-s_2^*s_1 - s_2^*s_1)x_1 - (is_2^*s_1 - is_1^*s_2)x_2 - (-s_1^*s_1 + s_2^*s_2)x_3.$$

Using matrices (82) and (85), we write the following expression

$$\begin{pmatrix} \bar{a}_+^* e^{i\frac{2\pi}{\lambda}(ct-r)} & \bar{a}_-^* e^{-i\frac{2\pi}{\lambda}(ct-r)} \end{pmatrix} \begin{pmatrix} \dfrac{1}{\sqrt{1-\frac{r_6^2}{r^2}}} & r\sin\theta+ir \\ \\ r\sin\theta-ir & -\dfrac{1}{\sqrt{1-\frac{r_6^2}{r^2}}} \end{pmatrix} \begin{pmatrix} \bar{a}_+ e^{-i\frac{2\pi}{\lambda}(ct-r)} \\ \bar{a}_- e^{i\frac{2\pi}{\lambda}(ct-r)} \end{pmatrix}, \tag{87}$$

Similarly to (86), we obtain the projections of the spin vector **s** of the considered wave vacuum disturbance on the axes $r,\ \theta,\ \varphi$ using the sum of matrices (85)

$$\langle s_r \rangle = \begin{pmatrix} \bar{a}_+^* e^{i\frac{2\pi}{\lambda}(ct-r)} & \bar{a}_-^* e^{-i\frac{2\pi}{\lambda}(ct-r)} \end{pmatrix} \begin{pmatrix} \dfrac{1}{\sqrt{1-\frac{r_6^2}{r^2}}} & 0 \\ \\ 0 & -\dfrac{1}{\sqrt{1-\frac{r_6^2}{r^2}}} \end{pmatrix} \begin{pmatrix} \bar{a}_+ e^{-i\frac{2\pi}{\lambda}(ct-r)} \\ \bar{a}_- e^{i\frac{2\pi}{\lambda}(ct-r)} \end{pmatrix} = \dfrac{1}{\sqrt{1-\frac{r_6^2}{r^2}}}(\bar{a}_-^*\bar{a}_+ - \bar{a}_+^*\bar{a}_-), \tag{88}$$

$$\langle s_\theta \rangle = \begin{pmatrix} \bar{a}_+^* e^{i\frac{2\pi}{\lambda}(ct-r)} & \bar{a}_-^* e^{-i\frac{2\pi}{\lambda}(ct-r)} \end{pmatrix} \begin{pmatrix} 0 & ir \\ -ir & 0 \end{pmatrix} \begin{pmatrix} \bar{a}_+ e^{-i\frac{2\pi}{\lambda}(ct-r)} \\ \bar{a}_- e^{i\frac{2\pi}{\lambda}(ct-r)} \end{pmatrix} = ir\left[\bar{a}_+^*\bar{a}_- e^{i\frac{4\pi}{\lambda}(ct-r)} - \bar{a}_-^*\bar{a}_+ e^{-i\frac{4\pi}{\lambda}(ct-r)}\right],$$

$$\langle s_\phi \rangle = \begin{pmatrix} \bar{a}_+^* e^{i\frac{2\pi}{\lambda}(ct-r)} & \bar{a}_-^* e^{-i\frac{2\pi}{\lambda}(ct-r)} \end{pmatrix} \begin{pmatrix} 0 & r\sin\theta \\ r\sin\theta & 0 \end{pmatrix} \begin{pmatrix} \bar{a}_+ e^{-i\frac{2\pi}{\lambda}(ct-r)} \\ \bar{a}_- e^{i\frac{2\pi}{\lambda}(ct-r)} \end{pmatrix} = r\sin\theta\left[\bar{a}_+^*\bar{a}_- e^{i\frac{4\pi}{\lambda}(ct-r)} + \bar{a}_-^*\bar{a}_+ e^{-i\frac{4\pi}{\lambda}(ct-r)}\right],$$

23

The initial phases of the conjugate pair of oscillations (82) are taken into account by the complexity of the amplitudes a+ and a−. Therefore, without loss of generality, we can set $\varphi_+ = \varphi_- = 0$, i.e. consider a+ and a− as real numbers. In this case, Ex. (86) take the form:

$$\langle s_r \rangle = \frac{1}{\sqrt{1-\frac{r_6^2}{r^2}}}(a_- a_+ - a_- a_+) = 0, \tag{89}$$

$$\langle s_\theta \rangle = ir\left[a_+ a_- e^{i\frac{4\pi}{\lambda}(ct-r)} - a_- a_+ e^{-i\frac{4\pi}{\lambda}(ct-r)}\right],$$

$$\langle s_\phi \rangle = r\sin\theta\left[a_- a_+ e^{i\frac{4\pi}{\lambda}(ct-r)} + a_- a_+ e^{-i\frac{4\pi}{\lambda}(ct-r)}\right].$$

When the amplitudes of the forward and backward waves are equal, $a_+ = a_- = a/4\pi r^2$, and also taking into account the formulas

$$\cos x = \frac{e^{ix}+e^{-ix}}{2}, \qquad \sin x = \frac{e^{ix}-e^{-ix}}{2i} \tag{90}$$

expressions (89) are simplified

$$\langle s_r \rangle = 0, \tag{91}$$

$$\langle s_\theta \rangle = -\frac{a^2}{8\pi^2 r^3}\sin\left[\frac{4\pi}{\lambda}(ct-r)\right] = -\frac{a^2}{8\pi^2 r^3}\sin\left[\frac{4\pi}{\lambda}(t\omega - kr)\right],$$

$$\langle s_\phi \rangle = \frac{a^2}{8\pi^2 r^3}\sin\theta\cos\left[\frac{4\pi}{\lambda}(ct-r)\right] = \frac{a^2}{8\pi^2 r^3}\sin\theta\cos[2(t\omega - kr)].$$

It turns out that the spin vector of the wave vacuum disturbance ("photon") rotates in a plane perpendicular to the direction of its propagation, and the magnitude of this vector decreases with increasing distance r from the center of the core of the "electron". Thus, the end of the spin vector describes a spiral that converges as it approaches the core of the "electron".

However, we have considered only one of the possible options. As an example, let's consider another option, when the metric (27′) is represented as a determinant of the matrix

$$\begin{pmatrix} cdt + r\sin\theta\, d\phi & \frac{1}{\sqrt{1-\frac{r_6^2}{r^2}}}dr + ird\theta \\ \frac{1}{\sqrt{1-\frac{r_6^2}{r^2}}}dr - ird\theta & cdt - r\sin\theta d\phi \end{pmatrix}. \tag{92}$$

Performing operations similar to (84) – (84), we obtain

$$\langle s_r \rangle = \left(\bar{a}_+^* e^{i\frac{2\pi}{\lambda}(ct-r)} \quad \bar{a}_-^* e^{-i\frac{2\pi}{\lambda}(ct-r)}\right)\begin{pmatrix} 0 & \frac{1}{\sqrt{1-\frac{r_6^2}{r^2}}} \\ \frac{1}{\sqrt{1-\frac{r_6^2}{r^2}}} & 0 \end{pmatrix}\begin{pmatrix} \bar{a}_+ e^{-i\frac{2\pi}{\lambda}(ct-r)} \\ \bar{a}_- e^{i\frac{2\pi}{\lambda}(ct-r)} \end{pmatrix} = \frac{1}{\sqrt{1-\frac{r_6}{r}}}\left(\bar{a}_-^*\bar{a}_+ e^{-i\frac{4\pi}{\lambda}(ct-r)} + \bar{a}_+^*\bar{a}_- e^{i\frac{4\pi}{\lambda}(ct-r)}\right),$$

$$\langle s_\theta \rangle = \left(\bar{a}_+^* e^{i\frac{2\pi}{\lambda}(ct-r)} \quad \bar{a}_-^* e^{-i\frac{2\pi}{\lambda}(ct-r)}\right)\begin{pmatrix} 0 & ir \\ -ir & 0 \end{pmatrix}\begin{pmatrix} \bar{a}_+ e^{-i\frac{2\pi}{\lambda}(ct-r)} \\ \bar{a}_- e^{i\frac{2\pi}{\lambda}(ct-r)} \end{pmatrix} = ir\left[\bar{a}_+^*\bar{a}_- e^{i\frac{4\pi}{\lambda}(ct-r)} - \bar{a}_-^*\bar{a}_+ e^{-i\frac{4\pi}{\lambda}(ct-r)}\right], \tag{93}$$

$$\langle s_\phi \rangle = \left(\bar{a}_+^* e^{i\frac{2\pi}{\lambda}(ct-r)} \quad \bar{a}_-^* e^{-i\frac{2\pi}{\lambda}(ct-r)}\right)\begin{pmatrix} r\sin\theta & 0 \\ 0 & -r\sin\theta \end{pmatrix}\begin{pmatrix} \bar{a}_+ e^{-i\frac{2\pi}{\lambda}(ct-r)} \\ \bar{a}_- e^{i\frac{2\pi}{\lambda}(ct-r)} \end{pmatrix} = r\sin\theta(\bar{a}_+^*\bar{a}_+ - \bar{a}_-^*\bar{a}_-).$$

With similar simplifications we obtain the components of the spin vector of the "photon" in this case

$$\langle s_r \rangle = \frac{a^2}{8\pi^2 r^4} \frac{1}{\sqrt{1 - \frac{r_6^2}{r^2}}} \cos[2(t\omega - kr)], \tag{94}$$

$$\langle s_\theta \rangle = -\frac{a^2}{8\pi^2 r^3} \sin\left[\frac{4\pi}{\lambda}(ct - r)\right],$$

$$\langle s_\phi \rangle = 0.$$

In order to fully describe the low-intensity interaction of a "photon" with the outer shell of a resting free valence "electron", it is necessary to consider all possible ways of representing the quadratic form (27′) as determinants of 2×2-matrices (i.e., Hermitian spin tensors) of type (83) and find the components of the "photon" spin vector for each of these cases. Then it is necessary to average the results obtained.

4 Isospin of the core of a free valence "electron"

We note once again that a quadratic form with any of the possible signatures from the ranks (21), presented in diagonal form, can be written in many ways as a determinant of a second-rank spin tensor, for example

$$\tag{95}$$

$$ds^{(+)2} = g_{00}dx^0 dx^0 - g_{11}x^1 dx^1 - g_{22}x^{22} dx^{22} - g_{33}x^3 dx^3 = \begin{pmatrix} y_0 dx^0 + y_3 dx^3 & y_1 dx^1 + iy_2 dx^2 \\ y_1 dx^1 - iy_2 dx^2 & y_0 dx^0 - y_3 dx^3 \end{pmatrix}_{det}$$

where $y_i = \sqrt{g_{ii}}$.

This matrix can be represented as an A4 matrix

$$A_4^{(+)} = \begin{pmatrix} y_0 dx^0 + y_3 dx^3 & y_1 dx^1 + iy_2 dx^2 \\ y_1 dx^1 - iy_2 dx^2 & y_0 dx^0 - y_3 dx^3 \end{pmatrix} = y_0 dx^0 \begin{pmatrix} 1 & 0 \\ 0 & 1 \end{pmatrix} - y_1 dx^1 \begin{pmatrix} 0 & -1 \\ -1 & 0 \end{pmatrix} - y_2 dx^2 \begin{pmatrix} 0 & -i \\ i & 0 \end{pmatrix} - y_3 dx^3 \begin{pmatrix} -1 & 0 \\ 0 & 1 \end{pmatrix}, \tag{96}$$

where $\sigma_0^{(+)} = \begin{pmatrix} 1 & 0 \\ 0 & 1 \end{pmatrix}, \quad \sigma_1^{(+)} = \begin{pmatrix} 0 & -1 \\ -1 & 0 \end{pmatrix}, \quad \sigma_2^{(+)} = \begin{pmatrix} 0 & -i \\ i & 0 \end{pmatrix}, \quad \sigma_3^{(+---)} = \begin{pmatrix} -1 & 0 \\ 0 & 1 \end{pmatrix}$ \hfill (97)

is a set of Pauli matrices.

Similarly, for a diagonalized quadratic form with the opposite signature $(- + + +)$ we have one of the options for its representation as an A4 matrix:

$$\tag{98}$$

$$ds^{(+)2} = -g_{00}dx^0 dx^0 + g_{11}dx^1 dx^1 + g_{22}dx^2 dx^0 + g_{33}dx^0 dx^0 = \begin{pmatrix} y_0 dx^0 + y_3 dx^3 & iy_1 dx^1 + y_2 dx^2 \\ iy_1 dx^1 - y_2 dx^2 & -y_0 dx^0 + y_3 dx^3 \end{pmatrix}_{det}$$

$$A_4^{(-)} = \begin{pmatrix} y_0 dx^0 + y_3 dx^3 & iy_1 dx^1 + y_2 dx^2 \\ iy_1 dx^1 - y_2 dx^2 & -y_0 dx^0 + y_3 dx^3 \end{pmatrix} = -y_0 dx^0 \begin{pmatrix} -1 & 0 \\ 0 & 1 \end{pmatrix} + y_1 dx^1 \begin{pmatrix} 0 & i \\ i & 0 \end{pmatrix} + y_2 dx^2 \begin{pmatrix} 0 & 1 \\ -1 & 0 \end{pmatrix} + y_3 dx^3 \begin{pmatrix} 1 & 0 \\ 0 & 1 \end{pmatrix},$$

$$\tag{99}$$

where $\sigma_0^{(+)} = \begin{pmatrix} -1 & 0 \\ 0 & 1 \end{pmatrix}, \quad \sigma_1^{(+)} = \begin{pmatrix} 0 & i \\ i & 0 \end{pmatrix}, \quad \sigma_2^{(+)} = \begin{pmatrix} 0 & 1 \\ -1 & 0 \end{pmatrix}, \quad \sigma_3^{(+)} = \begin{pmatrix} 1 & 0 \\ 0 & 1 \end{pmatrix}$ \hfill (100)

is a set of Cayley matrices.

Let's assume that all elements of length dx^i are equal to one ($dx^i =1$), then the A4 matrices (96) and (99) take the form

$$A_4^{(+)} = \begin{pmatrix} y_0 + y_3 & y_1 + iy_2 \\ y_1 - iy_2 & y_0 - y_3 \end{pmatrix} = \begin{pmatrix} y_0 & 0 \\ 0 & y_0 \end{pmatrix} - \begin{pmatrix} 0 & -y_1 \\ -y_1 & 0 \end{pmatrix} - \begin{pmatrix} 0 & -iy_2 \\ iy_2 & 0 \end{pmatrix} - \begin{pmatrix} -y_3 & 0 \\ 0 & y_3 \end{pmatrix},$$

(101)

$$A_4^{(-)} = \begin{pmatrix} y_0 + y_3 & iy_1 + y_2 \\ iy_1 - y_2 & -y_0 + y_3 \end{pmatrix} = -\begin{pmatrix} -y_0 & 0 \\ 0 & y_0 \end{pmatrix} + \begin{pmatrix} 0 & iy_1 \\ iy_1 & 0 \end{pmatrix} + \begin{pmatrix} 0 & y_2 \\ -y_2 & 0 \end{pmatrix} + \begin{pmatrix} y_3 & 0 \\ 0 & y_3 \end{pmatrix}.$$

As an example, we imagine the metric (6)

$$ds_1^{(+a)2} = \left(1 + \frac{r_7}{r} - \frac{r^2}{r_6^2}\right)c^2 dt^2 - \frac{dr^2}{\left(1 + \frac{r_7}{r} - \frac{r^2}{r_6^2}\right)} - r^2(d\theta^2 + \sin^2\theta\, d\phi^2),$$

(102)

determining the metric-dynamic state of the a-subcont in the core of the "electron", in the form of a spin-tensor determinant

$$\begin{pmatrix} \sqrt{1 + \frac{r_7}{r} - \frac{r^2}{r_6^2}}\, cdt - r\sin\theta\, d\phi & -\frac{1}{\sqrt{1 + \frac{r_7}{r} - \frac{r^2}{r_6^2}}}\, dr - ird\theta \\ \\ -\frac{1}{\sqrt{1 + \frac{r_7}{r} - \frac{r^2}{r_6^2}}}\, dr + ird\theta & \sqrt{1 + \frac{r_7}{r} - \frac{r^2}{r_6^2}}\, cdt + r\sin\theta\, d\phi \end{pmatrix}_{det}$$

(103)

We write this spin tensor taking into account $dx^i = 1$

$$\begin{pmatrix} \sqrt{1 + \frac{r_7}{r} - \frac{r^2}{r_6^2}} - r\sin\theta & -\frac{1}{\sqrt{1 + \frac{r_7}{r} - \frac{r^2}{r_6^2}}} - ir \\ \\ -\frac{1}{\sqrt{1 + \frac{r_7}{r} - \frac{r^2}{r_6^2}}} + ir & \sqrt{1 + \frac{r_7}{r} - \frac{r^2}{r_6^2}} + r\sin\theta \end{pmatrix}.$$

(104)

Note also that any binary event with probability of outcome ½ (e.g., a ball spinning clockwise or counterclockwise; a coin landing on heads or tails) can be described by spinors. For example, clockwise rotation is formally given by spinors (i.e., bra- and ket-vectors)

$$|Z+\rangle = \sqrt{\frac{1}{2}}\begin{pmatrix} 1 \\ 0 \end{pmatrix} \quad \text{and} \quad |Z+\rangle^* = \langle Z+| = \sqrt{\frac{1}{2}}(1\ 0),$$

(105)

such that $\langle Z+|Z+\rangle = \frac{1}{2}(1\ 0)\begin{pmatrix} 1 \\ 0 \end{pmatrix} = \frac{1}{2}.$

In this case, counterclockwise rotation is formally given by spinors

$$|Z-\rangle = \sqrt{\frac{1}{2}}\begin{pmatrix} 0 \\ 1 \end{pmatrix} \quad \text{and} \quad |Z-\rangle^* = \langle Z-| = \sqrt{\frac{1}{2}}(0\ 1),$$

(106)

such that $\langle Z-|Z-\rangle = \frac{1}{2}(0\ 1)\begin{pmatrix} 0 \\ 1 \end{pmatrix} = \frac{1}{2},\quad \langle Z-|Z+\rangle = \frac{1}{2}(0\ 1)\begin{pmatrix} 1 \\ 0 \end{pmatrix} = 0.$

Inside the core of the valence "electron" there are four layers (6) – (9), therefore, to study their isotopic rotation (isospin), we will use the following spinors

$$|Z +\rangle = \sqrt{\tfrac{1}{4}}\binom{1}{0} \quad \text{and} \quad |Z +\rangle^* = \langle Z +| = \sqrt{\tfrac{1}{4}}(1\ 0), \tag{107}$$

$$|Z -\rangle = \sqrt{\tfrac{1}{4}}\binom{0}{1} \quad \text{and} \quad |Z -\rangle^* = \langle Z -| = \sqrt{\tfrac{1}{4}}(0\ 1). \tag{108}$$

Using the spintensor (104) and spinors (107), we determine the 4-vector of isospin of the α-subcont

$$\langle s^{(+a)}\rangle = \sqrt{\tfrac{1}{4}}(1\ 0)\begin{pmatrix} \sqrt{1+\frac{r_7}{r}-\frac{r^2}{r_6^2}} - r\sin\theta & -\frac{1}{\sqrt{1+\frac{r_7}{r}-\frac{r^2}{r_6^2}}} - ir \\ -\frac{1}{\sqrt{1+\frac{r_7}{r}-\frac{r^2}{r_6^2}}} + ir & \sqrt{1+\frac{r_7}{r}-\frac{r^2}{r_6^2}} + r\sin\theta \end{pmatrix}\sqrt{\tfrac{1}{4}}\binom{1}{0} = \tag{109}$$

$$= \tfrac{1}{4}(1\ 0)\begin{pmatrix} \sqrt{1+\frac{r_7}{r}-\frac{r^2}{r_6^2}} & 0 \\ 0 & \sqrt{1+\frac{r_7}{r}-\frac{r^2}{r_6^2}} \end{pmatrix}\binom{1}{0} + \tfrac{1}{4}(1\ 0)\begin{pmatrix} 0 & -\frac{1}{\sqrt{1+\frac{r_7}{r}-\frac{r^2}{r_6^2}}} \\ -\frac{1}{\sqrt{1-\frac{r_7}{r}+\frac{r^2}{r_6^2}}} & 0 \end{pmatrix}\binom{1}{0} + \tfrac{1}{4}(1\ 0)\begin{pmatrix} 0 & -ir \\ ir & 0 \end{pmatrix}\binom{1}{0} +$$

$$+ \tfrac{1}{4}(1\ 0)\begin{pmatrix} -r\sin\theta & 0 \\ 0 & r\sin\theta \end{pmatrix}\binom{1}{0}$$

with components

$$s_t^{(+a)} = \tfrac{1}{4}(1\ 0)\begin{pmatrix} \sqrt{1+\frac{r_7}{r}-\frac{r^2}{r_6^2}} & 0 \\ 0 & \sqrt{1+\frac{r_7}{r}-\frac{r^2}{r_6^2}} \end{pmatrix}\binom{1}{0} = \tfrac{1}{4}\sqrt{1+\frac{r_7}{r}-\frac{r^2}{r_6^2}}, \tag{110}$$

$$s_r^{(+a)} = \tfrac{1}{4}(1\ 0)\begin{pmatrix} 0 & -\frac{1}{\sqrt{1+\frac{r_7}{r}-\frac{r^2}{r_6^2}}} \\ -\frac{1}{\sqrt{1+\frac{r_7}{r}-\frac{r^2}{r_6^2}}} & 0 \end{pmatrix}\binom{1}{0} = 0,$$

$$s_\theta^{(+a)} = \tfrac{1}{4}(1\ 0)\begin{pmatrix} 0 & -ir \\ ir & 0 \end{pmatrix}\binom{1}{0} = 0,$$

$$s_\phi^{(+a)} = \tfrac{1}{4}(1\ 0)\begin{pmatrix} -r\sin\theta & 0 \\ 0 & r\sin\theta \end{pmatrix}\binom{1}{0} = -\tfrac{1}{4}r\sin\theta.$$

Similarly, the 4-vectors of isospin are defined:

- b-subcont [for metric (7)]

$$s_t^{(+b)} = \tfrac{1}{4}\sqrt{1-\frac{r_7}{r}+\frac{r^2}{r_6^2}}, \quad s_r^{(+b)} = 0, \quad s_\theta^{(+b)} = 0, \quad s_\phi^{(+b)} = -\tfrac{1}{4}r\sin\theta.$$

27

- *c*-subcont [for metric (8)]

$$s_t^{(+c)} = \frac{1}{4}\sqrt{1 + \frac{r_7}{r} + \frac{r^2}{r_6^2}}, \quad s_r^{(+c)} = 0, \quad s_\theta^{(+c)} = 0, \quad s_\phi^{(+c)} = -\frac{1}{4}r\sin\theta,$$

- *d*-subcont [for metric (9)]

$$s_t^{(+b)} = \frac{1}{4}\sqrt{1 - \frac{r_7}{r} - \frac{r^2}{r_6^2}}, \quad s_r^{(+d)} = 0, \quad s_\theta^{(+d)} = 0, \quad s_\phi^{(+d)} = -\frac{1}{4}r\sin\theta.$$

The components of the general isospin vector of the subcont in the core of the "electron" are equal to

(111)

$$s_t^{(+)} = \frac{1}{4}\sqrt{s_t^{(+a)2} + s_t^{(+b)2} + s_t^{(+c)2} + s_t^{(+d)2}} = \frac{1}{4}\sqrt{\left(1 + \frac{r_7}{r} - \frac{r^2}{r_6^2}\right) + \left(1 - \frac{r_7}{r} + \frac{r^2}{r_6^2}\right) + \left(1 + \frac{r_7}{r} + \frac{r^2}{r_6^2}\right) + \left(1 - \frac{r_7}{r} - \frac{r^2}{r_6^2}\right)} = \frac{\sqrt{4}}{4} = \frac{1}{2},$$

$$s_r^{(+)} = 0, \quad s_\theta^{(+)} = 0, \quad s_\phi^{(+)} = \sqrt{s_\phi^{(+a)2} + s_\phi^{(+b)2} + s_\phi^{(+c)2} + s_\phi^{(+d)2}} = \frac{1}{4}\sqrt{4r^2\sin^2\theta} = \frac{1}{2}r\sin\theta.$$

Another type of isotopic rotation is possible, which is formally given by complex spinors

$$|Y+\rangle = \sqrt{\frac{1}{4}}\begin{pmatrix}i\\0\end{pmatrix} \quad \text{and} \quad |Y+\rangle^* = \langle Y+| = \sqrt{\frac{1}{4}}(i\ 0), \tag{112}$$

$$|Y-\rangle = \sqrt{\frac{1}{4}}\begin{pmatrix}0\\i\end{pmatrix} \quad \text{and} \quad |Y-\rangle^* = \langle Y-| = \sqrt{\frac{1}{4}}(0\ i) \tag{113}$$

such that $\langle Y+|Y+\rangle = \frac{1}{4}(i\ 0)\begin{pmatrix}i\\0\end{pmatrix} = -\frac{1}{4}, \quad \langle Y-|Y-\rangle = \frac{1}{4}(0\ i)\begin{pmatrix}0\\i\end{pmatrix} = -\frac{1}{4}.$

In this case, with a similar use of the spin tensor (104), the components of the general 4-vector of the isospin of the subcont in the core of the "electron" are equal to

$$s_t^{(+)} = -\frac{1}{2}, \quad s_r^{(+)} = 0, \quad s_\theta^{(+)} = 0, \quad s_\phi^{(+)} = \frac{1}{2}r\sin\theta. \tag{114}$$

Results (111) and (114) turned out to be analogous to the spin quantum number of classical quantum mechanics s = ±½. However, this is only the beginning of the study of the isospin properties of the diagonal quadratic form of type (6) or (102).

Within the framework of the Algebra of signature, the metric (102) can be represented as the sum of seven sub-metrics from the left rank in Ex. (23) with signatures from the left rank (21):

$$ds^{(+)2} = \left(1 + \frac{r_7}{r} - \frac{r^2}{r_6^2}\right)c^2dt^2 + \frac{dr^2}{\left(1 + \frac{r_7}{r} - \frac{r^2}{r_6^2}\right)} + r^2d\theta^2 + r^2\sin^2\theta\,d\phi^2 - \qquad - a_1\text{- subcont, } (+\ +\ +\ +) \tag{115}$$

$$-\left(1 + \frac{r_7}{r} - \frac{r^2}{r_6^2}\right)c^2dt^2 - \frac{dr^2}{\left(1 + \frac{r_7}{r} - \frac{r^2}{r_6^2}\right)} - r^2d\theta^2 + r^2\sin^2\theta\,d\phi^2 + \qquad - a_2\text{-subcont } (-\ -\ -\ +) \tag{116}$$

$$+\left(1 + \frac{r_7}{r} - \frac{r^2}{r_6^2}\right)c^2dt^2 - \frac{dr^2}{\left(1 + \frac{r_7}{r} - \frac{r^2}{r_6^2}\right)} - r^2d\theta^2 + r^2\sin^2\theta\,d\phi^2 - \qquad - a_3\text{-subcont, } (+\ -\ -\ +) \tag{117}$$

$$-\left(1 + \frac{r_7}{r} - \frac{r^2}{r_6^2}\right)c^2dt^2 - \frac{dr^2}{\left(1 + \frac{r_7}{r} - \frac{r^2}{r_6^2}\right)} + r^2d\theta^2 - r^2\sin^2\theta\,d\phi^2 + \qquad - a_4\text{-subcont, } (-\ -\ +\ -) \tag{118}$$

28

$$+\left(1+\frac{r_7}{r}-\frac{r^2}{r_6^2}\right)c^2dt^2+\frac{dr^2}{\left(1+\frac{r_7}{r}-\frac{r^2}{r_6^2}\right)}-r^2d\theta^2-r^2\sin^2\theta\,d\phi^2- \qquad -a_5\text{-subcont, }(+\ +\ -\ -) \qquad (119)$$

$$-\left(1+\frac{r_7}{r}-\frac{r^2}{r_6^2}\right)c^2dt^2+\frac{dr^2}{\left(1+\frac{r_7}{r}-\frac{r^2}{r_6^2}\right)}-r^2d\theta^2-r^2\sin^2\theta\,d\phi^2+ \qquad -a_6\text{-subcont, }(-\ +\ -\ -) \qquad (120)$$

$$+\left(1+\frac{r_7}{r}-\frac{r^2}{r_6^2}\right)c^2dt^2-\frac{dr^2}{\left(1+\frac{r_7}{r}-\frac{r^2}{r_6^2}\right)}+r^2d\theta^2-r^2\sin^2\theta\,d\phi^2. \qquad -a_7\text{-subcont, }(+\ -\ +\ -) \qquad (121)$$

Let us consider only one of the seven terms of this expression, for example, (118) with the signature $(-\,-\,+\,-)$ (the remaining terms of this expression are described similarly).

As already noted above, the sub-metric (118) (of the form $s^{(--+-)2}=-y_0^2-y_1^2+y_2^2-y_3^2$) can be represented as the determinant of one of the $A_4^{k(--+-)}$-matrices:

$$\begin{pmatrix}-y_0+iy_3 & y_1+y_2\\-y_1+y_2 & y_0+iy_3\end{pmatrix}\begin{pmatrix}y_0+iy_3 & y_1+y_2\\-y_1+y_2 & -y_0+iy_3\end{pmatrix}\begin{pmatrix}-y_0+iy_3 & -y_1+y_2\\y_1+y_2 & y_0+iy_3\end{pmatrix}\begin{pmatrix}y_0+iy_3 & -y_1+y_2\\y_1+y_2 & -y_0+iy_3\end{pmatrix} \qquad (122)$$

$$\begin{pmatrix}y_1+y_2 & -y_0+iy_3\\y_0+iy_3 & -y_1+y_2\end{pmatrix}\begin{pmatrix}y_1+y_2 & y_0+iy_3\\-y_0+iy_3 & -y_1+y_2\end{pmatrix}\begin{pmatrix}-y_1+y_2 & -y_0+iy_3\\y_0+iy_3 & y_1+y_2\end{pmatrix}\begin{pmatrix}-y_1+y_2 & y_0+iy_3\\-y_0+iy_3 & y_1+y_2\end{pmatrix}$$

$$\begin{pmatrix}-y_0+iy_1 & y_3+y_2\\-y_3+y_2 & y_0+iy_1\end{pmatrix}\begin{pmatrix}y_0+iy_1 & y_3+y_2\\-y_3+y_2 & -y_0+iy_1\end{pmatrix}\begin{pmatrix}-y_0+iy_1 & -y_3+y_2\\y_3+y_2 & y_0+iy_1\end{pmatrix}\begin{pmatrix}y_0+iy_1 & -y_3+y_2\\y_3+y_2 & -y_0+iy_1\end{pmatrix}$$

$$\begin{pmatrix}y_3+y_2 & -y_0+iy_1\\y_0+iy_1 & -y_3+y_2\end{pmatrix}\begin{pmatrix}y_3+y_2 & y_0+iy_1\\-y_0+iy_1 & -y_3+y_2\end{pmatrix}\begin{pmatrix}-y_3+y_2 & -y_0+iy_1\\y_0+iy_1 & y_3+y_2\end{pmatrix}\begin{pmatrix}-y_3+y_2 & y_0+iy_1\\-y_0+iy_1 & y_3+y_2\end{pmatrix}$$

$$\cdots\quad\cdots\quad\cdots\quad\cdots$$

$$\begin{pmatrix}y_0+y_2 & -y_1+iy_3\\y_1+iy_3 & -y_0+y_2\end{pmatrix}\begin{pmatrix}y_0+y_2 & y_1+iy_3\\-y_1+iy_3 & -y_0+y_2\end{pmatrix}\begin{pmatrix}-y_0+y_2 & -y_1+iy_3\\y_1+iy_3 & y_0+y_2\end{pmatrix}\begin{pmatrix}-y_0+y_2 & y_1+iy_3\\-y_1+iy_3 & y_0+y_2\end{pmatrix}$$

где $y_0=\sqrt{\left(1+\frac{r_7}{r}-\frac{r^2}{r_6^2}\right)}\,cdt,\quad y_1=\dfrac{dr}{\sqrt{\left(1+\frac{r_7}{r}-\frac{r^2}{r_6^2}\right)}},\quad y_2=rd\theta,\quad y_3=r\sin\theta\,d\phi.$

If we assume that each of the $A_4^{k(--+-)}$-matrices (122) is realized with some probability $c_k^2(t)$ (which can change with time t), then the average $A_4^{k(--+-)}$-matrix can be represented as

$$A_4^{(--+-)}=c_1^2(t)A_4^{1(--+-)}+c_2^2(t)A_4^{2(--+-)}+c_3^2(t)A_4^{3(--+-)}+\ldots+c_n^2(t)A_4^{n(--+-)} \qquad (123)$$

or $\quad A_4^{(--+-)}=\sum_{k=1}^{n}c_k^2(t)A_4^{k(--+-)},\quad$ where $\quad\sum_{i=1}^{n}c_i^2(t)=1.$ $\qquad (124)$

In the simplest case, when all $c_k^2=1/n$, Ex. (124) takes the form

$$A_4^{(--+-)}=\frac{1}{n}\sum_{i=1}^{n}A_4^{i(--+-)}. \qquad (125)$$

Some characteristics of the random processes under consideration can be obtained on the basis of spin-tensor analysis

$$s_4^{(--+-)} = \langle\psi_1|A_4^{1(--+-)}|\psi_1\rangle + \langle\psi_2|A_4^{2(--+-)}|\psi_2\rangle + \langle\psi_3|A_4^{3(--+-)}|\psi_3\rangle + \ldots + \langle\psi_m|A_4^{n(--+-)}|\psi_m\rangle, \tag{126}$$

where the "bra" and "ket" vectors have the form

$$\langle\psi_k| = (\bar{c}_k(t), 0) = \bar{c}_k(t)(1\ \ 0) \qquad |\psi_i\rangle = \begin{pmatrix} c_k(t) \\ 0 \end{pmatrix} = c_k(t)\begin{pmatrix} 1 \\ 0 \end{pmatrix}, \tag{127}$$

and / or

$$\langle\psi_i| = (i\bar{c}_k(t), 0) = \bar{c}_k(t)(i\ \ 0) \qquad |\psi_i\rangle = \begin{pmatrix} ic_k(t) \\ 0 \end{pmatrix} = c_k(t)\begin{pmatrix} i \\ 0 \end{pmatrix}, \tag{128}$$

where $c_k(t)$ and $\bar{c}_k(t)$ are complex conjugate probability amplitudes.

The chaotic fluctuations of all sub-layers (115) – (121) and layers (6) – (9) of the subcont inside the core of the "electron" can be described similarly.

A separate study, which is beyond the scope of this paper, should be devoted to the probabilistic description of intra-vacuum fluctuations. However, we note that all metrics and linear forms with which the Signature Algebra operates in this study are only the result of averaging extremely complex and intricate distortions of the $\lambda_{-12,-15}$-vacuum layers, sub-layers and sub-sub-layers … and interweaving of subcont currents (see Figures 1 and 15).

5 Infinite "electron" (continued)

In the previous paragraphs, the free valence "electron" was investigated as a result of elastic-plastic deformation of the outer side of the $\lambda_{-12,-15}$-vacuum. It was already noted that the valence "electron" is a kind of initial skeleton of this, on average, stable spherical vacuum formation.

Each solution metric (2) – (10) can be represented as a sum of seven similar sub-metrics with signatures from the left-hand side of the ranking expression (21) or (23). Each sub-metric can also be represented as a sum of seven similar sub-sub-metrics and this can continue ad infinitum.

In §2.8.3 in [5], each metric with the corresponding signature was conditionally assigned a color. The additive superposition of metrics with different signatures essentially means that their geodesic lines (i.e. color currents) are intertwined into bundles. The color dynamics of intertwined vacuum layers was described in the papers [4, 5].

Therefore, upon closer examination, the illusory (mathematical) fabric of stable $\lambda_{m,n}$-vacuum formations does not look as simplified as shown in Figures 7 and 14, but as shown in Figure 17.
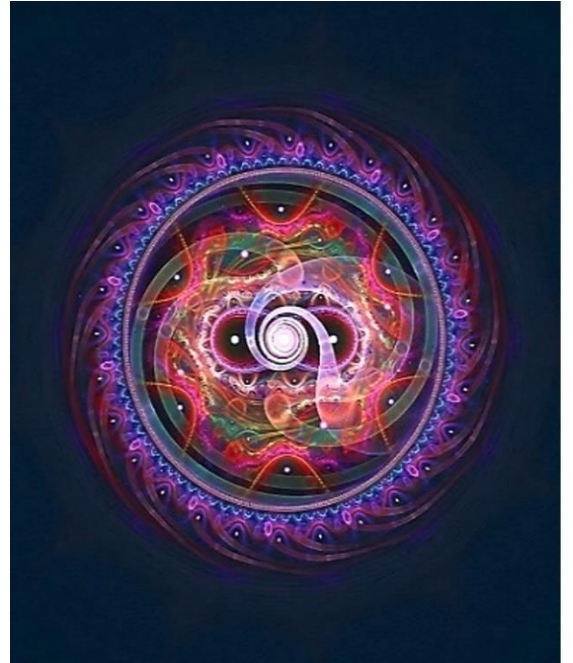
Fig. 17. Illustration of the interweaving of colored intra-vacuum currents. A similar illusion is created in the mind by the mathematical apparatus of the Algebra of signatures

In the theory developed here, the "electron" is infinite, but this infinity is discrete and self-similar (i.e. all layers of the $\lambda_{m,n}$-vacuum are similar to each other), therefore they are accessible for the deepest study by the mathematical methods of the Algebra of Signatures [1,2,3,4,5,6].

Note that, in turn, the geometrized mathematical apparatus of the Algebra of Signatures is based on the Algorithms for revealing the Great and Terrible Name of the GOD Yud-Key-Vav-Key (TETRAGRAMATON) [8].

6 The raqiya of a free valence "electron" 2

The *raqiya* of "electron" is a complex curved region of $\lambda_{-12,-15}$-vacuum adjacent to the abyss-crack surrounding its core (see Figures 1, 11, 12 and 18). The space of an average stable spherical vacuum formation (in particular, the "electron") is formed under the influence of two main factors.

First, the $\lambda_{-12,-15}$-vacuum in the region of the "electron" space is stretched so much that its radial elongation to infinity occurs due to an increase in the brokenness and twisting of the radial lines (see §1.2.2 and §5.2 in [5]). In this case, in the region of the "electron" space, the radial subcont currents change from laminar to turbulent flow (see Figure 18).
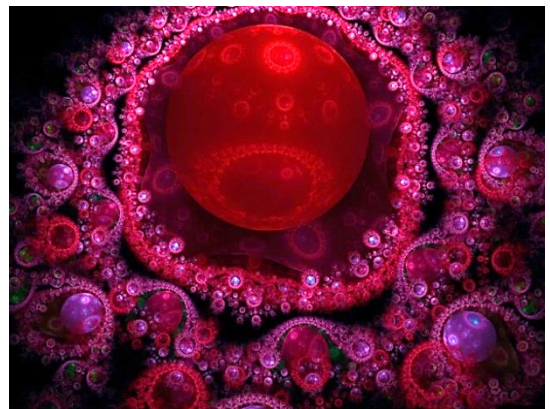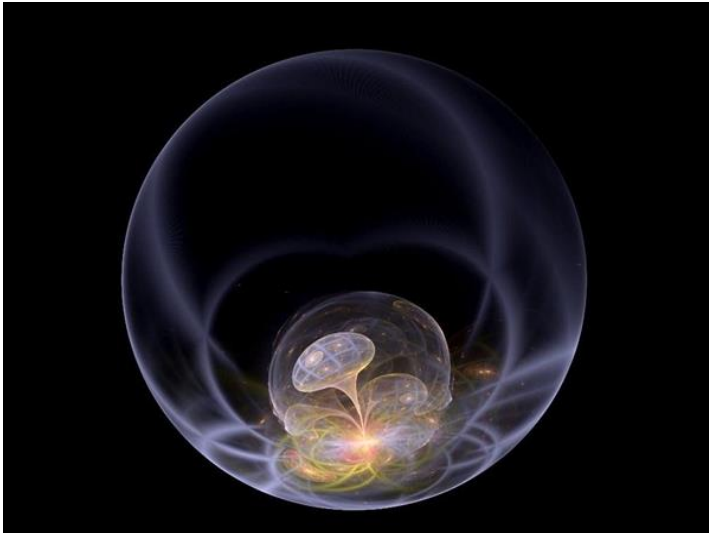
Fig. 18. Fractal illustrations of raqiya (i.e. multilayered and strongly curved area of $\lambda_{-12,-15}$-vacuum) surrounding the core of an average spherical stable vacuum formation (in particular, the "electron").

For example, humanity is one of the intelligent layers (noosphere) of raqiya of the "planet" Earth

Secondly, the *raqiya* of the "electron" is perceived as a multilayer and multilevel spherical abyss-crack (i.e. a spherical rupture of the $\lambda_{-12,-15}$-vacuum) between the "electron" core and its outer shell (Figure 11).

In §4.11 in [6] it is shown that in the *raqiya* of "electron" there are 24 spherical layers (among them 12 outer layers and 12 inner layers), which are connected with all spherical formations inside of which the "electron" core is located, in this case with the "Universe" with a radius of $r_2 \sim 10^{29}$ cm, and with all spherical formations that are inside the "electron" core, in this case with the proto-quark with a radius of $r_7 \sim 10^{-24}$ cm.

Today, the radius of the observable "Universe" is a very large value ($r_2 \sim 10^{29}$ cm), therefore in §1.1 we neglected the terms r^2/r_2^2 in the metrics (2) – (10). However, if we adhere to the opinion of cosmologists that the Universe is gradually expanding, then it is possible that the radius of the "Universe" was small. In this case, a spherical layer associated with the young "Universe" should have been noticeably manifested in the "electron's" *raqiya*. This could affect the properties of the "electron". That is, it is necessary to keep in mind that the "electron" could change during the evolution of the "Universe".

7 Rotation of the nucleus of a free valence "electron"

The core of any vacuum formation, including the core of an "electron", rotates relative to an outside observer (i.e., an observer located on the side of its outer shell), see Figure 19. At the same time, for an observer located inside the rotating core, this rotation may be practically unnoticeable.
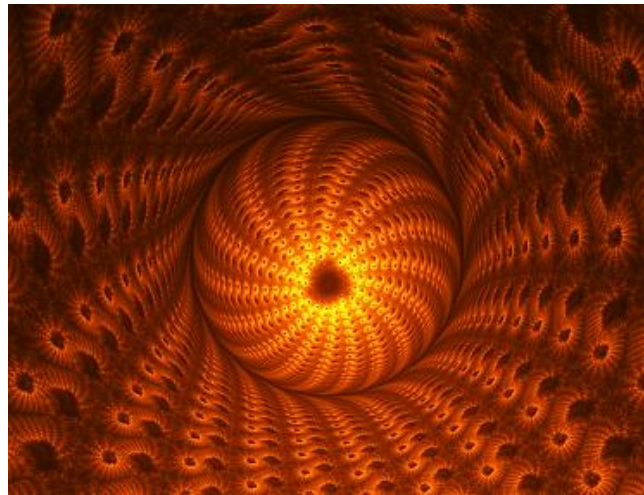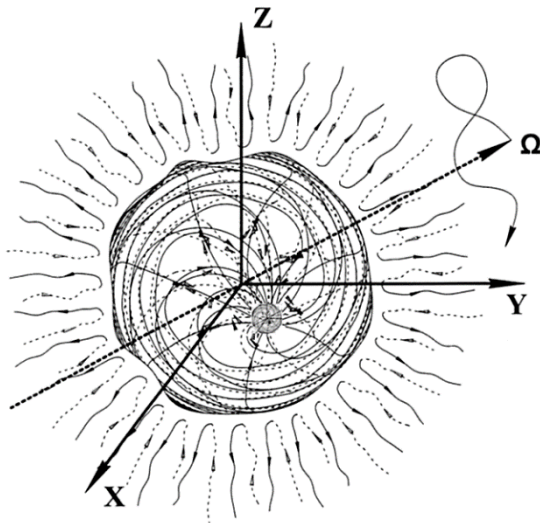

Fig. 19. The rotation of the "electron" core has two components: 1) rotation around the instantaneous axis, and 2) chaotic change in the direction of the rotation axis itself

Rotation of the core of a vacuum formation (in particular, the core of the "electron") is an extremely complex phenomenon that requires a separate extensive study. In this paper, only possible directions of these studies are outlined at the level of qualitative consideration.

First of all, we note that each point of each of the 4 transverse layers (n-subconts), which is on the periphery of the core of the "electron" (i.e. at $r \approx r_6$) should move with a speed close to the speed of light $v_r^{(+)} \approx v_\tau^{(+)} \approx c$ (see Exs. (68) – (71)), despite the fact that the total speed of the subcont (74) is zero on average. Motion with the speed of light is a condition for the existence of n-subconts on the edge of the abyss-crack (i.e. the spherical boundary between the core and the outer shell of the "electron" (see Figures 1 and 11).

Such a rotational motion of the periphery of the core can be qualitatively described as follows. If the surface of the "electron" core rotated like a solid sphere, then the speed of movement of points located on its equator $v_{re}^{(+)}$ would be maximum, i.e. close to the speed of light ($v_{re}^{(+)} \approx c$), while the speed of other points on this sphere would be noticeably less ($v_r^{(+)} < c$) (see Figure 20), and equal to zero at the poles.

In order for the speed of non-equatorial points on the surface of the core to also be close to the speed of light, in addition to the rotational motion with the entire sphere as a whole, they must also participate in one or several surface rotational motions: cyclones or anticyclones (see Figures 21 and 22) with an additional speed $v_{rc}^{(+)}$, so that $v_r^{(+)} + v_{rc}^{(+)} \approx c$.
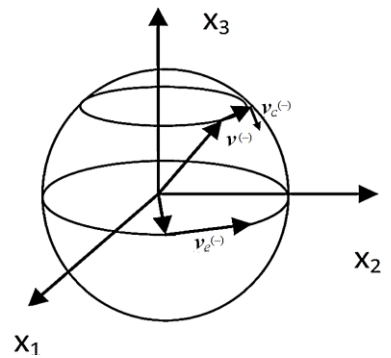
Fig. 20. Linear velocities of movement of points on a rotating sphere
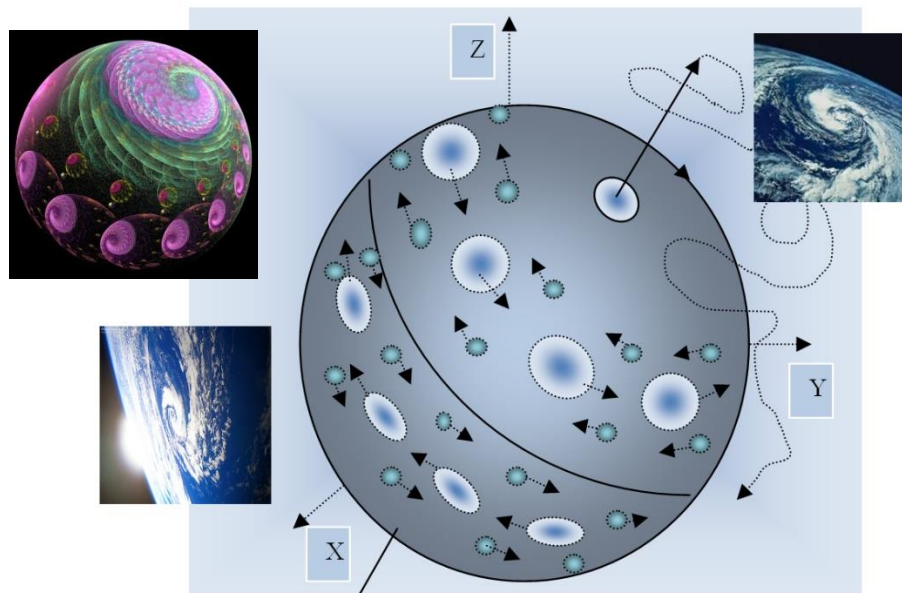
Fig. 21. Cyclones and anticyclones on the surface of the rotating core of a vacuum formation (in particular, an "electron") are similar to the circulation of air on the surface of a planet
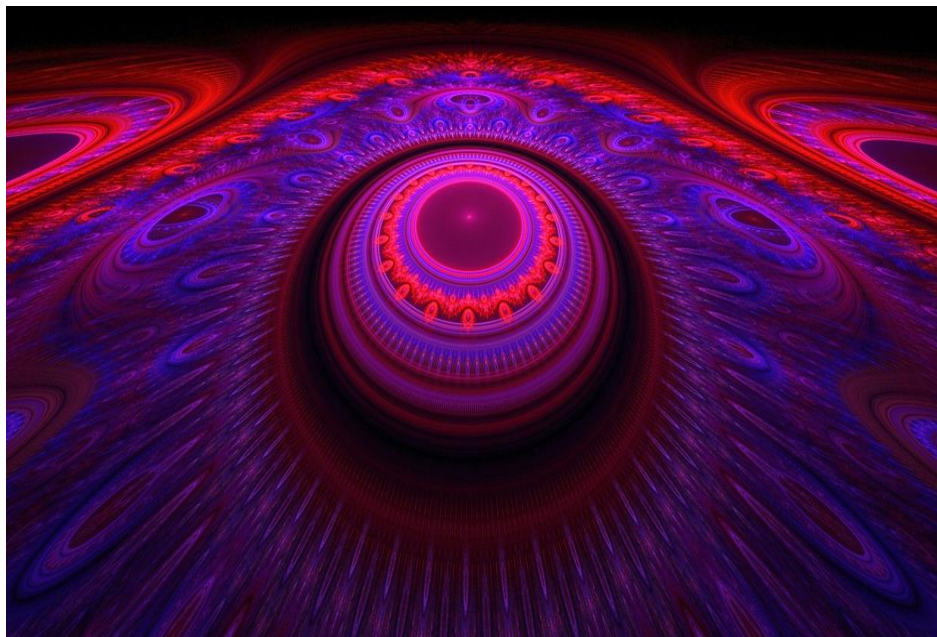
34

Fig. 22. Fractal illustrations of various zones on the surface of the rotating core of a vacuum formation
(in particular, the core of the "electron")

On the surface of the sphere under consideration (see Figures 21 and 22) there are still two points: the "north" and "south" poles, which do not participate in the rotational motion at all. But due to the boundary condition, they must also move at a speed close to the speed of light. Therefore, the axis of rotation of the "electron" core, passing through these poles, must also constantly move chaotically (i.e. change direction) at the speed of light.

As a result of the superposition of several of the above-mentioned reasons, the points located in the peripheral layer of the "electron" core must participate in an extremely complex surface motion, so that at the edge of the abyss-crack each point moves with a speed close to the speed of light. In this case, the instantaneous axis of rotation of the entire core as a whole must constantly shift along a practically chaotic trajectory (see Figures 11, 19 and 21).

Initially, it is unknown in which direction the "electron" core rotates, but it is known that there are only two such possibilities: "clockwise" and "counterclockwise", and the probability of any of these rotation directions is ½ (see §4). Due to the chaotic shift of the axis of rotation of the "electron", for any given direction it coincides with this direction part of the time, and the other equal part of the time this axis is oppositely directed. Therefore, the core of a free, stationary "electron" has an intrinsic angular momentum for any direction that is, on average, equal to zero.

Different longitudinal and transverse layers of the "electron" core move with different speeds (68) – (71) depending on the distance from its center r. If on the periphery of the core all four transverse layers of the subcont on average move practically only along the surface of a sphere with radius r_6, then as they approach the inner nucleolus the flow of the four intertwined layers of the subcont becomes more and more radial (see Figure 13). However, near the inner nucleolus these currents again wind up on the core of the "proto-quark" with radius r_7 (see Figure 23).
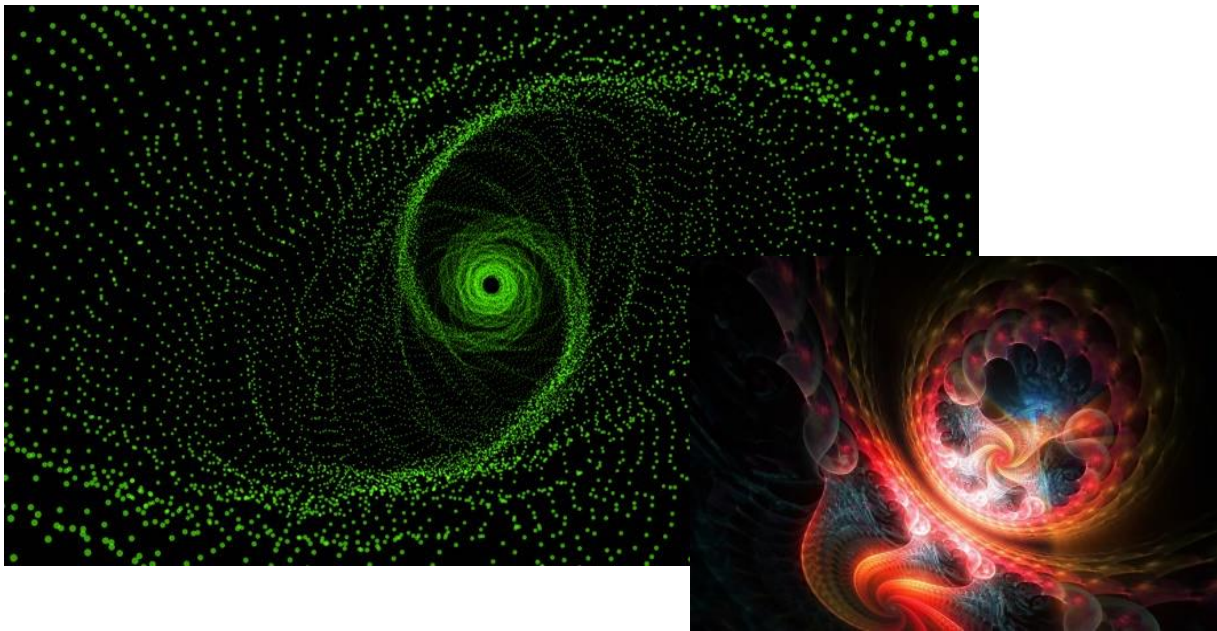
Fig. 23. Fractal illustrations of the rotational motion of subcont currents in the "electron" core. On the periphery of the "electron" core with radius r_6 and near its inner nucleolus with radius r_7, the velocity of all 4 longitudinal layers of the subcont, twisted into bundles, on average have a tangential component, and between the periphery of the "electron" core and the region of its inner nucleolus, on average, the radial component of the velocity of all 4 longitudinal layers of the subcont dominates.

Therefore, the projections of the velocities of the transverse layers of the subcont onto the surfaces of spheres with different radii $r_6 > r > r_7$ will be different. Because of this, the longitudinal layers of the "electron" core are also different (Fig. 24).
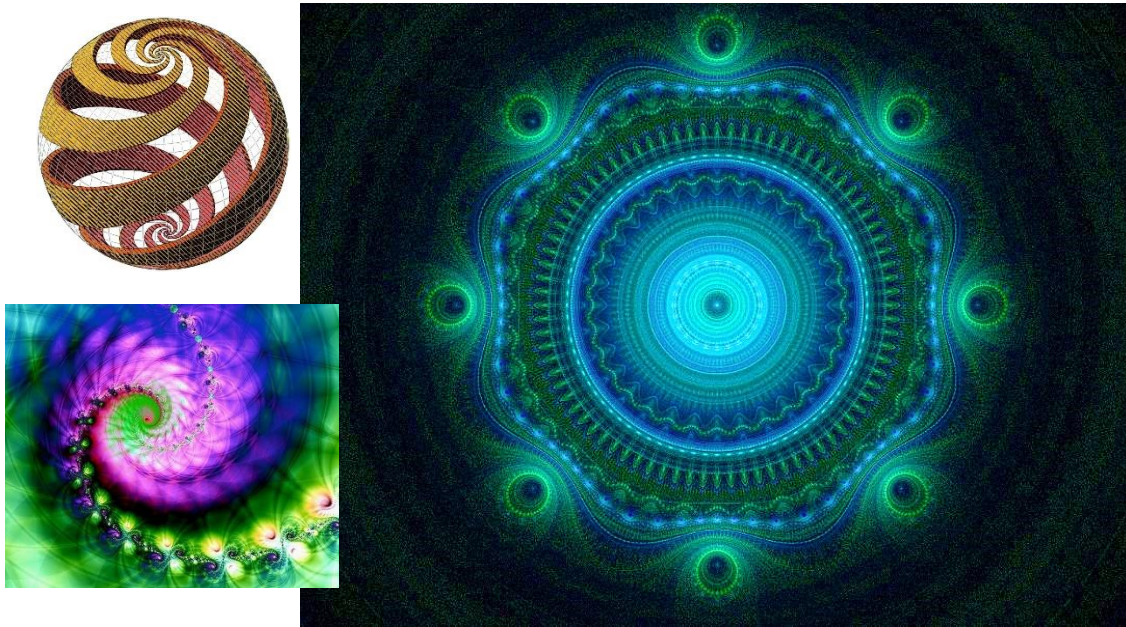
Fig. 24. Fractal illustration of the state of longitudinal and transverse layers of the "electron" core

We consider some aspects concerning the complex processes of subcont rotation in the "electron" core.

Let the point M, located at a distance r from the center of the "electron" core (i.e. between two raqiya $r_6 > r > r_7$), move around the instantaneous axis of rotation with a linear velocity (see Figure 23) [9]

$$\mathbf{v} = \mathbf{\omega} \times \mathbf{r}, \tag{129}$$

where $\mathbf{\omega} = \mathbf{e}\, d\varphi/dt$ (130)

Fig. 25. Determination of angular velocity of rotation [9]

is angular velocity of rotation of the core ($\mathbf{e}$ is a unit vector directed along the instantaneous axis of rotation).
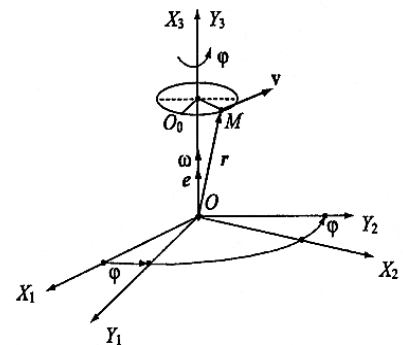
Let the reference frame x_1, x_2, x_3 (see Figure 25) remain motionless, and the system y_1, y_2, y_3 "chaotically" change its directions together with the instantaneous axis of rotation of the core of the "electron".

The coordinate axes of the reference and shifting reference frames in this case are related to each other by a system of three linear equations

$$y_\alpha = \beta_{\alpha 1}(t)\, x_1 + \beta_{\alpha 2}(t)\, x_2 + \beta_{\alpha 3}(t)\, x_3 , \tag{131}$$

where $\beta_{\alpha k}(t)$ ($\alpha, k = 1,2,3$) is direction cosines, which are random functions of time.

Let's differentiate Eqs. (131) [9]

$$\frac{dy_a}{dt} = \sum_{k=1}^{3} \frac{d\beta_{ak}(t)}{dt} x_k = \omega(t) \times y_a = \begin{pmatrix} x_1 & x_2 & x_3 \\ \omega_1(t) & \omega_2(t) & \omega_3(t) \\ \beta_{a1}(t) & \beta_{a2}(t) & \beta_{a3}(t) \end{pmatrix},$$

(132)

where $\omega_a(t)$ is the instantaneous value of the projection of the angular velocity vector $\boldsymbol{\omega}(t)$ onto the axes of the reference frame x_1, x_2, x_3 at time t.

Equating the coefficients at the unit vectors x_k, from equation (132) we obtain a system of equations for the rates of change of the direction cosines

$$d\beta_{a1}/dt = \beta_{a1}{}^{\bullet} = \omega_2 \beta_{a3} - \omega_3 \beta_{a2},$$

(133)

$$d\beta_{a2}/dt = \beta_{a\beta}{}^{\bullet} = \omega_3 \beta_{a1} - \omega_1 \beta_{a3},$$

(134)

$$d\beta_{a3}/dt = \beta_{a3}{}^{\bullet} = \omega_1 \beta_{a\beta} - \omega_2 \beta_{a1},$$

(135)

which can be represented in matrix form [9]

$$\begin{pmatrix} \beta_{a1}^{\bullet} \\ \beta_{a2}^{\bullet} \\ \beta_{a3}^{\bullet} \end{pmatrix} = \begin{pmatrix} 0 & -\omega_3 & \omega_2 \\ \omega_3 & 0 & -\omega_1 \\ -\omega_2 & \omega_1 & 0 \end{pmatrix} \begin{pmatrix} \beta_{a1} \\ \beta_{a2} \\ \beta_{a3} \end{pmatrix}.$$

(136)

Combining the three matrix equations into one, we obtain the Poisson matrix kinematic equation [9]

$$\begin{pmatrix} \beta_{11}^{\bullet} & \beta_{21}^{\bullet} & \beta_{31}^{\bullet} \\ \beta_{12}^{\bullet} & \beta_{22}^{\bullet} & \beta_{32}^{\bullet} \\ \beta_{13}^{\bullet} & \beta_{23}^{\bullet} & \beta_{33}^{\bullet} \end{pmatrix} = \begin{pmatrix} 0 & -\omega_3(t) & \omega_2(t) \\ \omega_3(t) & 0 & -\omega_1(t) \\ -\omega_2(t) & \omega_1(t) & 0 \end{pmatrix} \begin{pmatrix} \beta_{11} & \beta_{21} & \beta_{31} \\ \beta_{12} & \beta_{22} & \beta_{32} \\ \beta_{13} & \beta_{23} & \beta_{33} \end{pmatrix}.$$

(137)

which determines the displacement of point M along a sphere with radius r.

According to expressions (68) – (71), the velocities of the intra-vacuum layers in the core of the "electron" relative to the observer located inside the given core are equal to

$$v_r^{(+a)}(r) = c(-r_7/r + r^2/r_6{}^2)^{1/2} \quad - a\text{-subcont velocity};$$

(138)

$$v_r^{(+b)}(r) = c(r_7/r - r^2/r_6{}^2)^{1/2} \quad - b\text{-subcont velocity};$$

$$v_r^{(+c)}(r) = c(-r_7/r - r^2/r_6{}^2)^{1/2} \quad - c\text{-subcont velocity};$$

$$v_r^{(+d)}(r) = c(r_7/r + r^2/r_6{}^2)^{1/2} \quad - d\text{-subcont velocity}.$$

However, relative to an observer located outside the rotating (relative to him) core of the "electron", these velocities are decomposed into radial $v_{rr}^{(-m)}(r)$ and tangential $v_{rt}^{(-m)}(r)$ components

$$v_r^{(+a)}(r) = v_{rr}^{(+a)}(r) + v_{rt}^{(+a)}(r),$$

(139)

$$v_r^{(+b)}(r) = v_{rr}^{(+b)}(r) + v_{rt}^{(+b)}(r),$$

(140)

$$v_r^{(+c)}(r) = v_{rr}^{(+c)}(r) + v_{rt}^{(+c)}(r),$$

(141)

$$v_r^{(+c)}(r) = v_{rr}^{(+c)}(r) + v_{rt}^{(+c)}(r).$$

(142)

In this case, the tangential component of the velocity of each intra-vacuum layer can be estimated by the expression

$$v_{r\tau}^{(+m)}(r) \approx \boldsymbol{\omega}(t) \times \mathbf{s}^{(+m)} , \tag{143}$$

where $\mathbf{s}^{(+m)}$ is the spatial isospin vector of the m-th intra-vacuum layer.

For example, the tangential component of the velocity of the a-subcont inside the nucleus of the "electron" is approximately equal to

$$v_{r\tau}^{(+a)}(r) \approx \boldsymbol{\omega}(t) \times \mathbf{s}^{(+a)} , \tag{144}$$

where $\mathbf{s}^{(+a)}$ is the spatial isospin vector of the a-subcont with components (111):

$$s_r^{(-a)} = 0, \quad s_\theta^{(-a)} = 0, \quad s_\phi^{(-a)} = -\frac{1}{2} r \sin\theta. \tag{145}$$

From expression (139), taking into account the components of the isospin vector (145), we obtain an estimate of the modulus of the instantaneous value of the tangential component of the velocity of the a-subcont between two raqiya of the core of the "electron" ($r_6 > r > r_7$)

$$|v_{r\tau}^{(+a)}(r)| \approx \tfrac{1}{2}\, r\, \sin\theta\, [\omega_1(t)^2 + \omega_2(t)^2]^{\frac{1}{2}}, \tag{146}$$

provided that on the periphery of the core with radius r_6

$$|v_{r\tau}^{(+a)}(r_6)| \approx \tfrac{1}{2}\, r_6 \sin\theta\, [\omega_1(t)^2 + \omega_2(t)^2]^{\frac{1}{2}} = c, \tag{147}$$

and in the region of the inner nucleolus with radius r_7 the condition is satisfied

$$\|v_{r\tau}^{(+a)}(r_7)| \approx \tfrac{1}{2}\, r_7 \sin\theta\, [\omega_1(t)^2 + \omega_2(t)^2]^{\frac{1}{2}} = c. \tag{148}$$

From expression (139) it follows that the radial component of the velocity of the a-subcont inside the nucleus of the "electron" is approximately equal to

$$v_{rr}^{(-a)}(r) \approx v_r^{(-a)}(r) - v_{r\tau}^{(-a)}(r) \approx c(- r_7/r + r^2/r_6^2)^{1/2} - \tfrac{1}{2} r \sin\theta\, [\omega_1(t)^2 + \omega_2(t)^2]^{\frac{1}{2}}. \tag{149}$$

Based on the same analysis of the remaining expressions (140) – (142), the tangential and radial components of the velocities of the b-subcont, c-subcont and d-subcont inside the core of the "electron" can be obtained.

Once again, we note that this section does not contain complete solutions to the problems posed. Here, only the ways of describing the rotation of the core of a spherical vacuum formation, in particular the core of the "electron", are outlined. A separate, extensive study should be devoted to the rotation of various longitudinal and transverse layers of the core of a spherical vacuum formation.

8 Connection with quantum mechanics. Chaotic behavior of the core of the "electron" and its inner nucleolus

Before this paragraph, we considered the averaged stable metric-dynamic structure of a free valence "electron" based on the methods of differential geometry and the mathematical apparatus of the Algebra of signature. It turned out that in any stable spherical vacuum formation (in particular, in the "electron"), one can distinguish a core and an inner nucleolus (see Figures 5, 11 and 26).

In reality, the vacuum, like an elastic-plastic continuous medium, constantly and everywhere chaotically trembles, seethes

and distorts. The stable metric-dynamic structure of any spherical vacuum formation (in particular, the "electron") is only the result of simplification and averaging of complex vacuum fluctuations.

Chaotic vacuum deformations and curvatures need to be studied separately, but in this section, we will simplify the task. Let us assume that the core of the "electron" (with a radius of $r_6 \sim 10^{-13}$ cm) and the inner nucleolus (with a radius of r7 ~ 10–24 cm) are separate particles that, under the influence of complex vacuum fluctuations, wander chaotically in the vicinity of a certain central point (i.e., the center of the stochastic system, Figure 26). This approach largely coincides with the initial provisions of Nelson's stochastic quantum mechanics [10,11,12].
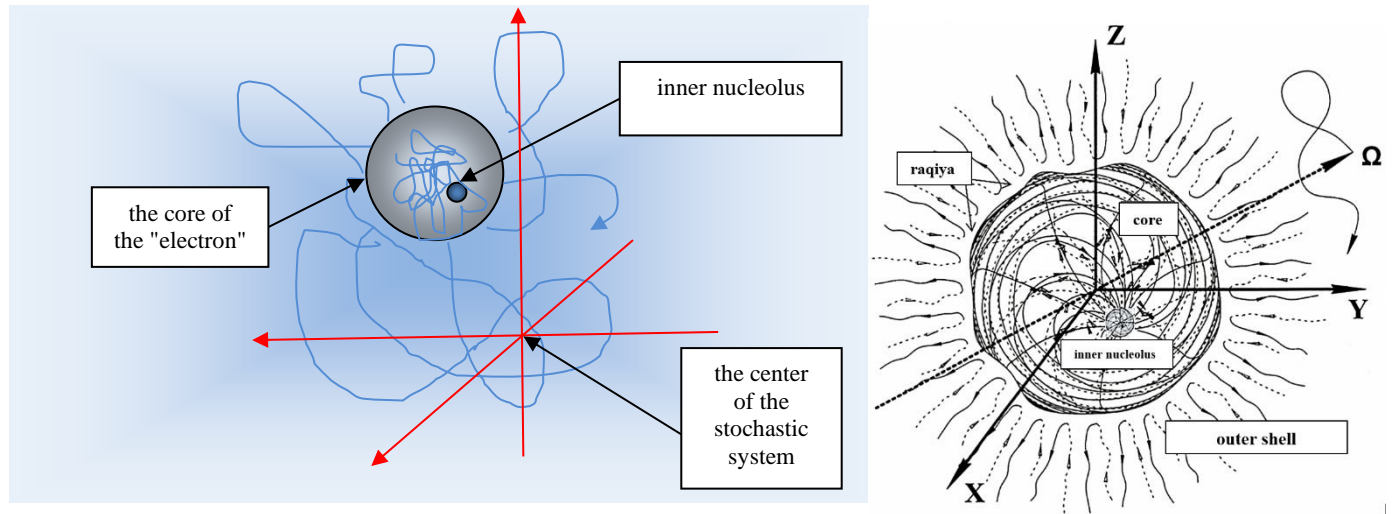
Fig. 26. Chaotically wandering core of the "electron", inside which
the inner nucleolus wanders chaotically too

Chaotic vacuum deformations and curvatures should be studied separately, but in this section we will simplify the task. Let us assume that the nucleus of the "electron" (with a radius of $r_6 \sim 10^{-13}$cm) and the inner nucleolus (with a radius of $r_7 \sim 10^{-24}$ 4 cm) are separate particles that, under the influence of complex vacuum fluctuations, wander chaotically in the vicinity of a certain central point (i.e., the center of the stochastic system, Figure 26). This approach largely coincides with the initial provisions of stochastic quantum mechanics by Edward Nelson [10,11,12].

It is more correct to consider the joint chaotic behavior of the core of the "electron" and its inner nucleolus. That is, to study the core of the "electron" as a chaotically wandering particle with a constantly chaotically shifting geometric center (i.e. its center of inertia).

We deliberately avoid using the concept of the "center of mass" of a particle, since there is no mass in geometrized vacuum physics. Stable vacuum formations are only stable deformations revealed from the seething vacuum by averaging its fluctuations.

However, we will simplify the problem even more and consider the nucleus of the "electron" as a small structureless particle (with a radius $r_6 \sim 10^{-1}$cm), which wanders chaotically in a much larger seething region of vacuum with a characteristic size of the order of $r_a \sim 10^{-10}$ cm.

The chaotic behavior of the nucleolus (i.e. the nucleus of the "proto-quark") inside the nucleus of the "electron" has already been partially considered in §4.9 in [6].

In the same way as it was done in §4.9 in [6] for the inner nucleolus, for the "electron" core in the stationary case one can write the functional of the average efficiency of the stochastic system (144) in [6] (for a more detailed consideration of this random process see [13])

$$w = \int_{-\infty}^{\infty}\int_{-\infty}^{\infty}\int_{-\infty}^{\infty}\left(-\frac{\eta_r^2}{2}\psi(x,y,z)\nabla^2\psi(x,y,z) + \psi^2(x,y,z)[<u(x,y,z)> - <\varepsilon(x,y,z)>]\right)dxdydz.$$

The condition for finding the extremal of this functional is the stationary Schrödinger-Euler-Poisson equation [13]

$$-\frac{3\eta_r^2}{2}\left\{\frac{\partial^2\psi(x,y,z)}{\partial x^2} + \frac{\partial^2\psi(x,y,z)}{\partial y^2} + \frac{\partial^2\psi(x,y,z)}{\partial z^2}\right\} + 2[<u(x,y,z)> - <\varepsilon(x,y,z)>]\psi(x,y,z) = 0, \qquad (150)$$

where $\eta_r = \frac{2\sigma_r^2}{\tau_{rcor}}$,

here

$$\sigma_r = \frac{1}{\sqrt{3}}\sqrt{\sigma_x^2 + \sigma_y^2 + \sigma_z^2} \qquad (151)$$

is standard deviation of random 3-dimensional trajectory of chaotically wandering core of "electron" relative to conditional center of the considered stochastic system (see Figure 26);

$$\tau_{rcor} = \frac{1}{3}\left(\tau_{xcor} + \tau_{ycor} + \tau_{zcor}\right) \qquad (152)$$

is autocorrelation interval of the given 3-dimensional stationary random process.

In non-stationary case the efficiency functional of the given stochastic system takes the form (see (59) in [13])

$$(153)$$
$$\overline{<s_r(t)>} = \int_{t_1}^{t_2}\int_{-\infty}^{\infty}\int_{-\infty}^{\infty}\int_{-\infty}^{\infty}\left(-\frac{\eta_r^2}{2}\psi(\vec{r},t)\nabla^2\psi(\vec{r}) + [<u(\vec{r},t)> - <\varepsilon(\vec{r},t_0)>]\psi^2(\vec{r},t) \pm i\frac{\eta_r^2}{D}\psi(\vec{r},t)\frac{\partial\psi(\vec{r},t)}{\partial t}\right)dxdydzdt.$$

To find the extremal of this functional is the time-dependent Schrödinger-Euler-Poisson equation (67) in [13]

$$\pm i\frac{\eta_r^2}{D}\frac{\partial\psi(\vec{r},t)}{\partial t} = -\frac{3\eta_r^2}{2}\nabla^2\psi(\vec{r},t) + 2[<u(\vec{r},t)> - <\varepsilon(\vec{r},t_0)>]\psi(\vec{r},t). \qquad (154)$$

In other words, the average behavior of a chaotically wandering core of an "electron" under certain conditions (see [13]) is described by the equations of quantum mechanics. The stochastic Schrödinger-Euler-Poisson equations (150) and (154) coincide with the corresponding Schrödinger equations up to a constant coefficient η_r.

Moreover, taking into account in the article [13] two fundamental principles at once: "Minimum action" and "Maximum entropy" in one efficiency functional of the form (153), allows us to obtain for a stochastic system of the "chaotically wandering particle" type not only differential equations of the Schrödinger equation type, but also other stochastic equations depending on the initial conditions, for example, the self-diffusion equation (see equation (73) in [13]), etc.

In general, the variational method proposed in the article [13] allows us to obtain equations describing quantum and non-quantum stochastic systems of any scale (such as chaotically wandering core or nuclei: "proto-quark", "electron", "biological cell", "planet", "star", "galaxy", etc.). In this case, there are no deviations from ordinary empirical expectations and classical logic, and it is also possible to do without involving hypothetical de Broglie waves that are not observed in experiments.

Without involving the hypothesis of de Broglie waves, it is also possible to explain the results of an experiment on the diffraction of microparticles (in particular, electrons) on a crystal.

Using the usual methods of probability theory and the laws of geometric optics, the author obtained formula (2.2) in [14]

$$D(\nu, \omega/\vartheta, \gamma) = \frac{1}{2\pi^2 l_2}\left(\frac{\cos^2(\pi n_1) - \cos(\pi n_1)\cos\left(\sqrt{\frac{a^2+b^2}{d^2}}l_2/\eta\right)}{\left(\pi n_1/l_2\right)^2 - \left(\sqrt{\frac{a^2+b^2}{d^2}}l_2/\eta\right)^2} - \frac{\cos\left(\pi n_1 + \sqrt{\frac{a^2+b^2}{d^2}}l_2/\eta\right) - 1}{\left(\pi n_1/l_2 + \sqrt{\frac{a^2+b^2}{d^2}}/\eta\right)^2}\right)\left|\frac{d(a_\nu' b_\omega' - a_\omega' b_\nu') + c_\nu'(ba_\omega' - ab_\omega')}{d^2\sqrt{a^2+b^2}}\right|, \quad (155)$$

where

$a = \cos\nu\cos\omega + \cos\vartheta\cos\gamma;$ $b = \cos\nu\sin\omega + \cos\vartheta\sin\gamma;$ $d = \sin\nu + \sin\vartheta;$ $a_\nu' = -\sin\nu\cos\omega;$

$b_\nu' = -\sin\nu\sin\omega;$ $c_\nu' = \cos\nu;$ $a_\omega' = -\cos\nu\sin\omega;$ $b_\omega' = \cos\nu\cos\omega;$

$$\eta = \frac{l_1^2(\pi^2 n_1^2 - 6)}{6\pi^2 r_{cor5}}, \quad (156)$$

here

l_1 is the thickness of one reflective layer (i.e. horizontal atomic plane) of the crystal (see Figure 2.1 in [14]);
$l_2 = l_1 n_1$ is the depth of the multilayer surface of the single crystal, effectively participating in the elastic scattering of electrons;
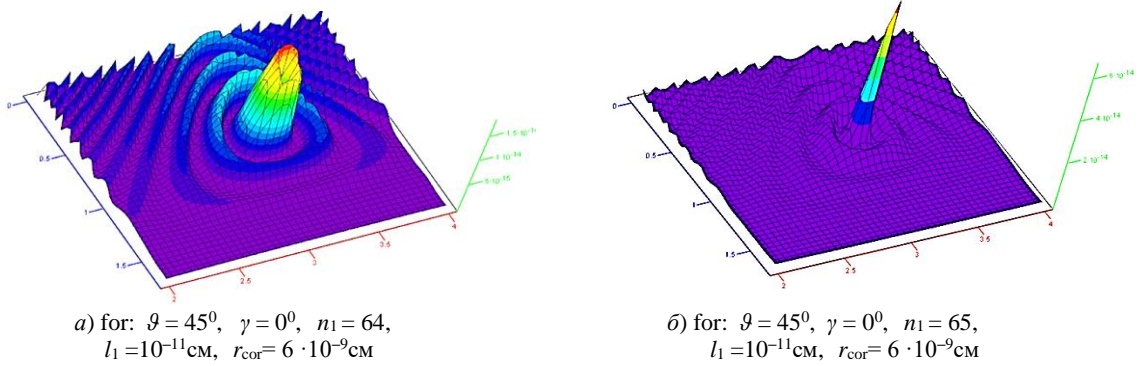n_1 is the number of uneven layers of the single crystal (sinusoidal type), lying in the interval [0, l2];
r_{cor} is the autocorrelation radius of one uneven layer of the crystal of the sinusoidal type. This autocorrelation radius is approximately equal to the average radius of curvature of the sinusoidal irregularities of one layer of the crystal;
ϑ, γ are the angles that define the direction of motion of microparticles (in particular, electrons) incident on the surface of the crystal (see Figure 1.2 in [14]);
ν, ω are angles that define the direction of movement of microparticles (in particular, electrons) reflected from the surface of the crystal towards the detector (see Figure 1.2 in [14]).

Calculations using formula (155) allow us to obtain ring-shaped scattering diagrams of microparticles (in particular, electrons) on a crystal (see Figure 27), corresponding to experimental electronograms (see Figure 28).

а) for: $\vartheta = 45^0$, $\gamma = 0^0$, $n_1 = 64$, $l_1 = 10^{-11}$см, $r_{cor} = 6 \cdot 10^{-9}$см

б) for: $\vartheta = 45^0$, $\gamma = 0^0$, $n_1 = 65$, $l_1 = 10^{-11}$см, $r_{cor} = 6 \cdot 10^{-9}$см

Fig. 27. Volume diagrams of elastic scattering of electrons on a multilayer surface of a single crystal, calculated using formula (155) for different values of the parameters ϑ, l_1, n_1 and r_{cor}

Fig. 28. Experimental electron diffraction patterns obtained as a result of electron diffraction on the surface of crystals

The number of crystal layers n_1, which are penetrated by incident microparticles (in particular, electrons), depends on their velocity $n_1 = f(v)$. The results of calculations using formula (155) as a function of n_1 (see Figure 29a), these calculations are in good agreement with the results of the experiment of K. Davisson and L. Germer (1927) on the diffraction of electrons on a nickel crystal [15] (see Figure 29b).


a)

b)
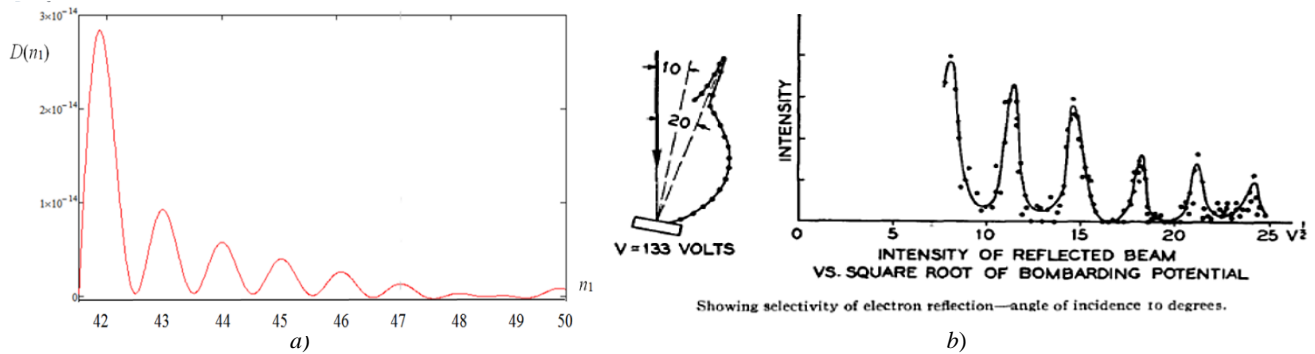
Fig. 29. a) Result of calculation using formula (155) as a function of the number of layers n1 of the reflecting surface of the crystal, which in turn depend on the velocity v of the microparticles falling on this surface. with the following constant parameters $\gamma = 0^0$, $v = 45^0$, $\omega = 0^0$, $l_1 = 10^{-11}$ cm, $r_{cor} = 9 \cdot 10^{-9}$ cm; b) Intensity of the electron beam I scattered by a nickel single crystal at a constant value of the reflection angle, depending on the square root of the voltage U accelerating the particles in the electron gun (electron generator). This experimental dependence was first obtained in 1927 by Clinton Davisson and Lester Germer [15] and served as one of the reasons for accepting Louis de Boyle's hypothesis on the wave properties of matter

The greatest surprise in quantum physics is caused by the diffraction of electrons on two slits. Richard Feynman said: –"This phenomenon is absolutely, absolutely impossible to explain in a classical way. In this phenomenon lies the very essence of quantum mechanics."

Indeed, if an electron is a point particle, then no reasonable explanation can be given for this experiment.

However, if we consider the "electron" as a stable, on average, spherical vacuum formation in which we can distinguish a core and an outer shell (see Figures 1 and 5), then the mysterious charm surrounding this double-slit experiment can easily dissipate. This phenomenon can be explained by wave disturbances of the outer shell of the "electron", which simultaneously penetrates both slits, while the core of this "electron" passes through only one of them.
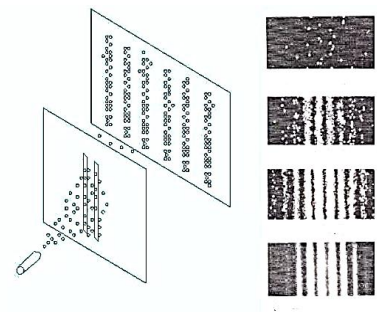
Fig. 30. Electron diffraction on two slits

Much research is still needed to describe numerous quantum effects using the methods of stochastic quantum mechanics and fully geometrized vacuum physics, but it is already possible to confidently assert that the phenomena of the microworld are fundamentally no different from random processes in the macroworld.

There is much to suggest that Einstein's rejection of quantum indeterminism was not unfounded. However, weakened determinism is not due to the restriction of the rigidity of administration and censorship by the "hypothetical imperative", but to the imposition of conditions of energetic optimality on an acceptable level of freedom. Weakened determinism is based on the extremity of the efficiency functional, which unites both fundamental principles: "Minimum action" (i.e. energetic limitation and reasonable expediency) with "Maximum entropy" (i.e. accessible freedom, within the framework of recognized necessity).

9 Free "positron"

If in all the previous paragraphs we replace the set of metrics (1) with the signature $(+ - - -)$, defining the averaged stable metric-dynamic state of a free resting valence "electron", with the set of antipodal metrics (11) with the signature $(- + + +)$, and also replace the terms:
- "outer side of the $\lambda_{-12,-15}$-vacuum" with "inner side of the $\lambda_{-12,-15}$-vacuum";
- "subcont" with "antisubcont";
- "convexity" with "concavity";
- the notations $ds_i^{(+---)}, ds_i^{(+)}, l_i^{(+)}, g_{ij}^{(+)}, v_\theta^{(+)}, E_{vi}^{(+)}, a_i^{(+)}, A_4^{(+)}$ with $ds_i^{(-+++)}, ds_i^{(-)}, l_i^{(-)}, g_{ij}^{(-)}, v_\theta^{(-)}, E_{vi}^{(-)}, a_i^{(-)}, A_4^{(-)}$,

then we obtain a completely analogous, but completely opposite metric-dynamic model of an on average stable spherical vacuum formation – a free resting valence "positron".

If we add the set of metrics (1) to the set of antipodal metrics (11), we get zero. That is, the "electron" and "positron" completely compensate each other's manifestations.

10 Quasi-stationary interactions of "particles" and "antiparticles"

10.1 Simplified quasi-stationary "electron" - "positron" interaction

There are no separately existing "electrons" and "positrons". Consideration of these stable vacuum formations separately is possible only within the framework of a simplified mathematical model.

If the cores of the "electron" and "positron" are separated from each other, then subcont - antisubcont currents constantly circulate between the raqiya of these vacuum formations (see Figures 31 and 32).
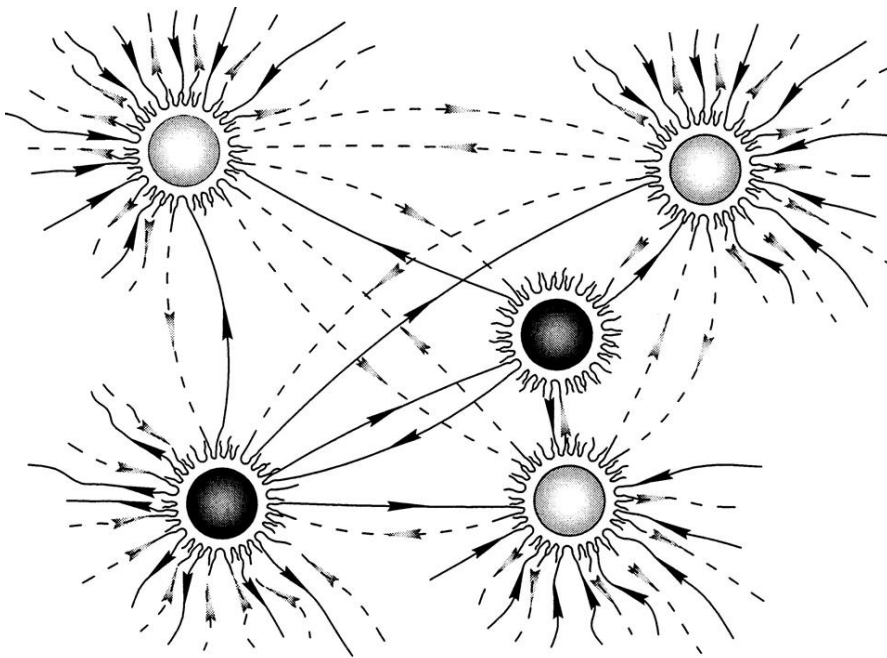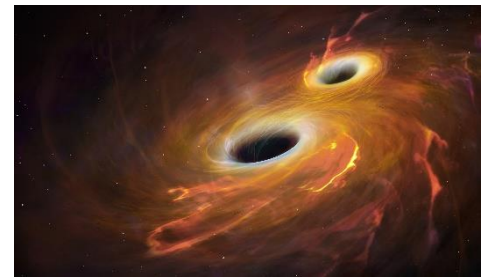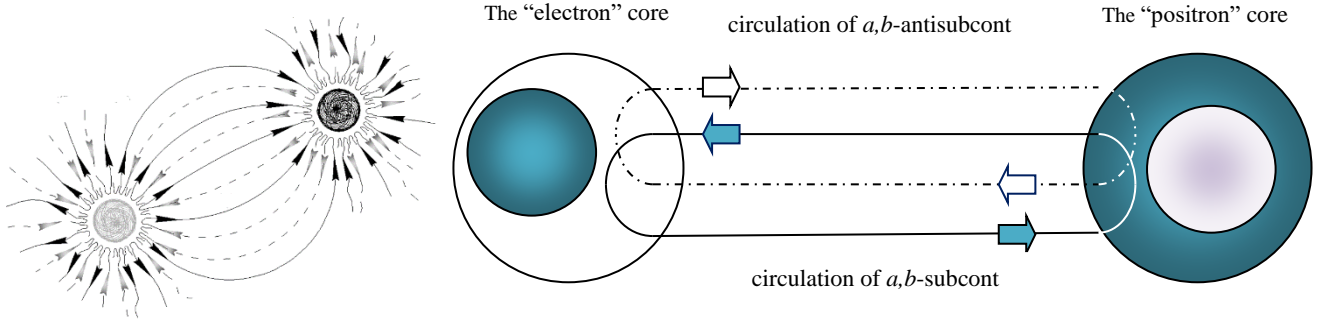

Fig. 31. Subcont - antisubcont currents between a raqiyas of the "particles" and "antiparticles"

Fig. 32. Schematic representation of the average circulation of *a,b*-subcont and *a,b*-antisubcont between the "electron" and "positron" raqiyas

In §2.2 it was shown that in the outer shell of the "electron" the *a*-subcont flows in the form of thin currents twisted in spirals around all radial directions to the "electron's" raqiya (i.e. spherical abyss-crack) (see Figures. 6 and 7), and the *b*-subcont flows out from the "electron's" raqiya in the form of thin currents in all directions along a multitude of counter-spirals.

As a result, the acceleration vector of the subcont (or the geometrized vector of the eclectic intensity of the subcont) in the outer shell of the "electron" has components (59)

$$a_{\alpha r}^{(+)} = E_{vr}^{(+ab)} = \frac{c^2 r_6}{2r^2 \sqrt{1 - \frac{r_6^2}{r^2}}}, \qquad a_{\alpha \theta}^{(+)} = E_{v\theta}^{(+ab)} = 0, \qquad a_{\alpha \phi}^{(+)} = E_{v\phi}^{(+ab)} = 0. \tag{157}$$

In the outer shell of the "positron" similar but opposite processes occur: the *a*-antisubcont flows in the form of thin currents from all sides to the "positron" raqiya along a multitude of spirals, and the *b*-antisubcont flows out from the spherical abyss-crack (i.e., raqiya) of the "positron" in the form of thin currents in all directions along a multitude of counter-spirals. As a result, the acceleration vector of the antisubcont (or the geometrized vector of the eclectic tension of the antisubcont) in the outer shell of the "positron" has the components

$$a_{\alpha r}^{(-)} = E_{vr}^{(-ab)} = \frac{c^2 r_6}{2r^2 \sqrt{1 - \frac{r_6^2}{r^2}}}, \qquad a_{\alpha \theta}^{(-)} = E_{v\theta}^{(-ab)} = 0, \qquad a_{\alpha \phi}^{(-)} = E_{v\phi}^{(-ab)} = 0. \tag{158}$$

Earlier we assumed that in the outer shells of the free "electron" and "positron" these subcont and antisubcont currents and countercurrents began and ended at the periphery of the Universe (see Figures 7 − 9). Now we will take into account that some of these currents and countercurrents circulate between the "particle" and "antiparticle" raqiyas (in particular, between the "electron" and "positron" raqiyas, see Figures 31 and 32).

In this case, between the "electron" and "positron" raqiyas there are four intertwined subcont-antisubcont currents with accelerations of the form (55) and (56)

I $\qquad a_r^{(+a)} = -\dfrac{c^2 r_6}{2r^2 \sqrt{\left(1 - \frac{r_6}{r}\right)}} \qquad$ – *a*-subcont; $\hfill$ (159)

H $\qquad a_r^{(+b)} = \dfrac{c^2 r_6}{2r^2 \sqrt{1 + \frac{r_6}{r}}} \qquad$ – *b*-subcont; $\hfill$ (160)

V $\qquad a_r^{(-a)} = \dfrac{c^2 r_6}{2r^2 \sqrt{\left(1 - \frac{r_6}{r}\right)}} \qquad$ – *a*-antisubcont; $\hfill$ (161)

H′ $\qquad a_r^{(-b)} = -\dfrac{c^2 r_6}{2r^2 \sqrt{1 + \frac{r_6}{r}}} \qquad$ – *b*-antisubcont. $\hfill$ (162)

45

The twisting of the four subcont – antisubcont currents can be explained using a four-sided Mobius strip (see Figures 33). In this case, each of the four vacuum currents with accelerations (159) – (162) flows along its side of the four-sided Mobius strip, transforming into each other at the inflection points located in the "electron" and "positron" raqiyas.

Thus, the "electron" attracts the "positron" with acceleration

$$a_r^{(e+\bar{e})} = \frac{1}{\sqrt{4}} \sqrt{a_r^{(+a)2} + a_r^{(+b)2} + a_r^{(-a)2} + a_r^{(-b)2}} = \frac{c^2 r_6}{2r^2 \sqrt{\left(1 - \frac{r_6^2}{r^2}\right)}}. \qquad (163)$$

Рис. 33. The four-sided Mobius strip, and the circulation of spirally coiled subcont-antisubcont currents along one of its sides

Similarly, the "positron" attracts the "electron" with the same acceleration (since the action is equal to the reaction)

$$a_r^{(\bar{e}+e)} = \frac{1}{\sqrt{4}} \sqrt{a_r^{(-a)2} + a_r^{(-b)2} + a_r^{(+a)2} + a_r^{(+b)2}} = \frac{c^2 r_6}{2r^2 \sqrt{\left(1 - \frac{r_6^2}{r^2}\right)}}.$$

The total radial acceleration with which the "electron" and "positron" are attracted to each other on average is

$$a_r^{(e,\bar{e})} = a_r^{(e+\bar{e})} + a_r^{(\bar{e}+e)} = \frac{c^2 r_6}{r^2 \sqrt{\left(1 - \frac{r_6^2}{r^2}\right)}}, \qquad (163)$$

where, in this case, r is the distance between the centers of the "electron" and "positron".

The graph of function (163) is shown in Figure 34. This function determines the acceleration of the convergence of the core of the "electron" and the core of the "positron" depending on the distance between their centers.

For $r \gg r_6$, Ex. (163) is simplified

$$a_r^{(e+\bar{e})} = \frac{c^2 r_6}{r^2}, \qquad (164)$$

and corresponds to the strength of the Coulomb interaction between an electron and a positron in classical electrostatics

$$F_r^{(e+\bar{e})} = \frac{e^2}{4\pi\varepsilon_0 \, r^2}. \qquad (165)$$
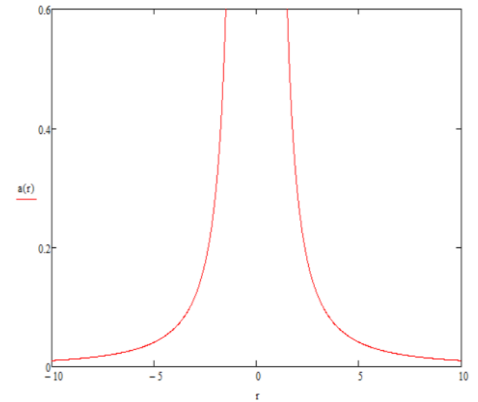
Comparing Ex. (164) and (165), we find the correspondence

$$\frac{e^2}{4\pi\varepsilon_0 m_e} \cong c^2 r_6, \text{ where } m_e \text{ is the rest mass of the electron.} \qquad (166)$$

Based on relation (166), we can estimate the radius of the core of the "electron"


Fig. 34. Graph of function (163) for the conventionally accepted $c = r_6 = 1$. This function determines the acceleration of the approach of the cores of the "electron" and "positron" depending on the distance between their centers.

$$r_6 \cong \frac{e^2}{4\pi\varepsilon_0 c^2 m_e} \cong 2{,}8179403267 \times 10^{-13} \text{cm,} \qquad (167)$$

in modern physics, this value is usually called the "classical radius of the electron" or the "Lorentz radius" or the "Thomson scattering length".

10.2 Simplified quasi-stationary "electron" – "electron" interaction

As shown in Figures 35 and 36, between the "electron" 1 and "electron" 2 only subcont currents and countercurrents circulate (i.e. only subcont exchange process take place), the antisubcont does not circulate between them.

The "electron 1" core

Circulation of *a,b*-subcont
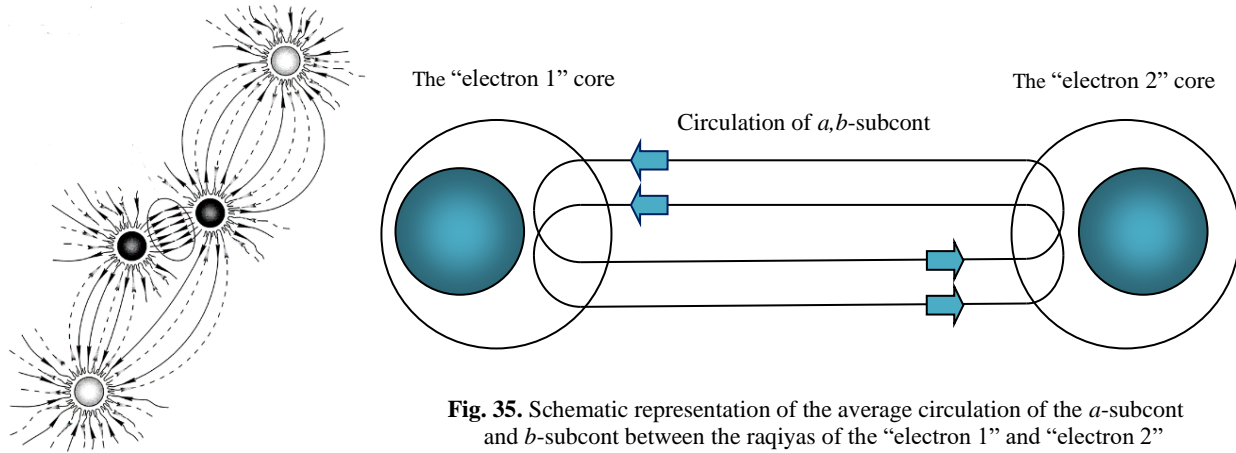
The "electron 2" core

Fig. 35. Schematic representation of the average circulation of the *a*-subcont and *b*-subcont between the raqiyas of the "electron 1" and "electron 2"

The region of interaction of two "electrons"
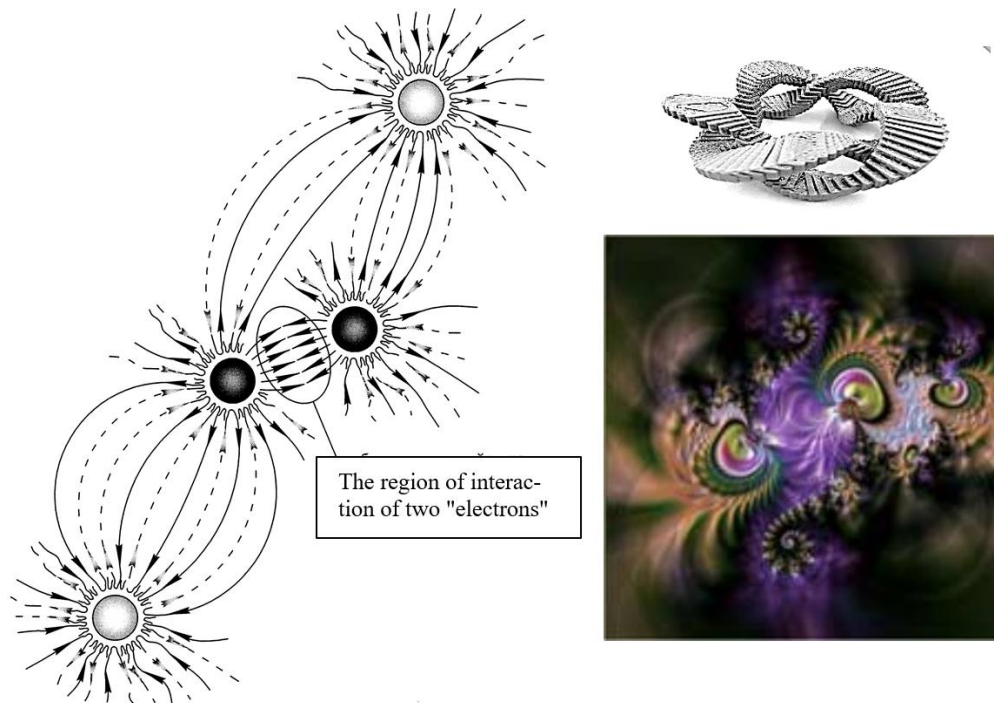
Fig. 36. The region of interaction of two "electrons"

As shown in §2, the a_1-subcont with acceleration (55) flows to the raqiya of the "electron1" and the b_1-subcont with acceleration (56) flows away from it (see Figure 35). The total radial component of the acceleration of the subcont in the outer shell of the "electron 1", repulsive the core of the "electron 2", is on average equal to (58)

$$a_{r1}^{(+a1b1)} = \frac{1}{\sqrt{2}} \sqrt{a_r^{(+a1)2} + a_r^{(+b1)2}} = \frac{c^2 r_6}{2r^2 \sqrt{1 - \frac{r_6^2}{r^2}}}. \qquad (168)$$

In this case, the b_1-subcont, which flows away from the raqiya of "electron 1", flows into the raqiya of "electron 2" in the form of an a_2-subcont and flows out of it in the form of a b_2-subcont (see Figure 35). As a result, "electron 2" repulsive the core of the "electron 2" with a similar acceleration

$$a_{r2}^{(+a2b2)} = \frac{1}{\sqrt{2}} \sqrt{a_r^{(+a2)2} + a_r^{(+b2)2}} = \frac{c^2 r_6}{2r^2 \sqrt{1 - \frac{r_6^2}{r^2}}}. \qquad (169)$$

Thus, "electron 1" and "electron 2" on average repel each other with a common acceleration

$$a_r^{(e_1 + e_2)} = a_{r1}^{(+a1b1)} + a_{r2}^{(+a2b2)} = \frac{c^2 r_6}{r^2 \sqrt{\left(1 - \frac{r_6^2}{r^2}\right)}}, \qquad (170)$$

where, in this case, r is the distance between the centers of "electron 1" and "electron 2".

For $r \gg r_6$, Ex. (170) is simplified

$$a_r^{(e_1 + e_2)} = \frac{c^2 r_6}{r^2}, \qquad (171)$$

and corresponds to the force of Coulomb repulsion of two electrons from each other (165).

A similar consideration of the "positron 1" – "positron 2" interaction leads to the same result

$$a_r^{(e_1 + e_2)} = a_{r1}^{(+a1b1)} + a_{r2}^{(+a2b2)} = \frac{c^2 r_6}{r^2 \sqrt{\left(1 - \frac{r_6^2}{r^2}\right)}}. \qquad (172)$$

For the case under consideration, it would be correct to solve Einstein's vacuum equations, taking into account the vacuum stresses that arise during the interactions of the "particles". However, this is a difficult task. In addition, in the simplified model proposed here, we assumed that at each fixed moment of time, the interaction between two "particles" is quasi-stationary. That is, we conditionally assume that the "electron" and "positron" or "electron 1" and "electron 2" in a Coulomb-type interaction move so slowly that at each moment they can be considered as if motionless. In fact, the shape and structure of the "electron" and "positron" change during the movement (this is planned to be shown in the next article of this series). These approximations are justified by the fact that they bring clarity to the geometric nature of electric charge (see §2.2.2) and provide an explanation of Coulomb's law based on simplified metric-dynamic models of the valence "electron" and valence "positron".

CONCLUSION

In this article (i.e. in Part 7 of "Geometrized Physics of Vacuum Based on the Algebra of Signature") averaged metric-dynamic models of only two mutually opposite stable spherical vacuum formations are considered: a free "electron" (i.e. a conditional "convexity" of the $\lambda_{-12,-15}$-vacuum) and a free "positron" (i.e. a conditional "concavity" of the $\lambda_{-12,-15}$-vacuum).

The study of simplified metric-dynamic models of the "electron" and "positron" allowed us to demonstrate the use of the mathematical apparatus and methodology of geometrized vacuum physics, which includes [1,2,3,4,5,6]: vacuum differential geometry (i.e., the nullified general theory of relativity), the Algebra of signature (i.e., the metric knot topology), and the effective probability theory (i.e., stochastic quantum mechanics). These mathematical tools are suitable for a detailed study of all stable and unstable spherical vacuum formations presented in §4 of [6]: "quarks", "leptons", "baryons", "mesons" and "bosons", "atoms" and "molecules".

In addition, the "electron" and "positron" are artificially extracted from the general hierarchical cosmological model presented in §§1–3 in [6]. This is done by leaving for consideration only those terms from the hierarchical sets of metrics (23) – (27) and (28) – (32) in [6] that contain radii $r_6 \sim 10^{-13}$ cm (corresponding to the size of the nucleus of the "electron" and "positron"). In this hierarchical cosmological model, all spherical vacuum formations of different scales nested in one another (like matryoshka dolls, see Figure 1 in [6]) are similar to one another. Therefore, if in all equations and expressions of this article instead of radii from the hierarchical sequence (44a) in [6]:

$r_2 \sim 10^{29}$ cm is radius corresponding to the size of the observable Universe,
$r_6 \sim 10^{-13}$ cm is radius corresponding to the size of the "electron" core,
$r_7 \sim 10^{-24}$ cm is radius corresponding to the size of the "proto-quark" core

substitute from the same hierarchy of radii, for example:

$r_2 \sim 10^{29}$ cm is radius corresponding to the size of the observable Universe,
$r_4 \sim 10^{8}$ cm is radius corresponding to the size of the core of a planet or star,
$r_6 \sim 10^{-13}$ cm radius corresponding to the size of the core of the "electron",

then we obtain metric-dynamic models of "planets";

or, for example:

$r_2 \sim 10^{29}$ cm is radius corresponding to the size of the observable Universe,
$r_3 \sim 10^{19}$ cm is the radius corresponding to the size of the core of the galaxy,
$r_4 \sim 10^{8}$ cm is radius corresponding to the size of the core of a planet or star,

then we get metric-dynamic models of "galaxies", etc.

On closer examination, "electron" and "positron" are not mathematical points, as they are treated in classical electrodynamics and in a number of quantum theories. "Electron" and "positron" are infinitely complex objects occupying the entire Universe. Four spherical regions can be distinguished in them: the outer shell, the shell, the nucleus and the inner nucleolus, which require separate extensive studies.

No matter how much we study "electron" and "positron" as, on average, stable vacuum formations, they will still remain unknown. This article considers only some aspects related to free resting "electron" and "positron" and their interaction with each other at a simplified level of quasi-static vacuum electrostatics.

Many questions related to the uniform and accelerated motion of the "electron" and "positron", their state in the composition of an atom (see ranking expressions (105) – (110) in [6]), their interaction with high-frequency and low-frequency "photons" and other "bosons", questions of their annihilation, the nature of electric current, etc. were left outside the scope of consideration.

Among the positive results of this article, it can be noted that within the framework of the theory developed here, the problem of the connection between the deterministic vacuum theory of relativity and quantum mechanics is easily solved, and the existence of the so-called "mass gap" is logically substantiated.

Vacuum is similar to an elastic-plastic continuous medium (trembling jelly), which constantly and everywhere chaotically seethes, bizarrely bends and twists into spirals, topological knots are tied and untied in it, etc. Einstein's vacuum equations are, in essence, conservation laws, i.e. conditions for ensuring the stability of averaged local and global vacuum formations. Metric-solutions of these vacuum equations allow us to obtain averaged (i.e. simplified) metric-dynamic models (mental frameworks) of stable spherical vacuum formations. However, the averaged stable structure of "particles" is illusory – it is only a mental construction, i.e. the result of the ability of our thinking to simplify infinitely complex situations.
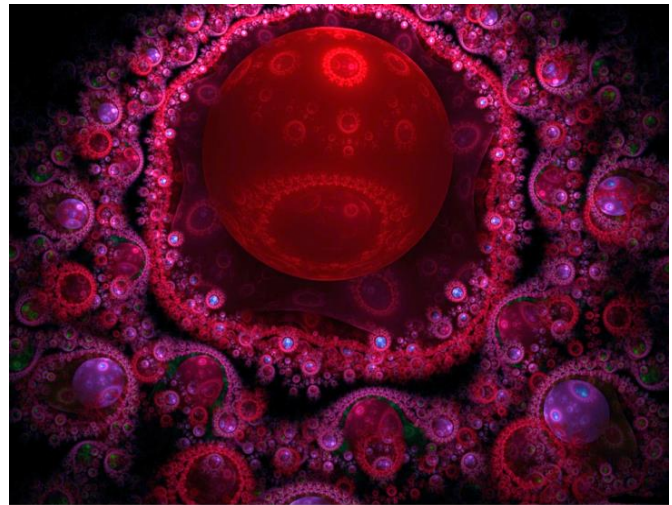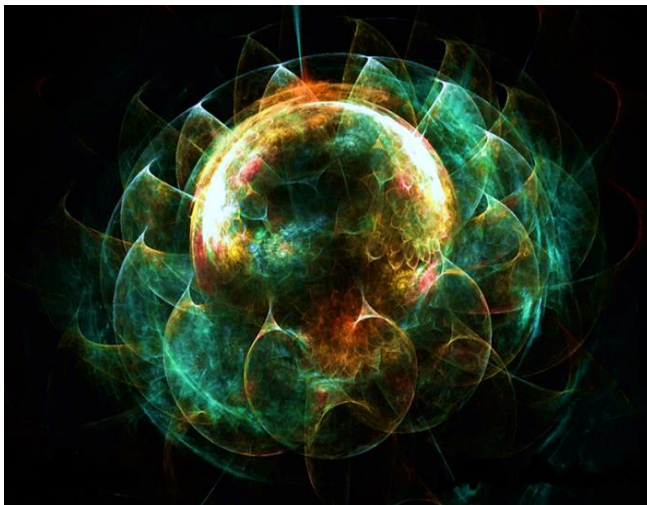
In addition, the nuclei of spherical vacuum formations, extracted from the seething chaos by averaging and simplification, themselves move chaotically as structureless particles (corpuscles) under the influence of the seething vacuum medium (see Figure 26). However, the arbitrariness of the behavior of a randomly wandering nucleus (corpuscle) is only apparent. When averaging the chaotic behavior of a nucleus, it turns out that it obeys the laws of effective probability, which are a compromise between two opposite global aspirations of any stochastic system for "Minimum Action" (i.e., for energy conservation) and for "Maximum Entropy" (i.e., for ultimate freedom). The equations of stochastic quantum mechanics, describing the average behavior of a chaotically wandering particle, turned out to be conditions for the extremum of the averaged efficiency functional (see [13]).

It may seem that deterministic Einstein vacuum equations and stochastic diffusion equations and Schrödinger equations relate to different laws of nature. In fact, they all have their roots in a deep understanding of the dichotomy of "Order and Chaos" and in the philosophical definition of "Freedom as cognized necessity" (Baruch Spinoza, Georg Hegel). Einstein vacuum equations and the equations of stochastic mechanics are different forms of manifestation of the extremality of one efficiency functional. If we neglect the chaotic component of the particle's motion (i.e. if we consider only the average trajectory of its

motion), then the search for the extremality of the efficiency functional of such a stochastic system can move on to the Lagrangian formalism of classical mechanics (see expression (18a) in [13]).

Thus, in the geometrized vacuum physics developed here, random fluctuations are first eliminated by averaging in order to reveal the average structure of stable vacuum formations. Then, chaotic fluctuations are returned to consideration as:
- dynamic chaos due to the study of the average behavior of chaotically wandering nuclei (corpuscles) of, on average, stable spherical vacuum formations;
- topological chaos due to the study of nodal superpositions of metrics with 16 different signatures (see §1);
- relic chaos due to the study of fluctuations of the vacuum itself.

Within the framework of the proposed "geometrized vacuum physics" there are no contradictions between the general theory of relativity, probability theory and quantum mechanics.

In the "geometized physics of vacuum" the concept of "mass" is absent. As has been repeatedly noted in articles [1,2,3,4,5,6], the heuristically introduced physical quantity "mass" with the dimension of kilogram (which corresponds to the weight of one liter of purified water at a temperature of 4 ^{0}C and normal atmospheric pressure at the latitude and longitude of Paris) is convenient for applied problems. But this quantity is completely impossible to introduce into a completely geometrized theory.

In the theory developed here, the subject of study is stable and unstable spherical vacuum formations (i.e. local and global averaged deformations of the corpuscular type vacuum) of various scales. In this case, such concepts as charge, mass, spin, color and other characteristics of particles in the fully geometrized physics developed here are expressed through the properties of 3-dimensional space illuminated by light rays (i.e. through the properties of the $\lambda_{m,n}$-vacuum): the speed of light in a vacuum, the radius of the "particle" core, the signatures of the metric, etc.

Although the terminology and basic concepts in "geometrized vacuum physics" differ from modern quantum field theory, one can try to answer one of the "Millennium Prize Problems", which is formulated as "The Yang–Mills existence and mass gap problem".

First, we note that Einstein's vacuum equations, taking into account all 16 signatures,

$$
\begin{array}{llll}
(+ + + +)^1 & (+ + + -)^5 & (- + + -)^9 & (+ + - +)^{13} \\
(- - - +)^2 & (- + + +)^6 & (- - + +)^{10} & (- + - +)^{14} \\
(+ - - +)^3 & (+ + - -)^7 & (+ - - -)^{11} & (+ - + +)^{15} \\
(- - + -)^4 & (+ - + -)^8 & (- + - -)^{12} & (- - - -)^{16}
\end{array}
\tag{173}
$$

is a special case of the Yang–Mills equations [16].

Recall that the Yang–Mills equations are a system of partial differential equations for a connection on a vector bundle. They arise as the Euler–Lagrange equations from the Yang–Mills action functional.

Secondly, within the framework of the fully geometrized theory developed here, the problem of the existence of a mass gap is easily solved.

Secondly, within the framework of the fully geometrized theory developed here, the problem of the existence of a *mass gap* can be easily solved.

Recall that in quantum field theory the mass gap is the difference in energy between the vacuum and the next highest energy state. The vacuum energy is zero by definition, and if we assume that all energy states can be treated as particles in plane waves, the mass gap is equal to the mass of the lightest particle (i.e., the electron).

In previous articles [4,5,6] it was shown that Einstein vacuum equations (140) in [5]

$$
R_{ik} \pm \Lambda_a \, g_{ik} = 0,
\tag{174}
$$

have flat solutions (10) and (20)

$$ds_5^{(+---)2} = c^2 dt^2 - dr^2 - r^2(d\theta^2 + sin^2\theta\, d\phi^2),$$

$$ds_5^{(-+++)2} = -c^2 dt^2 + dr^2 + r^2(d\theta^2 + sin^2\theta\, d\phi^2),$$

which determine the stable metric-dynamic state of the undeformed section of the two-sided $\lambda_{-12,-15}$-vacuum.

The next stable, but already deformed, state of the outer side of the $\lambda_{-12,-15}$-vacuum, i.e. (subcont), is determined by the set of metric-solutions (2) – (5) and (6) – (9) of the same vacuum equation, which allow us to construct an averaged metric-dynamic model of the "electron". Similarly, the stable deformed state of the inner side of the $\lambda_{-12,-15}$-vacuum (i.e. antisubcont) is determined by the set of metric-solutions (12) – (15) and (16) – (19) of the same vacuum equation (174), which allow us to construct an averaged metric-dynamic model of the "positron".

Here we are not talking about the difference in the rest masses (or rather energies) of the vacuum and the electron, but about the two nearest stable states of the $\lambda_{-12,-15}$-vacuum. We call the first stable undeformed state of a section of the $\lambda_{-12,-15}$-vacuum "emptiness" (or rather, the Einstein void), and we call the next simplest stable deformed state of one side of the $\lambda_{-12,-15}$-vacuum "electron". The difference between these two average stable states of the $\lambda_{-12,-15}$-vacuum, caused by the internal discrete properties of the Einstein vacuum equation. This is the easily explainable reason for the existence of the so-called "mass gap" in the Yang-Mills theory.

However, the internal discreteness of Einstein vacuum equations does not lie in the fact that they are quantized by the methods of quantum field theory, but in the fact that the solutions of these levels are discrete in nature, both from the point of view of the hierarchical discontinuity of the sizes of the cores of stable vacuum formations, and from the point of view of the countable classification of topological nodes, associated with the limitedness of the discrete set of 16 possible signatures (173).

In conclusion, it should be noted that it is necessary to distinguish between living and non-living "electrons" and "positrons". They differ in that in living vacuum formations, what we perceive as chaos is a complex genetic code (i.e. a closed information flow). Living "electrons" and "positrons" are male and female (Fermi-bacteria or viruses). Non-living "electrons" and "positrons" are only compacted vacuum shells, revealed from senseless chaos by means of averaging.

The article is accompanied by fractal illustrations. Some fractals convey the essence of natural manifestations in an amazing way. Sometimes it is necessary to write several pages of text to explain what a fractal conveys in one image.
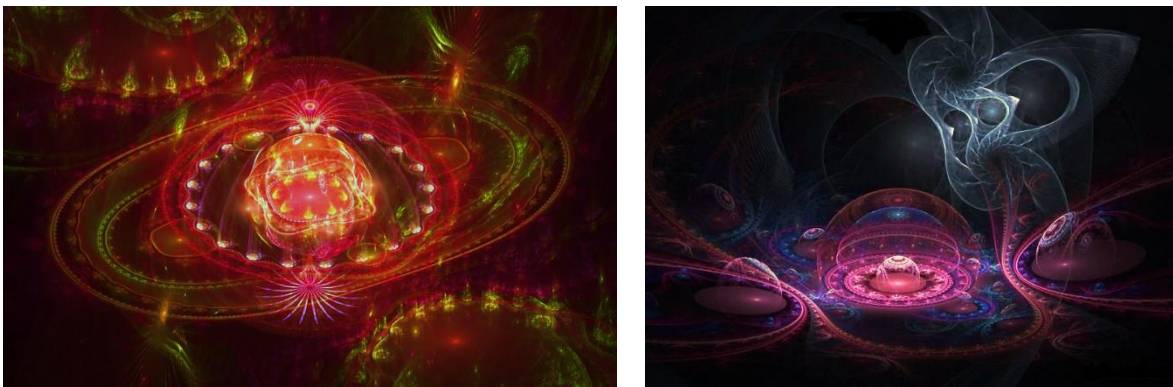
Unfortunately, it is almost impossible to find the authors of these masterpieces on the Internet, so the fractals are provided without indicating their creators. We compensate for this by expressing heartfelt gratitude to these devotees of beauty, starting with Gaston Maurice Julia and Benoit Mandelbrot, with the hope that their efforts will serve to expand our knowledge of the bottomless depths of reality around us.

REFERENCES

[1] Batanov-Gaukhman, M. (2023). Geometrized Vacuum Physics. Part I. Algebra of Stignatures. Avances en Ciencias e Ingeniería, 14 (1), 1-26, https://www.executivebs.org/publishing.cl/avances-en-ciencias-e-ingenieria-vol-14-nro-1-ano-2023-articulo-1/ ; and viXra:2403.0035, and Preprints, 2023060765. https://doi.org/10.20944/preprints202306.0765.v3, Available in Russian: https://doi.org/10.24108/preprints-3113027 .

[2] Batanov-Gaukhman, M. (2023). Geometrized Vacuum Physics. Part II. Algebra of Signatures. Avances en Ciencias e Ingeniería, 14 (1), 27-55, https://www.executivebs.org/publishing.cl/avances-en-ciencias-e-ingenieria-vol-14-nro-1-ano-2023-articulo-2/: and Preprints, 2023070716, https://doi.org/10.20944/preprints202307.0716.v1. and viXra:2403.0034. Available in Russian: https://doi.org/10.24108/preprints-3113028 .

[3] Batanov-Gaukhman, M. (2023). Geometrized Vacuum Physics. Part III. Curved Vacuum Area. Avances en Ciencias e Ingeniería Vol. 14 nro 2 año 2023 Articulo 5, https://www.executivebs.org/publishing.cl/avances-en-ciencias-e-ingenieria-vol-14-nro-2-ano-2023-articulo-5/; and Preprints 2023, 2023080570. https://doi.org/10.20944/preprints202308.0570.v4. and viXra:2403.0033 . Available in Russian: https://doi.org/10.24108/preprints-3113032 .

[4] Batanov-Gaukhman, M., (2024). Geometrized Vacuum Physics. Part IV: Dynamics of Vacuum Layers. Avances en Ciencias e Ingeniería Vol. 14 nro 3 año 2023 Articulo 1 https://www.executivebs.org/publishing.cl/avances-en-ciencias-e-ingenieria-vol-14-nro-3-ano-2023-articulo-1/, and Preprints.org. https://doi.org/10.20944/preprints202310.1244.v3. and viXra:2403.0032 . Available in Russian: https://doi.org/10.24108/preprints-3113039

[5] Batanov-Gaukhman, M., (2024). Avances en Ciencias e Ingeniería Vol. 14 nro 3 año 2023 Articulo 2 https://www.executivebs.org/publishing.cl/avances-en-ciencias-e-ingenieria-vol-14-nro-3-ano-2023-articulo-2/ and Geometrized Vacuum Physics Part 5: Stable Vacuum Formations, viXra:2405.0002 . Available in Russian: https://doi.org/10.24108/preprints-3113040

[6] Batanov-Gaukhman, M. (2024) Geometrized Vacuum Physics Part 6: Hierarchical Cosmological Model, viXra:2408.0010

[7] Landau L.D., Lifshitz E.M. (1971) The Classical Theory of Fields / Course of theoretical phys-ics, V. 2 Translated from the Russian by Hamermesh M. University of Minnesota – Pergamon Press Ltd. Oxford, New York, Toronto, Sydney, Braunschwei, p. 387.

[8] Gaukhman, M.Kh. (2007) Algebra of signatures "NAMES" (orange Alsigna). – Moscow: LKI, p.228, ISBN 978-5-382-00077-0, (www.alsigna.ru).

[9] Chelnokov Yu.N. (2006) Quaternion and biquaternion models and methods of solid mechanics and their positions. – Moscow: Fizmatlit (in Russian).

[10] Nelson, E. (1966) Derivation of the Schrödinger Equation from Newtonian Mechanics. Phys. Rev. *150 (4): 1079 –1085,* doi·10.1103/physrev.150.1079.

[11] Nelson, E. (1967) *Dynamical Theories of Brownian Motion*, Princeton University Press, Princeton, N.J., zbMATH Google Scholar.

[12] Nelson, E. (1985) Quantum fluctuations. Princeton: Princeton University Press.

[13] Batanov-Gaukhman M. (2024) Development of the Stochastic Interpretation of Quantum Mechanics by E. Nelson. Derivation of the Schrödinger-Euler-Poisson Equations. *Recent Progress in Materials* **2024**; 6(2): 014; 10.21926/rpm.2402014, or arXiv:2011.09901v10 . Available in Russian:

[14] Batanov-Gaukhman M. (2024) Stochastic Model of Microparticle Scattering On a Crystal. Avances en Ciencias e Ingeniería (ISSN: 0718-8706), vol. 12 №3. https://www.executivebs.org/publishing.cl/avances-en-ciencias-e-ingenieria-vol-12-nro-3-ano-2021-articulo-4/ or arXiv:2110.00372v1

[15] Davisson, C. J. & Germer, L. H. (1928) Reflection of Electrons by a Crystal of Nickel, Proceedings of the National Academy of Sciences of the United States of America. vol.**14** (4), pp. 317–322. doi:10.1073/pnas.14.4.317, PMC 1085484, PMID 16587341.

[16] Krivonosov, L. N., Lukyanov V. A. (2009) Relationship between the Yang–Mills equations and the Einstein and Maxwell equations // Zh. SFU. Ser. Math. and physical T. 2, No. 4. P. 432–448 (in Russian).